X-Ray Nano-Analytics and Microscopy

Part I

Christian G. Schroer
DESY & Universität Hamburg

HELMHOLTZ RESEARCH FOR GRAND CHALLENGES

Universität Hamburg
DER FORSCHUNG | DER LEHRE | DER BILDUNG

DESY.

DESY: Bright Light for Science

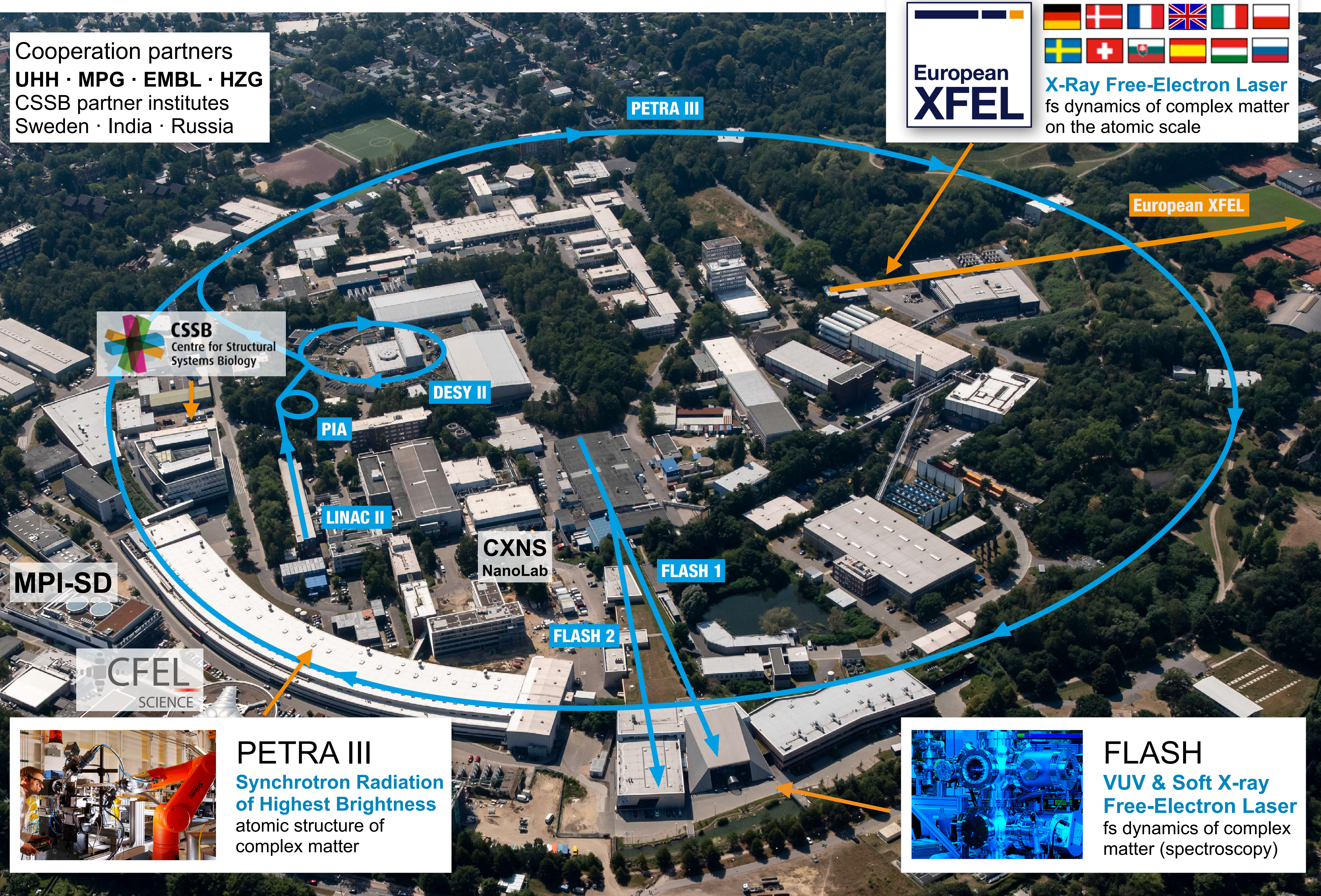

X-ray Scanning Microscopy

Broad field of applications:

> Main advantage: large penetration depth

→ *in-situ* and *operando* studies

→ 3D bulk analysis without destructive sample preparation

> X-ray analytical contrasts: XRD, XAS, XRF, ...

→ elemental, chemical, and structural information

Today: „mesoscopic gap“

real-space resolution: down to about 10 nm

XRD and XAS: atomic scale

Many interesting physics and chemistry (e. g. catalysis) at the 1 - 10 nm scale!

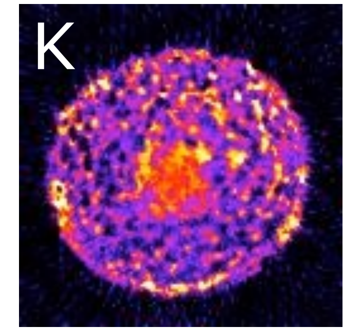

C. G. Schroer, APL **79**, 1912 (2001).

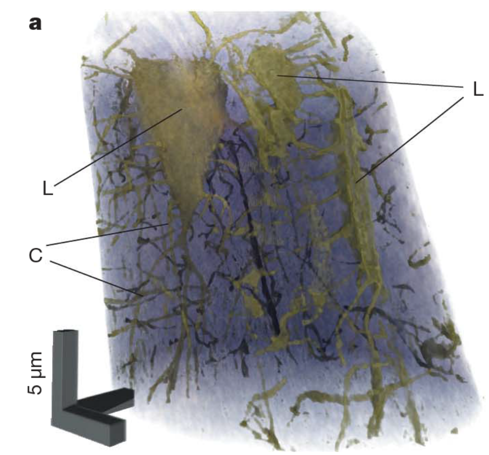

M. Dierolf, et al., Nature **467**, 436 (2010).

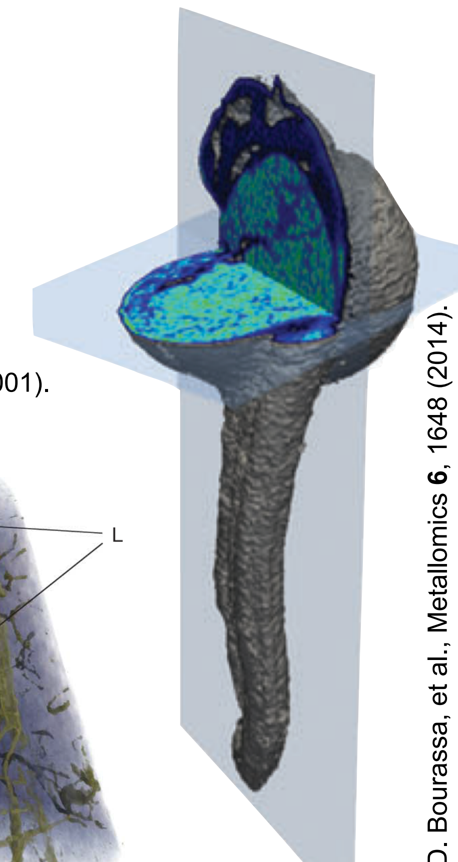

D. Bourassa, et al., Metallomics **6**, 1648 (2014).

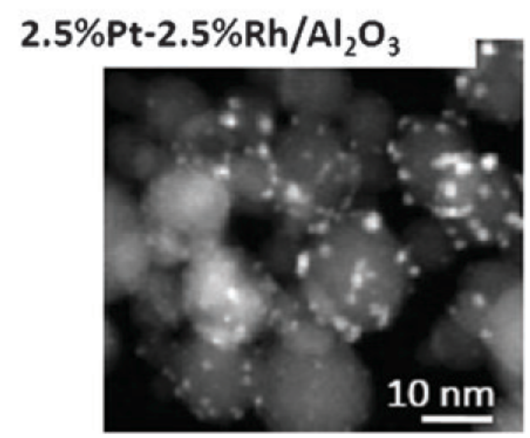

catalysts

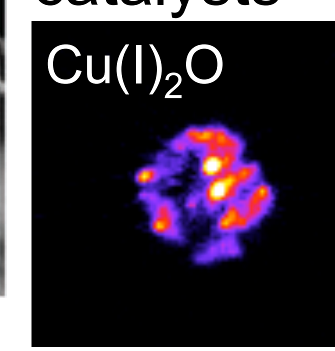

C. G. Schroer, et al., APL **82**, 3360 (2003).

X-ray Microscopy

Many interesting physics and chemistry questions:

investigate local states:

- individual defects (0D): changes in electron density, charge ordering
- (structural) domain boundaries (2D), e. g., in multiferroics
- mesoscopic dynamics at (solid-state) phase transitions
- catalytic nanoparticles (under reaction conditions)
- ...

Mesoscale also very important for nanotechnology (e. g., defects in devices)!

ferroelectric phase transition

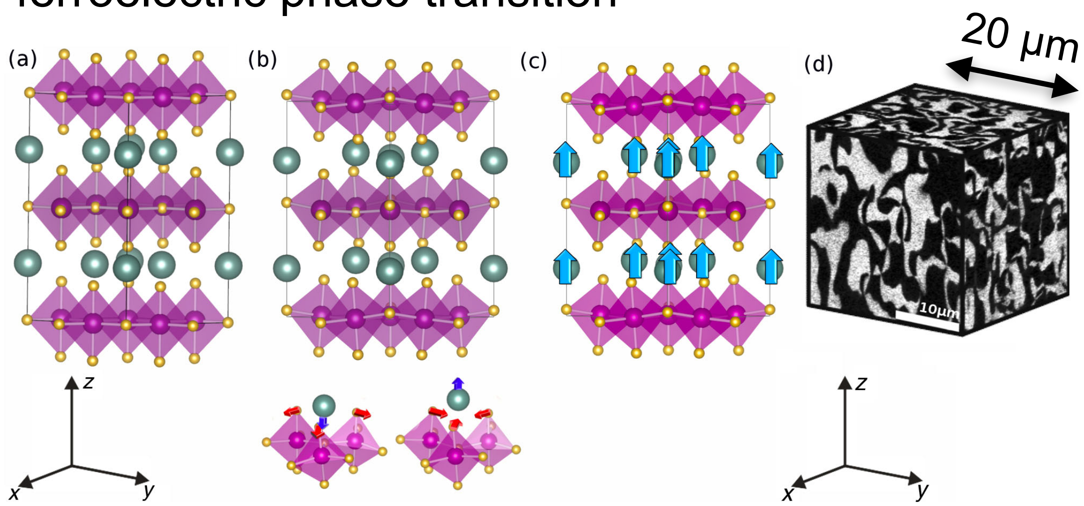

Griffin, et al., PRX **2**, 041022 (2012).

variation of supercond. gap

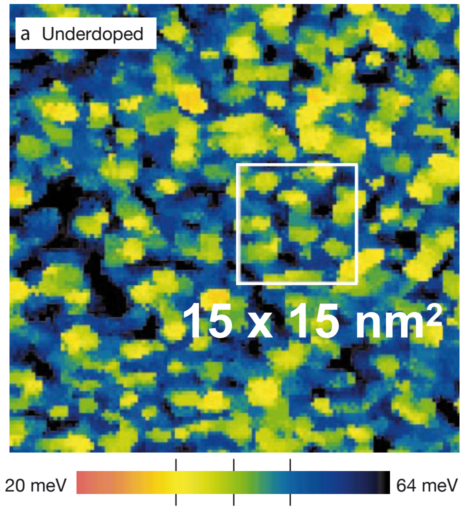

Lang, et al., Nature **415**, 412 (2002).

nanoelectromechanical switch

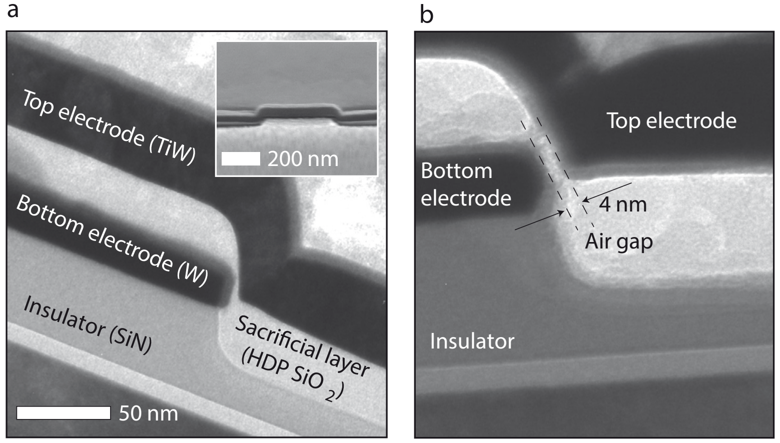

Lee, et al., Nature Nanotech. **8**, 36 (2012).

Current State of X-Ray Microscopy

Conventional X-ray microscopy

→ optics limit spatial resolution: diffraction limit

$$d=\frac{\lambda}{2n\sin\alpha}$$

(typically: a few tens of nanometers)

optics are technology limited!

Theoretical extrapolation of X-ray optical performance to the atomic level.

[PRB **74**, 033405 (2006); H. Yan, et al., PRB **76**, 115438 (2007)]

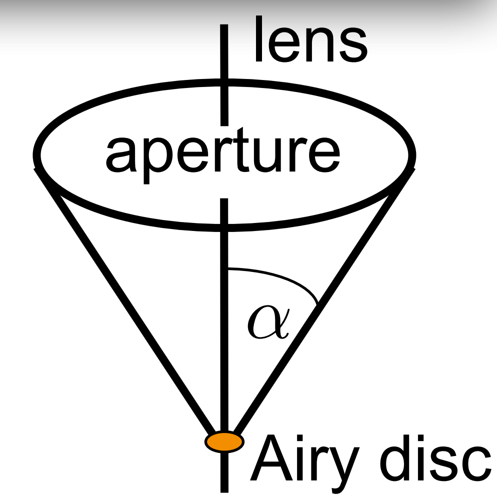

Coherent X-ray imaging techniques (CXDI, ptychography)

→ no imaging optics needed!

→ limited by statistics of far-field diffraction patterns ...

highest resolution: a few nanometers, focusing coherent beam

[PRL **101**, 090801 (2008); Y. Takahashi, et al., PRB **80**, 054103 (2009);
A. Schropp, et al., APL **100**, 253112 (2012); T. Aidukas, et al., Nature **632**, 81 (2024)]

Spectral Brightness

10000x more light per decade (since 1965)

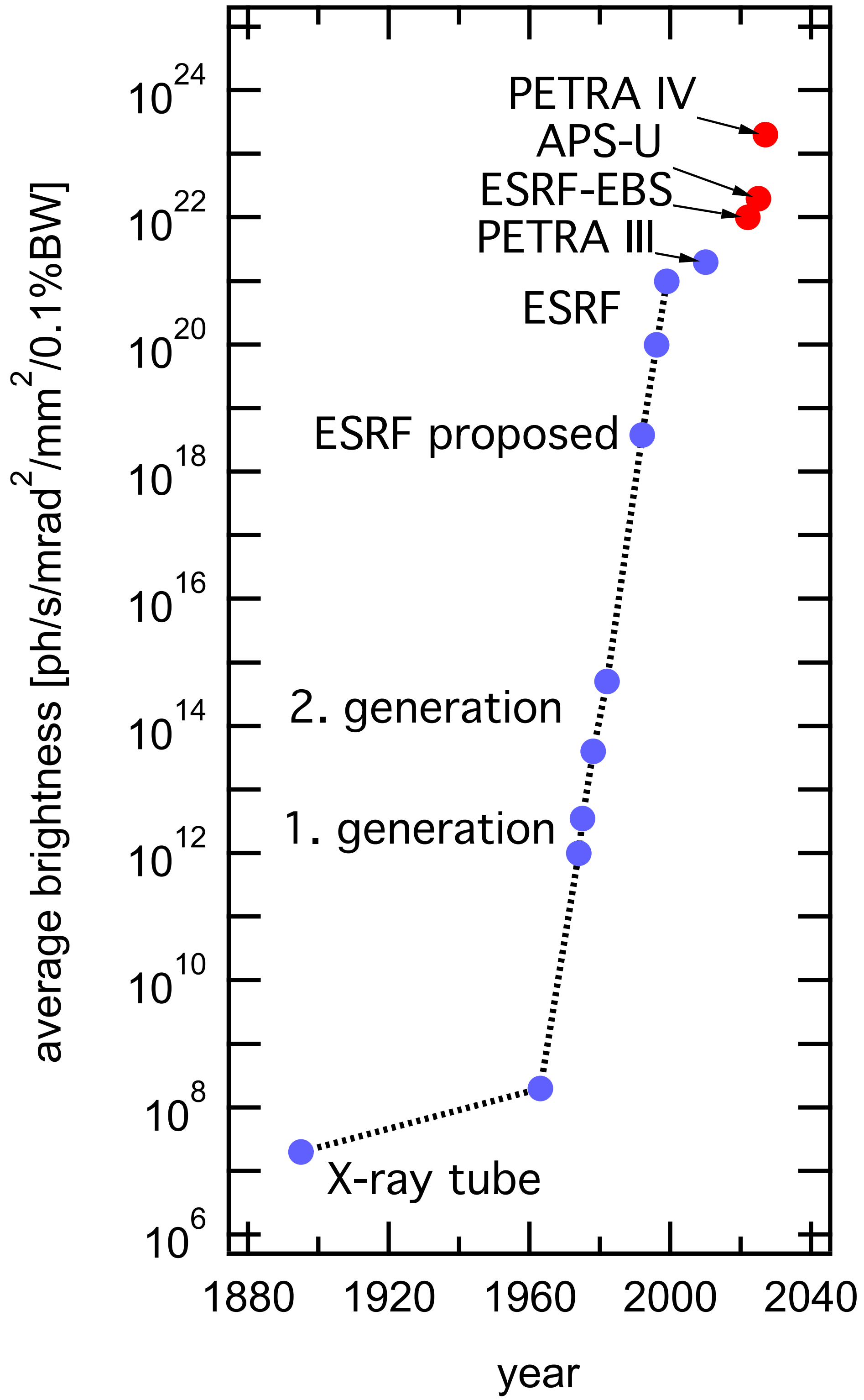

Spectral brightness:

$$B_{\mathrm{sp}} = \frac{F}{\Omega \cdot A \cdot \Delta E/E}$$

Flux per phase-space volume

coherent flux:

$$F_c \propto B_{\mathrm{sp}} \cdot \lambda^2 \cdot \frac{\Delta E}{E}$$

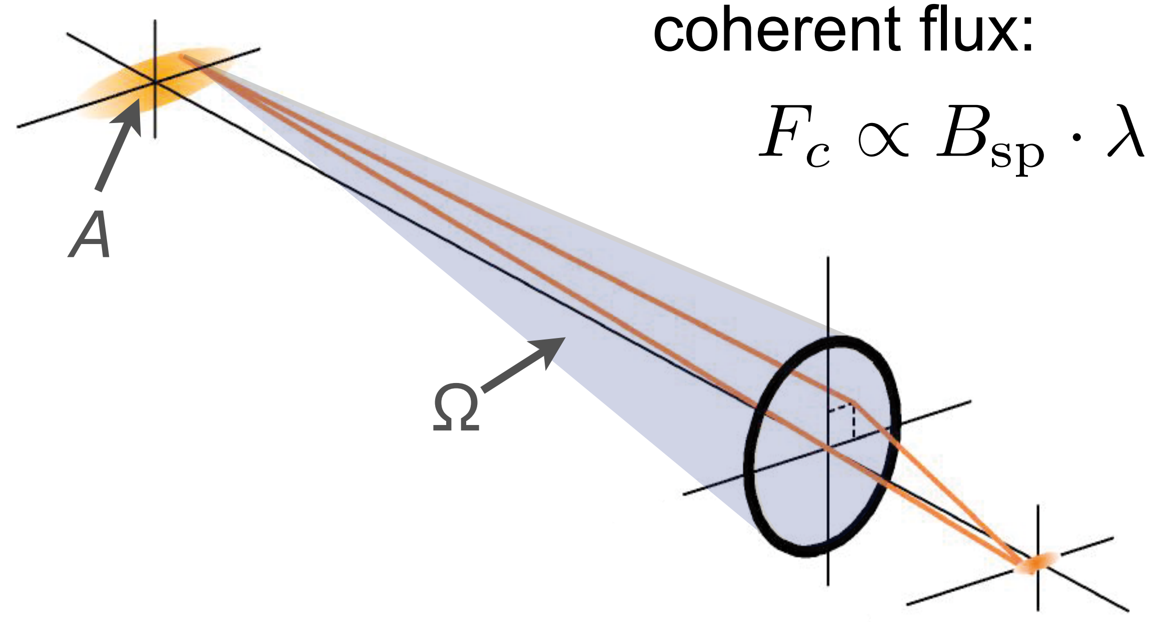

Improvements in brightness:

- > faster measurements (time resolution)
- > nano-imaging (spatial resolution)
- > spectroscopy (energy resolution)

Spectral Brightness

10000x more light per decade (since 1965)

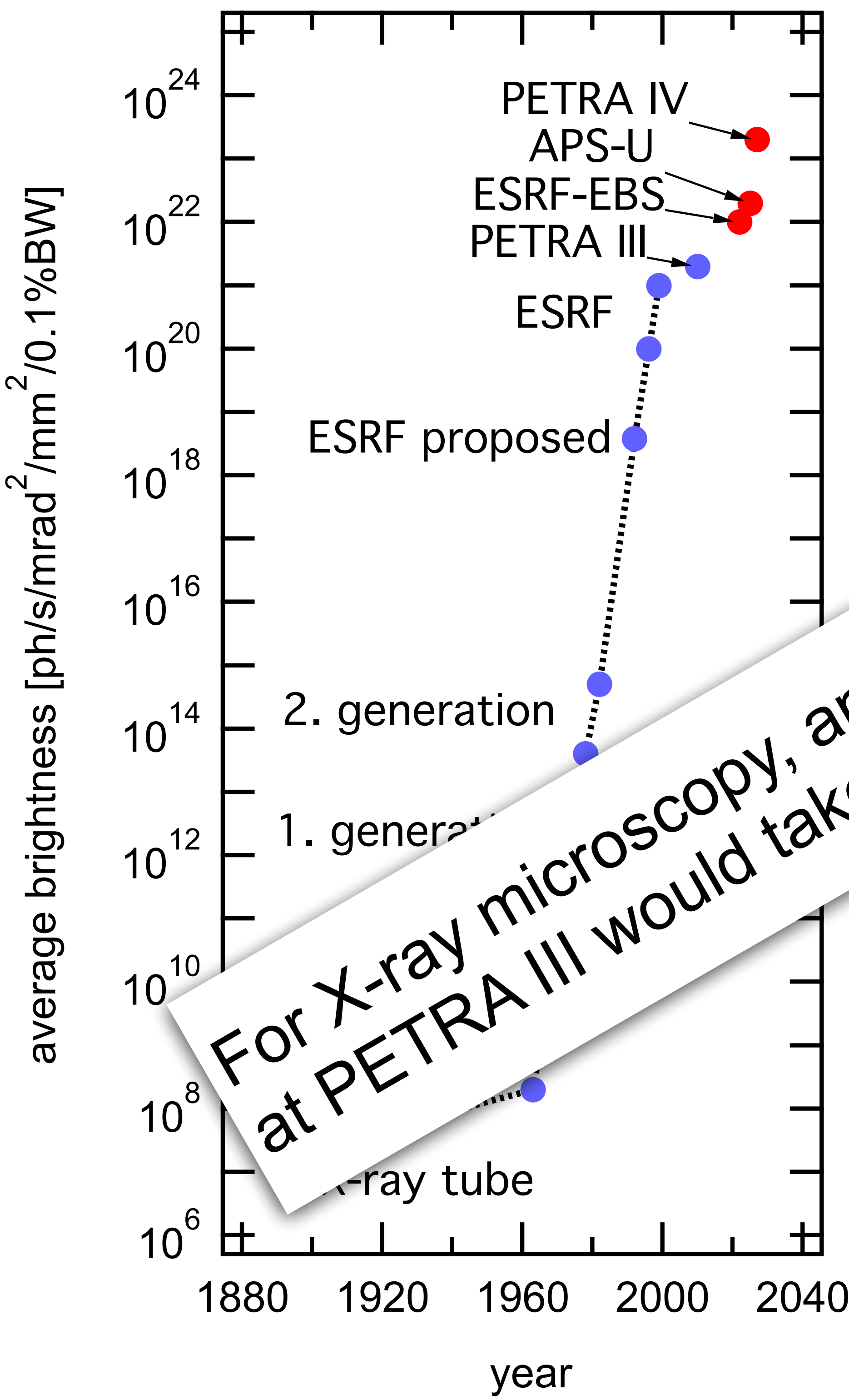

Spectral brightness:

$$B_{\mathrm{sp}} = \frac{F}{\Omega \cdot \ldots}$$

Flux per phase ...

...erent flux:

$$F_c \propto B_{\mathrm{sp}} \cdot \lambda^2 \cdot \frac{\Delta E}{E}$$

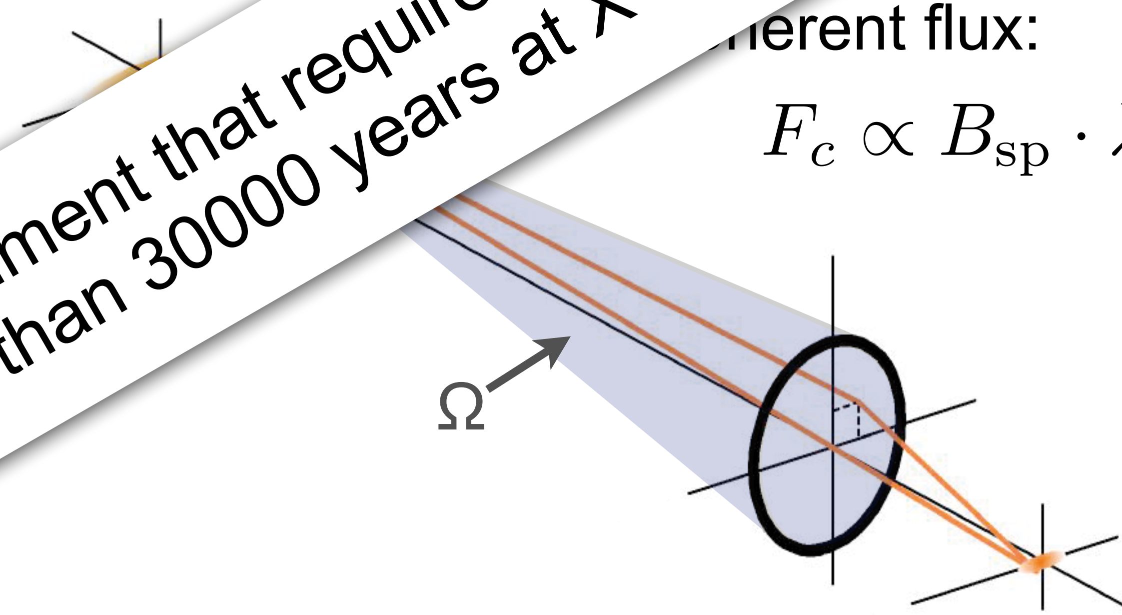

For X-ray microscopy, an experiment that requires 1 s of exposure time at PETRA III would take more than 30000 years at X-ray tube!!!

Improvements in brightness:

- > faster measurements (time resolution)
- > nano-imaging (spatial resolution)
- > spectroscopy (energy resolution)

Nanofocusing Optics

reflection:

> mirrors (25 nm)
H. Mimura, et al., APL **90**, 051903 (2007)

> capillaries

> wave guides (~10 nm)
S. P. Krüger, et al., J. Synchrotron Rad. **19**, 227 (2012)

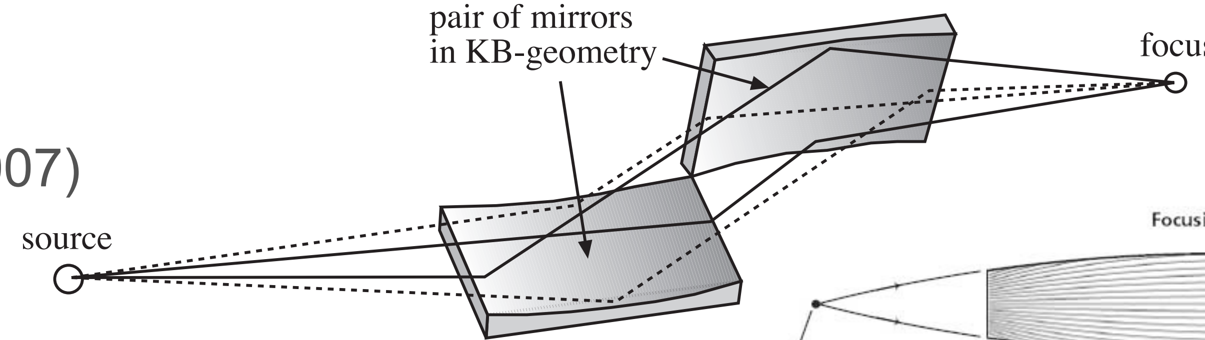

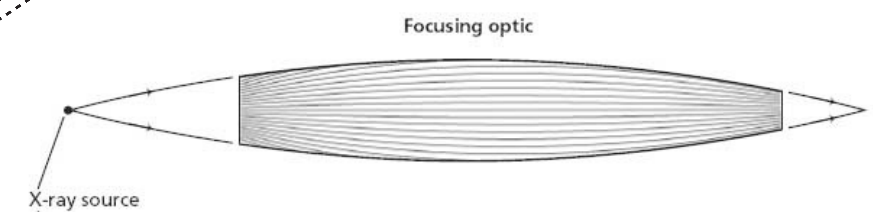

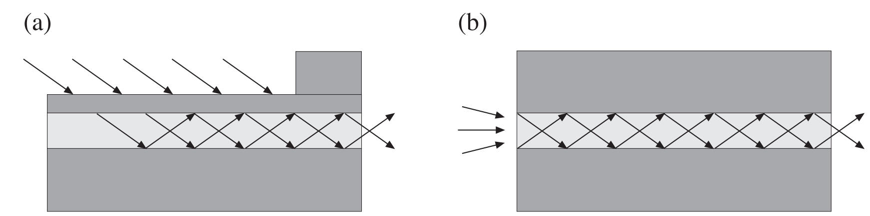

diffraction:

> Fresnel zone plates (< 10 nm)
J. Vila-Comamala, et al., Ultramic. **109**, 1360 (2009)

> multilayer mirrors (7 nm)
H. Mimura, et al., Nat. Phys. **6**, 122 (2010)

> multilayer Laue lenses (8 nm x 7 nm)
S. Bajt, et al., Light: Sci. & App. **7**, 17162 (2018)

> bent crystals

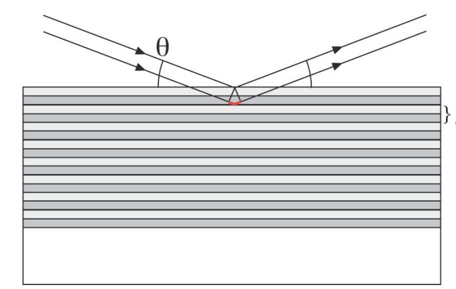

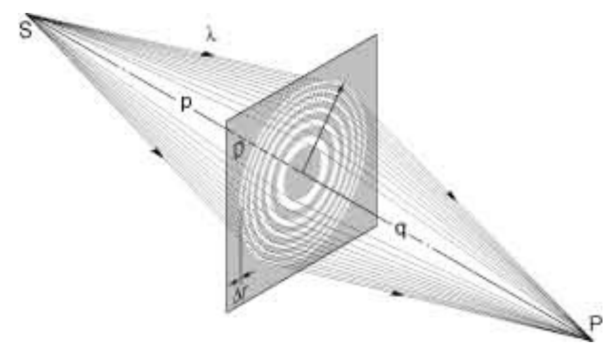

refraction:

> lenses (43 nm, 18 nm)
C. G. Schroer, et al., AIP Conf. Ser. **1365**, 227 (2011)
J. Patommel, et al., APL **110**, 101103 (2017)

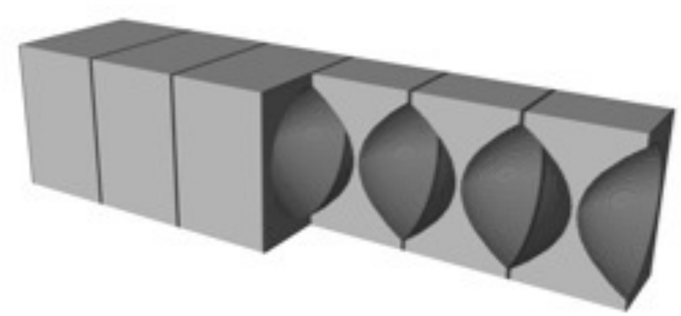

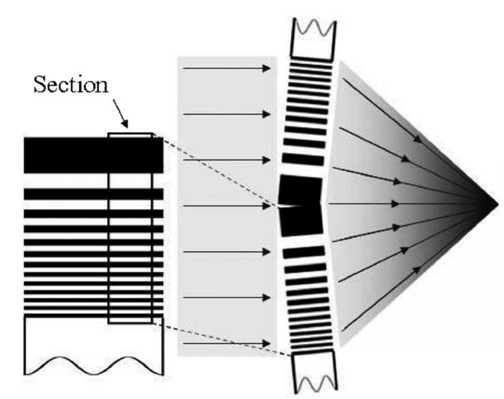

X-Ray Microscopy Techniques: Full-Field Imaging

Projection imaging:

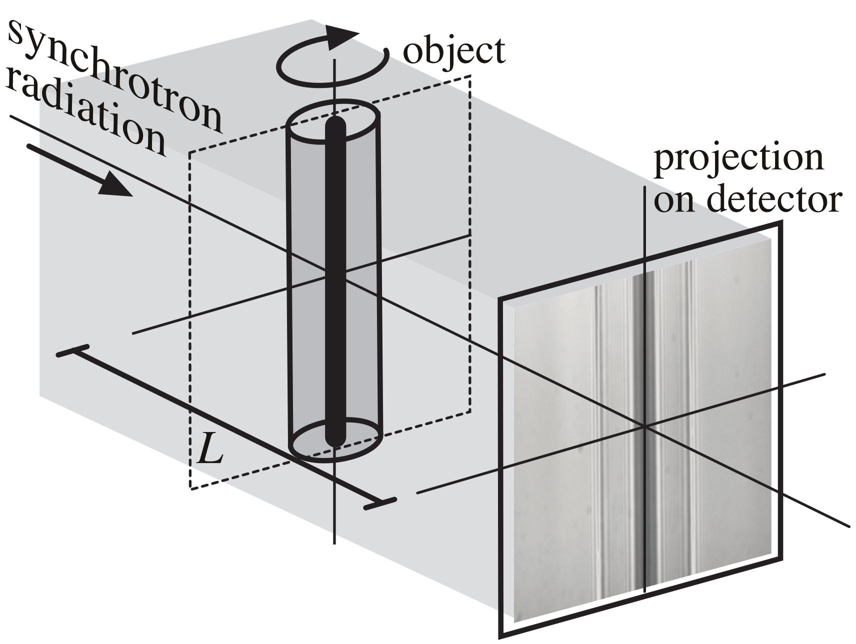

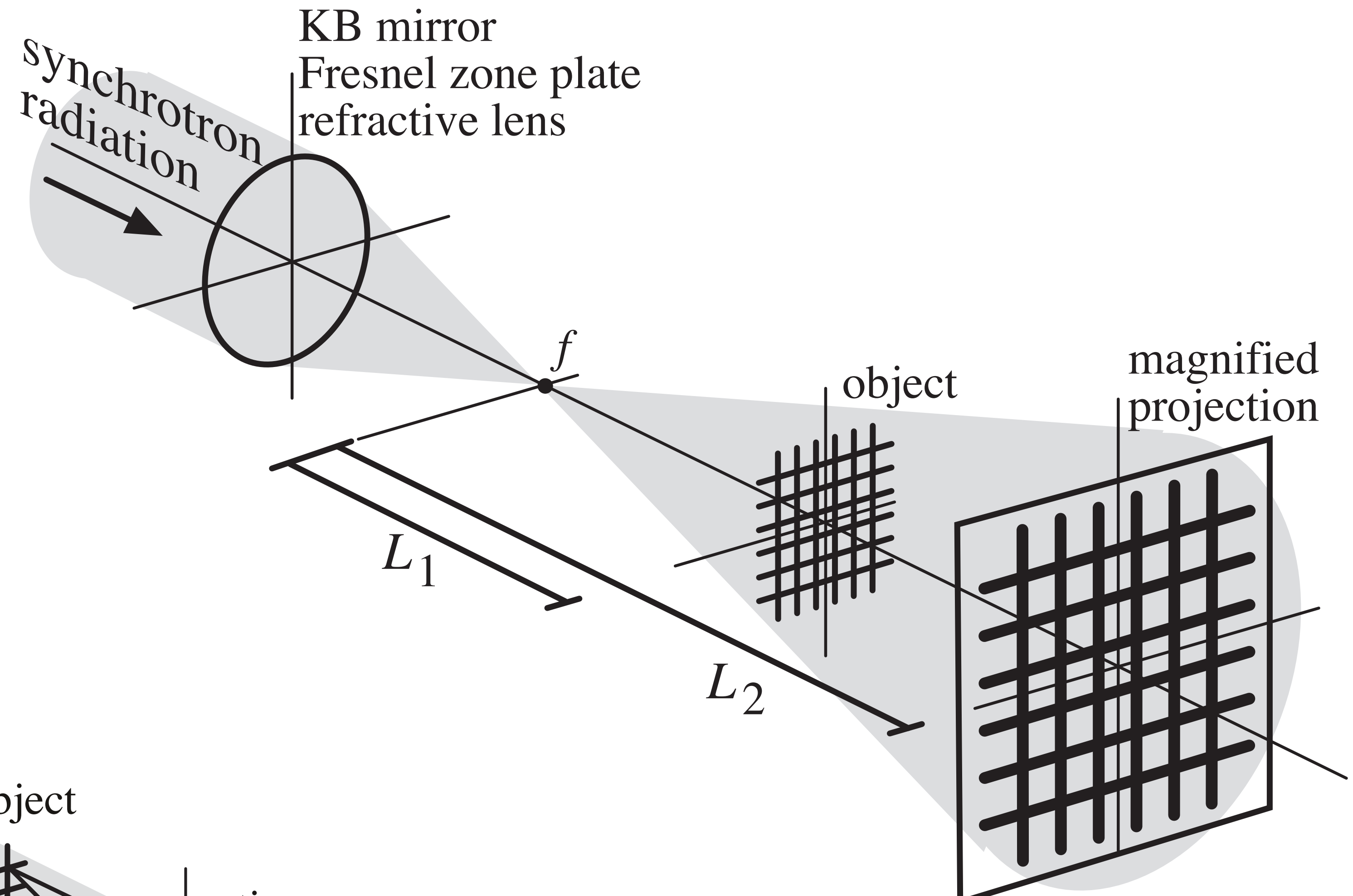

Imaging through objective lens:

x-rays focused by condensor (aperture matching)

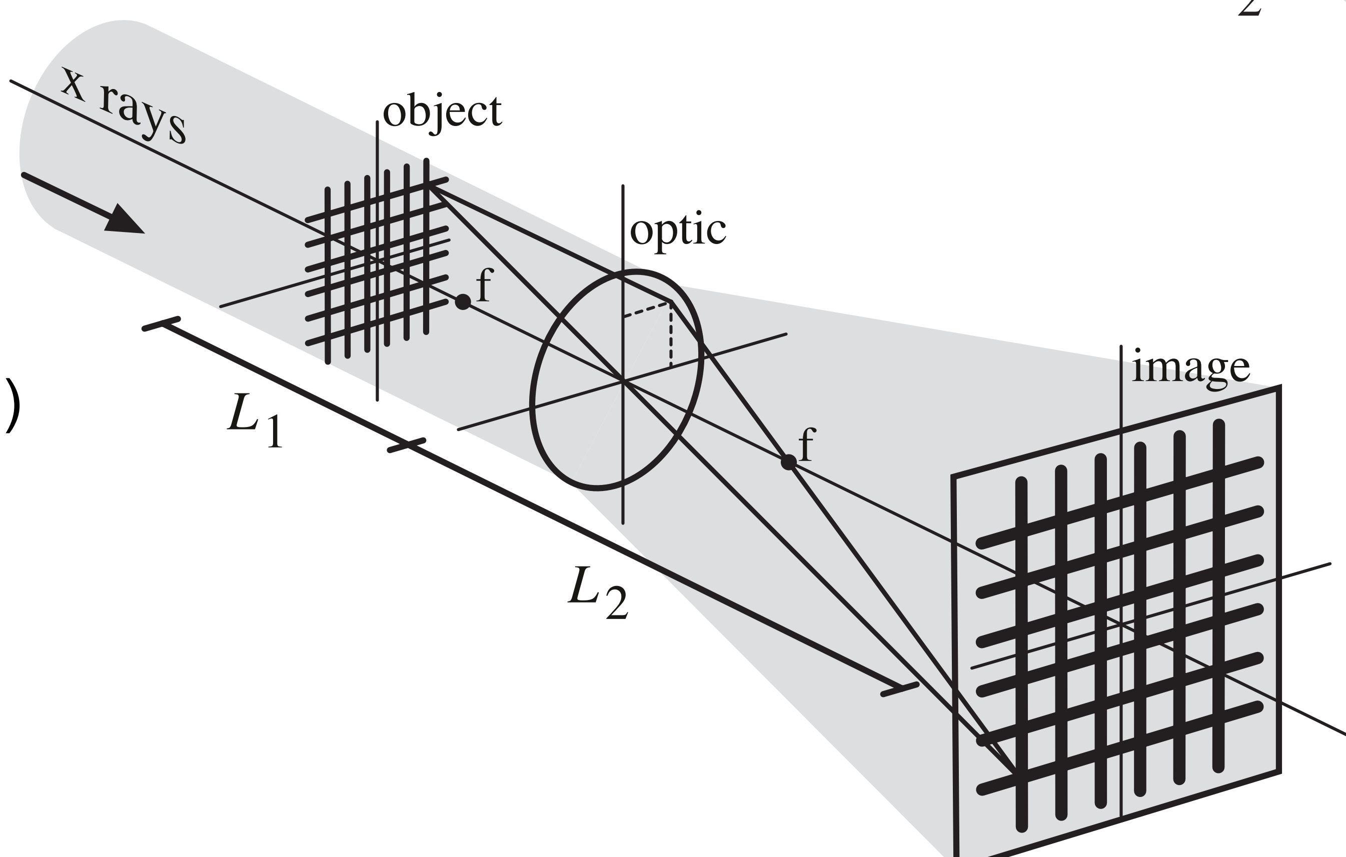

Cuneiform scripts from the ancient Near East document the first two-thirds of recorded human history.

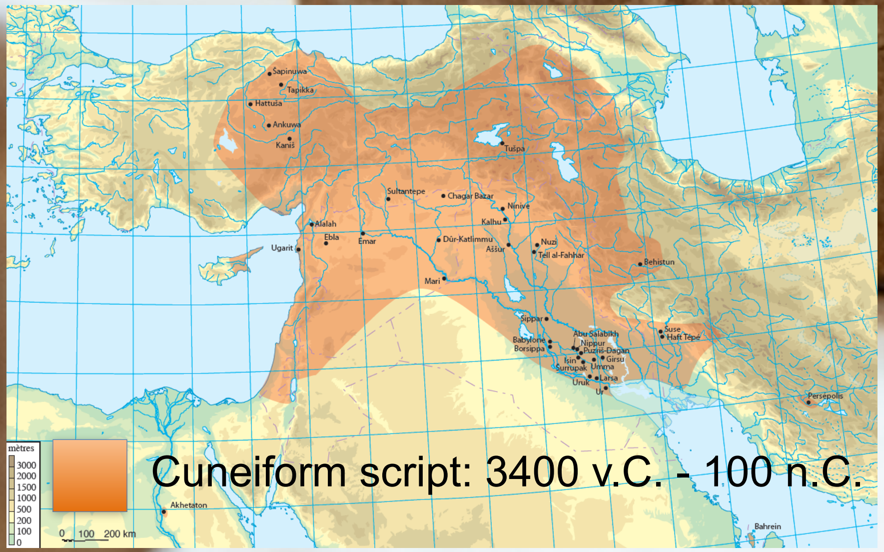

Over one million cuneiform scripts tell the story of daily life (in 16 languages)

The envelope was invented in 2400 BC:

> Letters: confidentiality and material integrity

> Legal texts: sealed envelope guarantees the validity of the document

Today there are thousands of unopened cuneiform letters and documents!

→ As time capsules, they provide an insight into life in early cultures

Cécile Michel (CNRS)

A Computer Tomograph for the Museum…

Excellence cluster:
Understanding written Artefacts

Universität Hamburg
DER FORSCHUNG | DER LEHRE | DER BILDUNG

CENTRE FOR THE STUDY OF MANUSCRIPT CULTURES

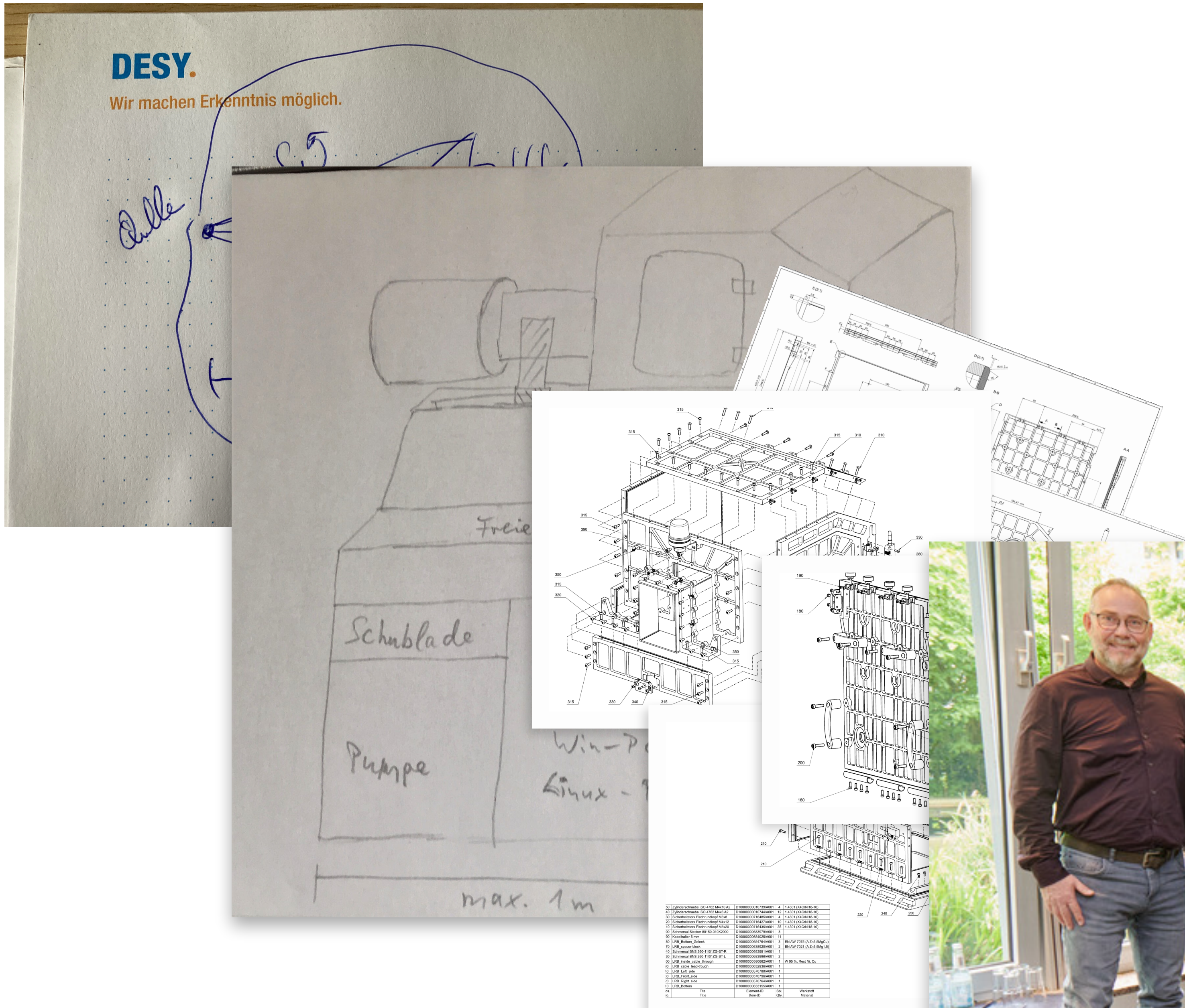

Arrival at the Louvre…

Assembly and Commissioning

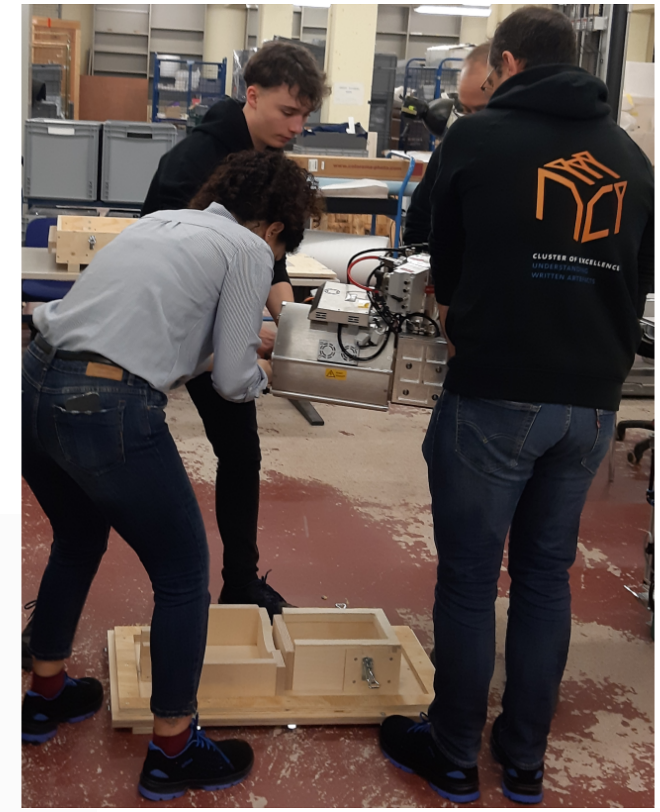

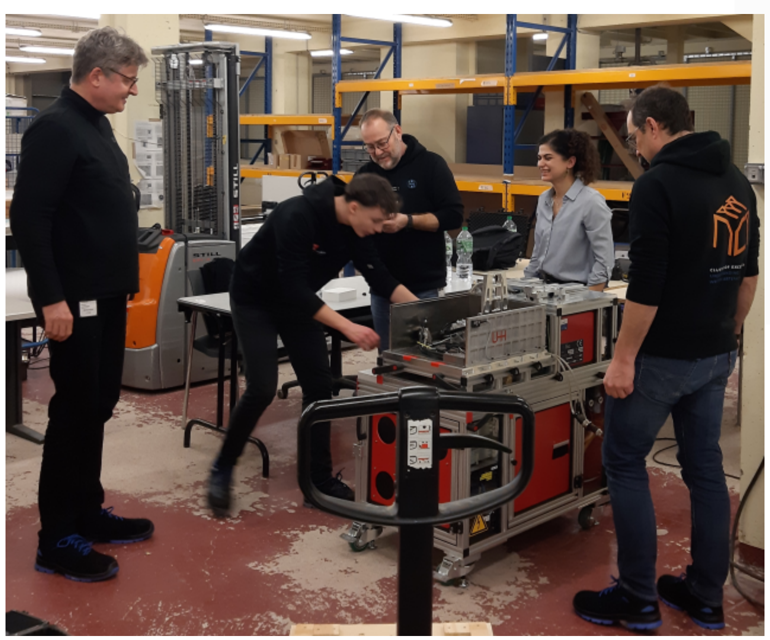

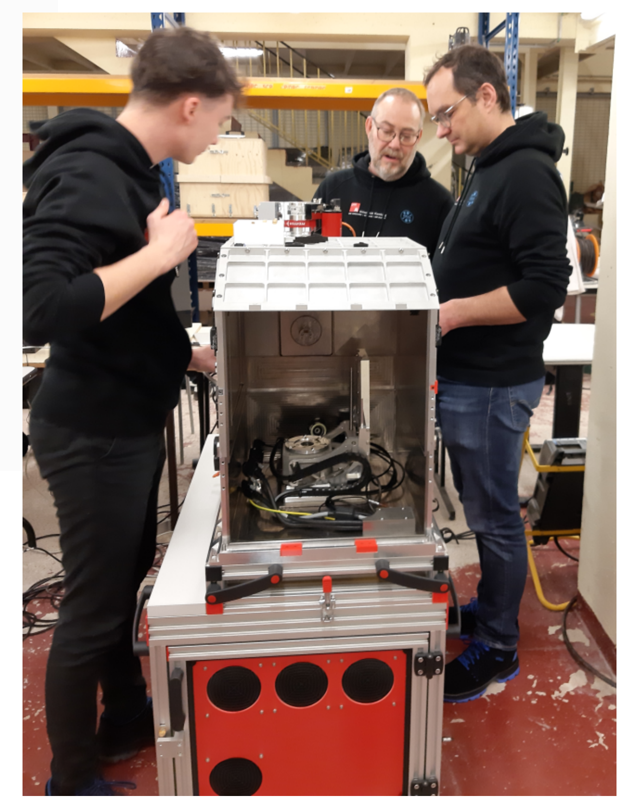

Preparing the Cuneiform Tablets

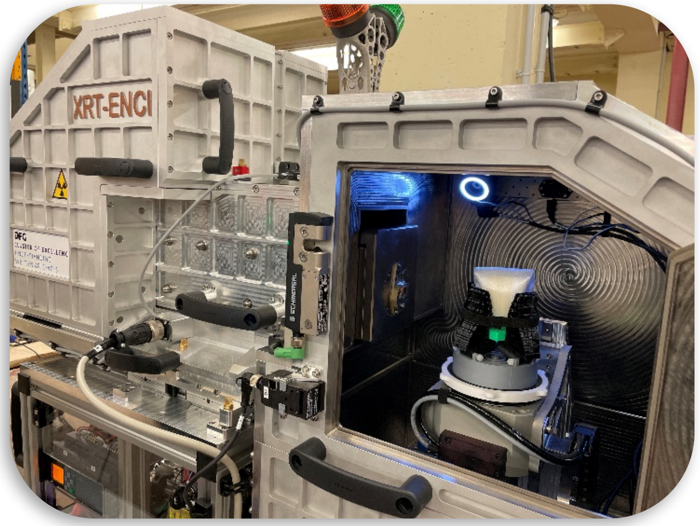

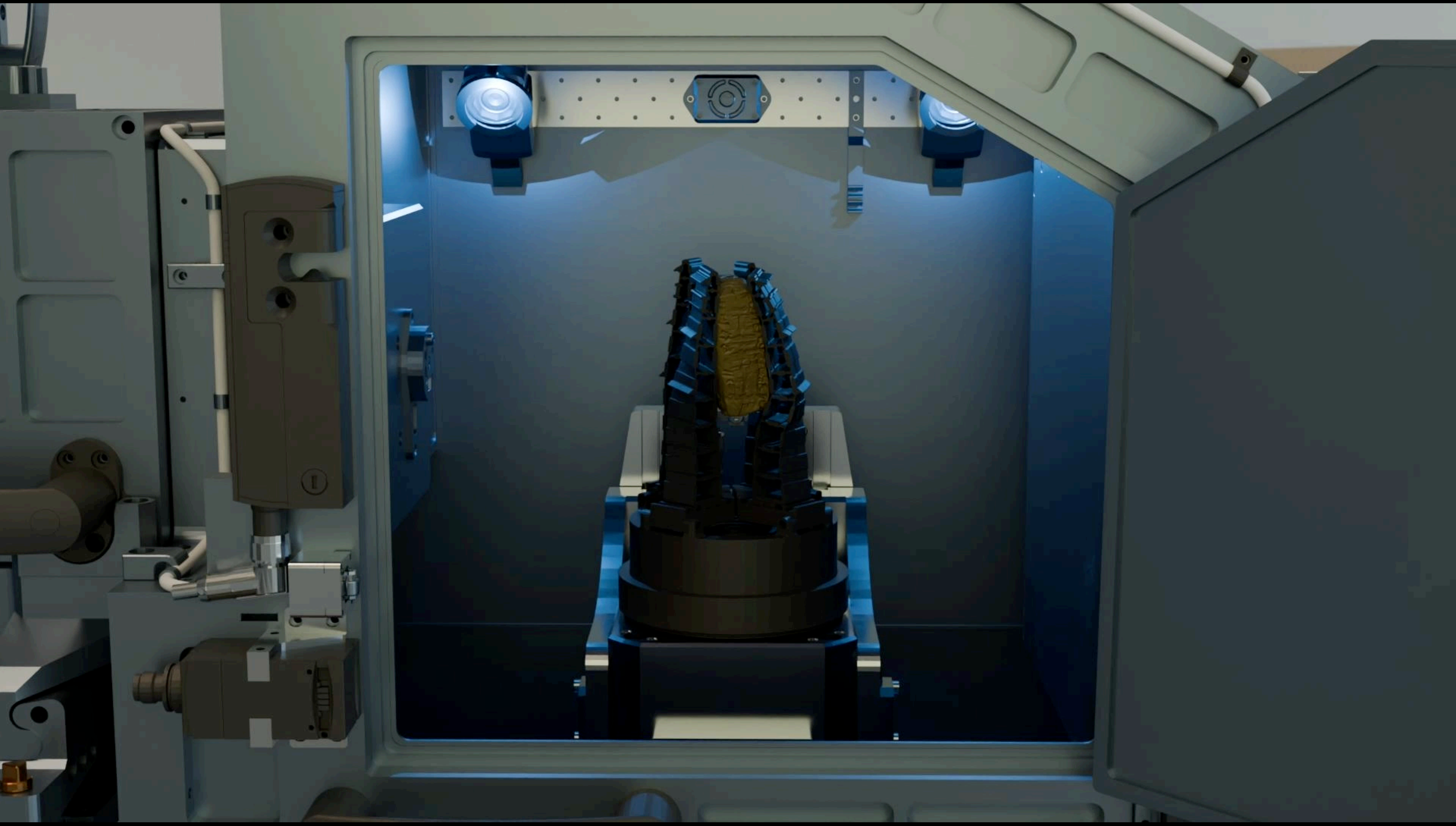

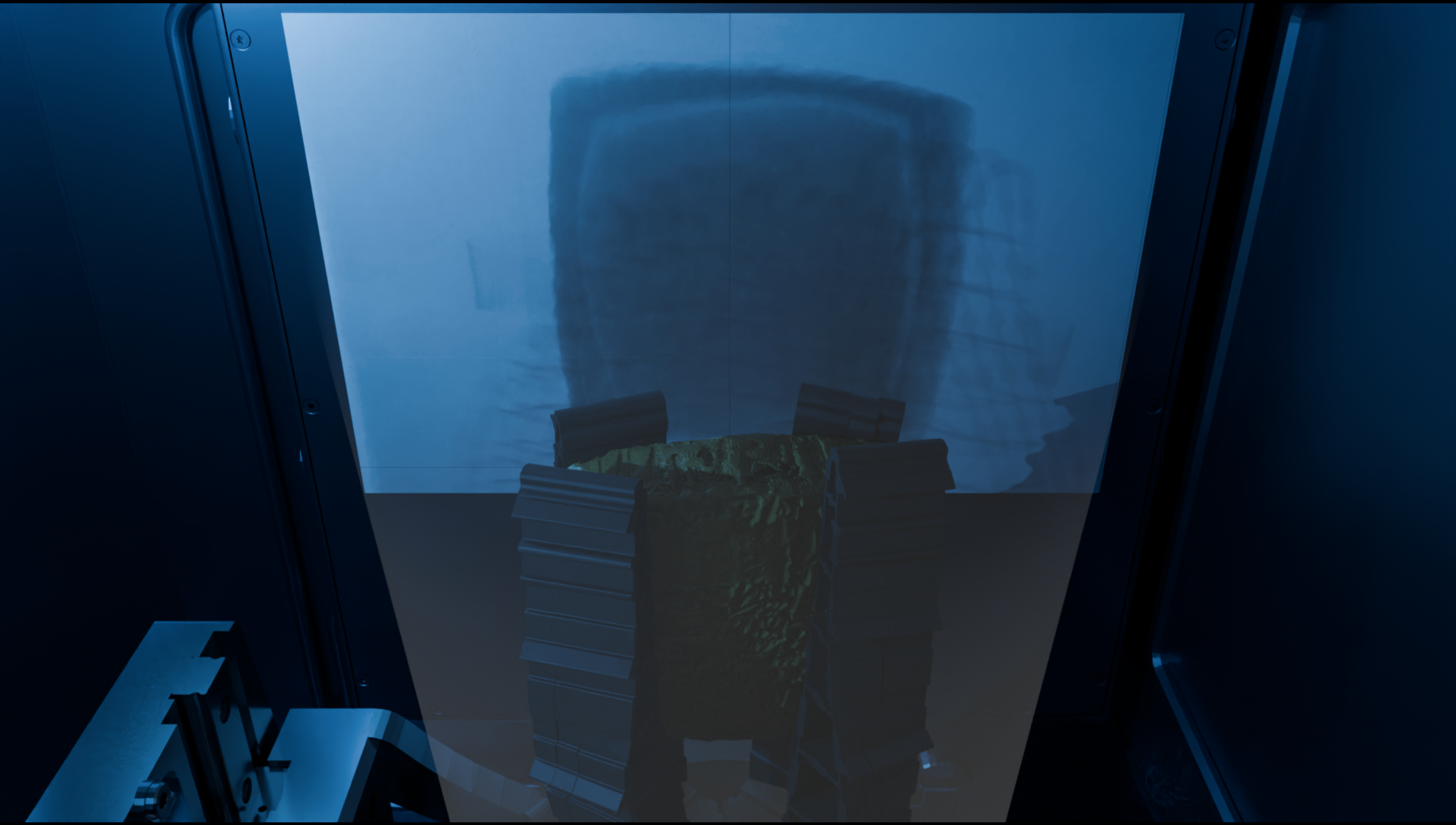

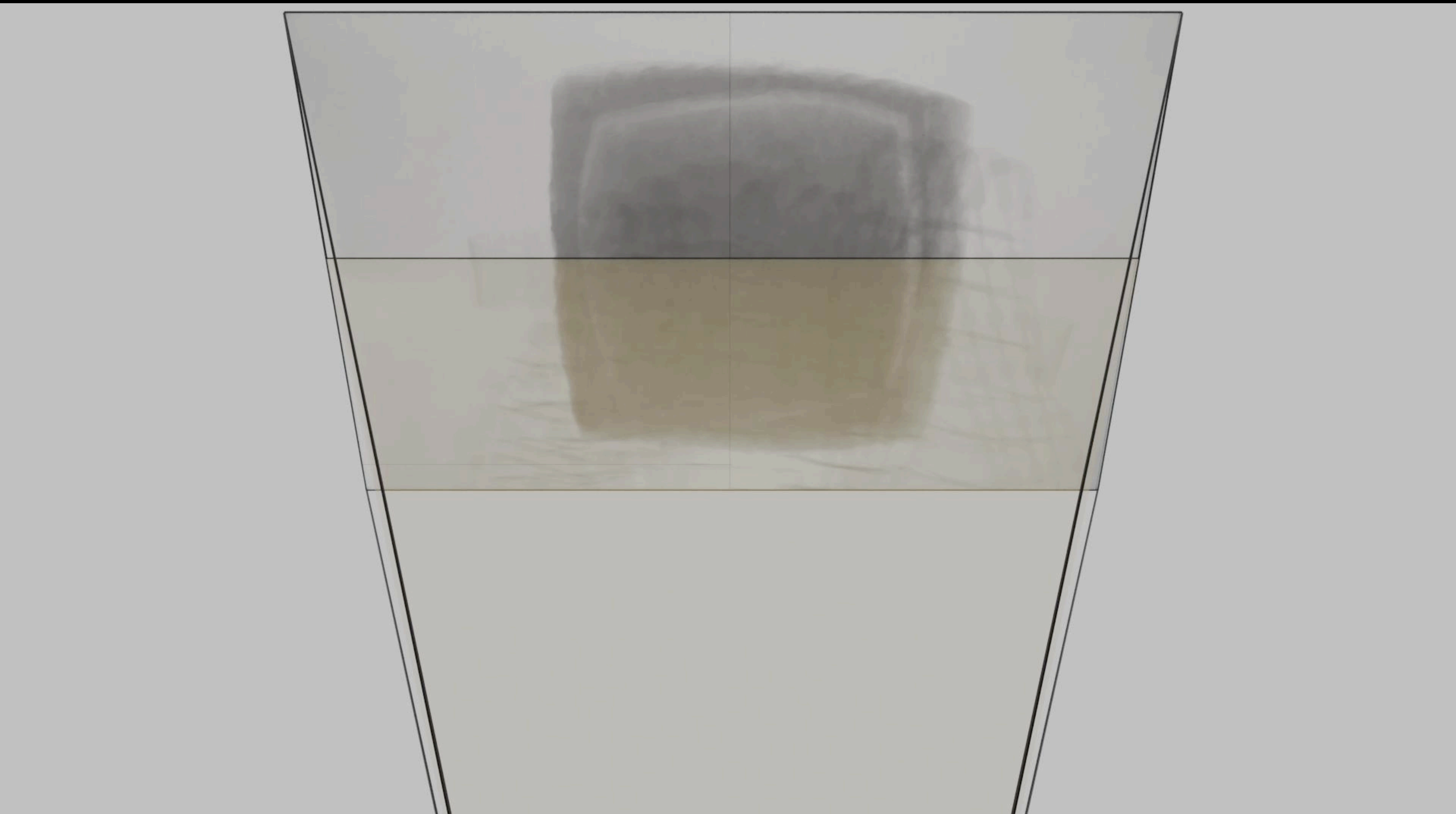

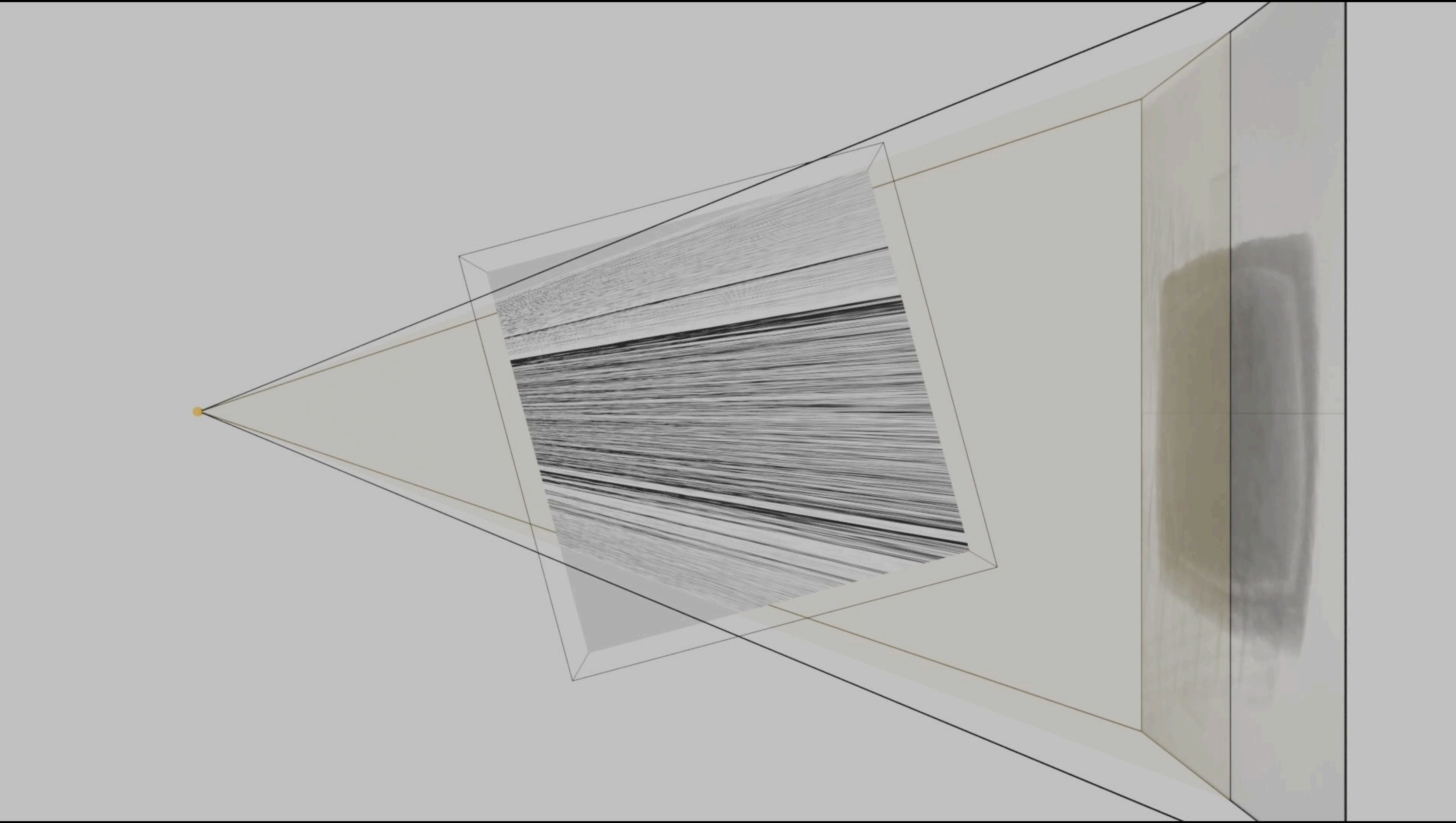

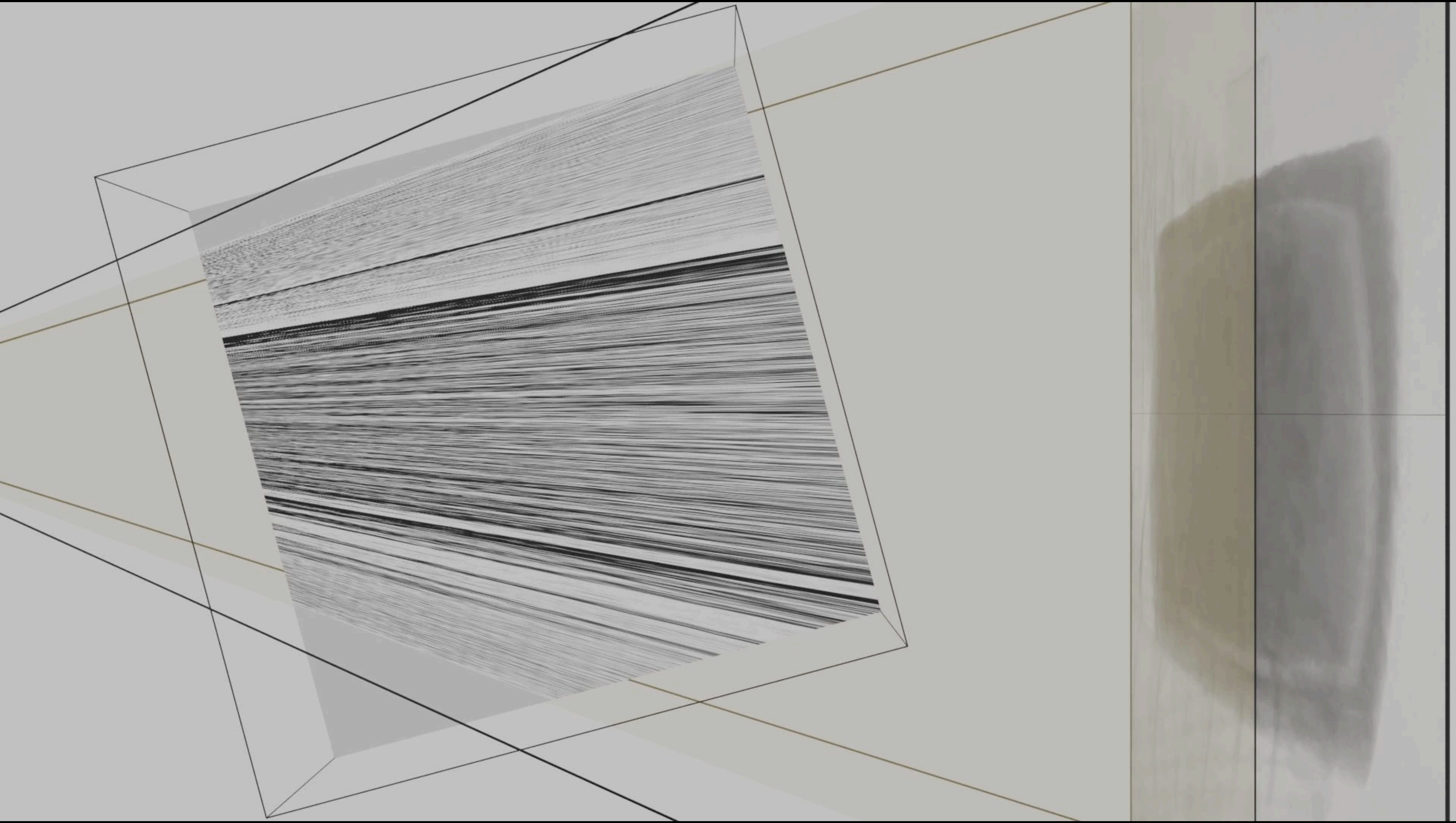

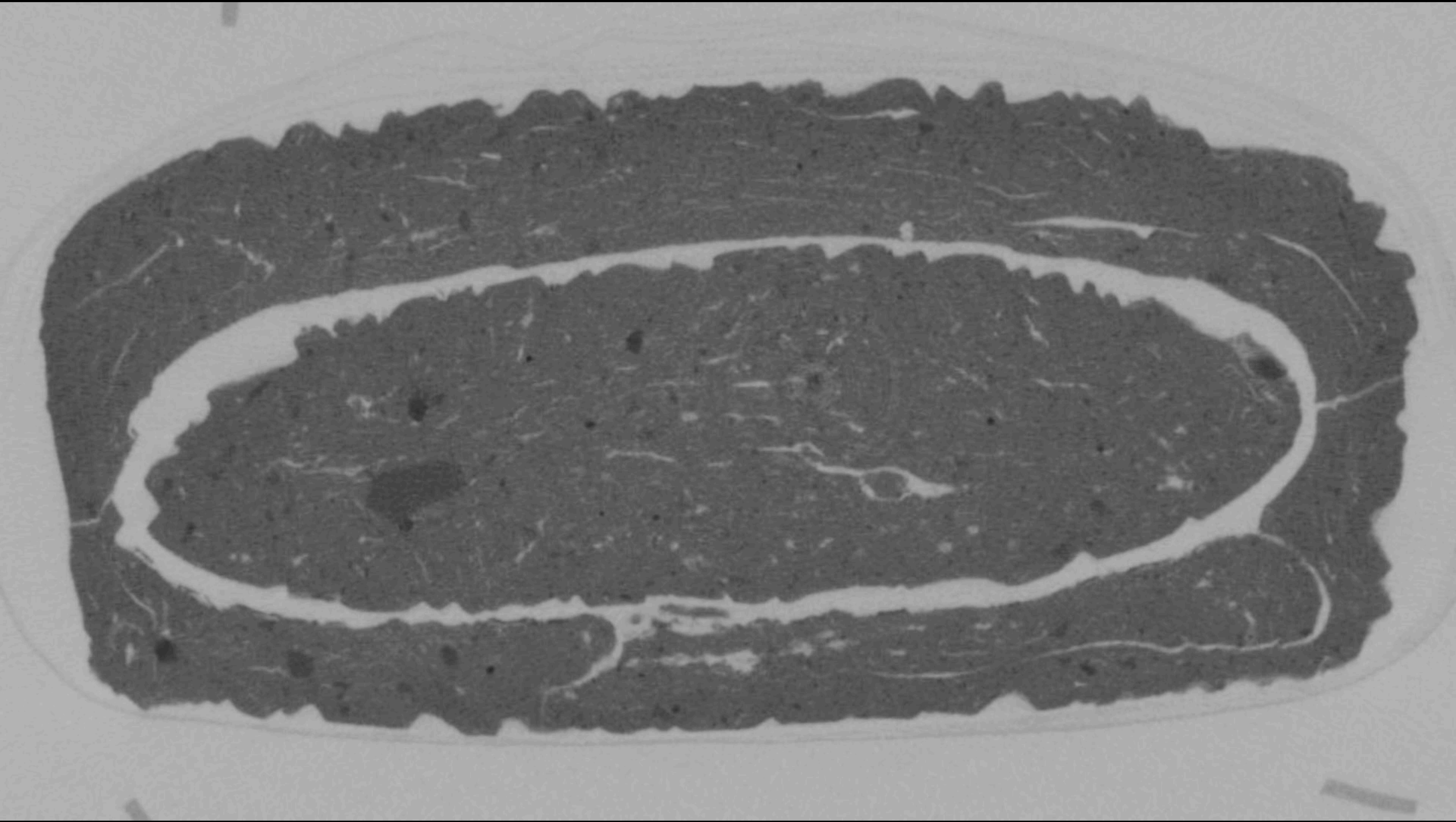

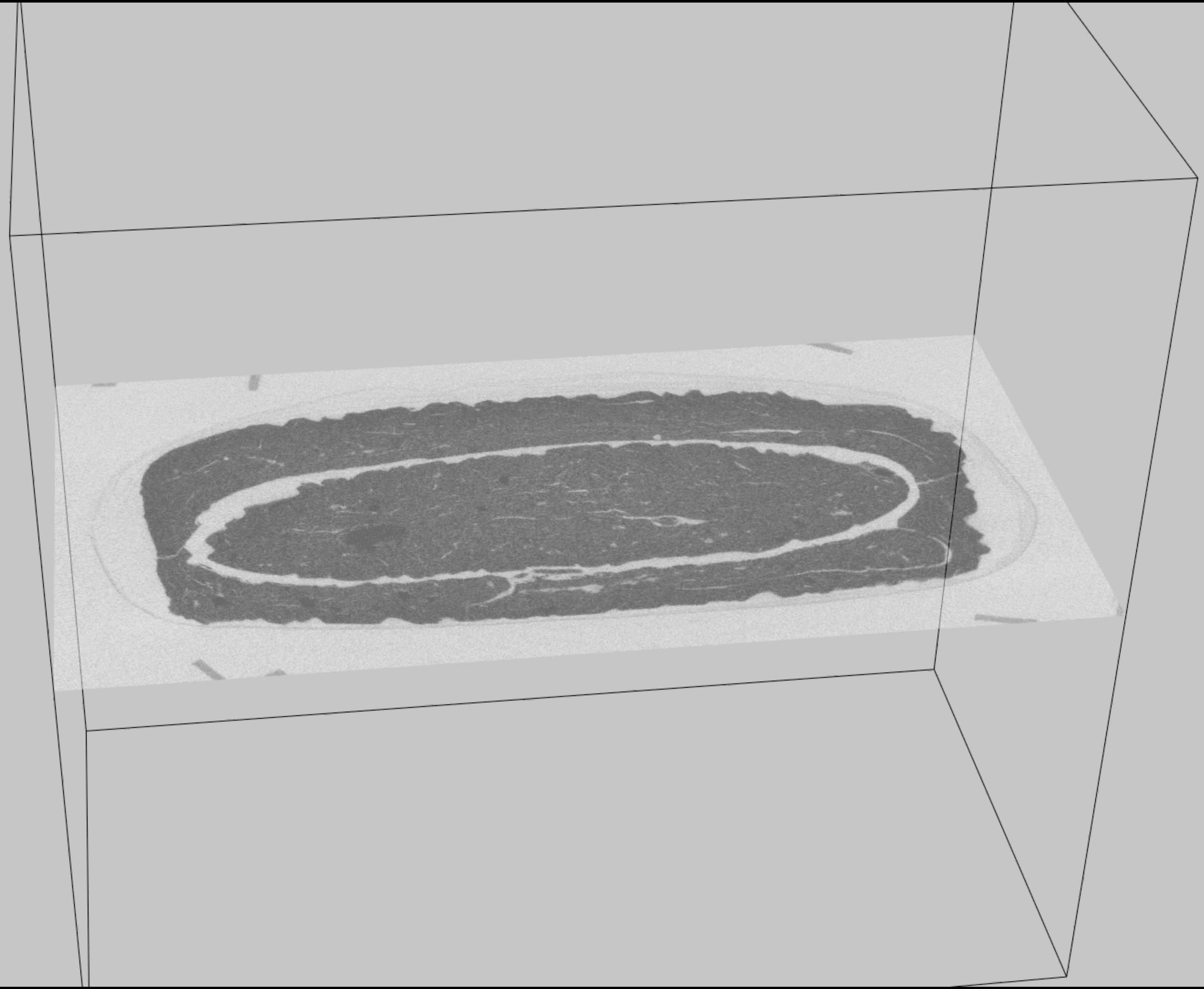

What is written there?

Old Assyrian (ca. 1950 - 1850 B.C.)

Place of discovery:
  Cappadocia, Kanesh

Collection:
  Louvre (Paris), AO 8295

Enlil-bani has loaned 2/3 minas, 2 2/3 shekels and 15 grains (340 g) of refined silver to Assur-malik, son of Uzua. From the week of Iddin-Abum, month 5, year of Enna-Suen, son of Shu-Ishar, within five weeks he will pay. If he has not paid, he will add as interest half a shekel per mina and per month.

Witnesses: Shu-Belum, son of Kulumaya, and Amur-Assur, son of Assur-tab.

Tracking the development of malaria parasites in mosquitoes

High-throughput tomography and AI-supported segmentation enable statistically robust analyses

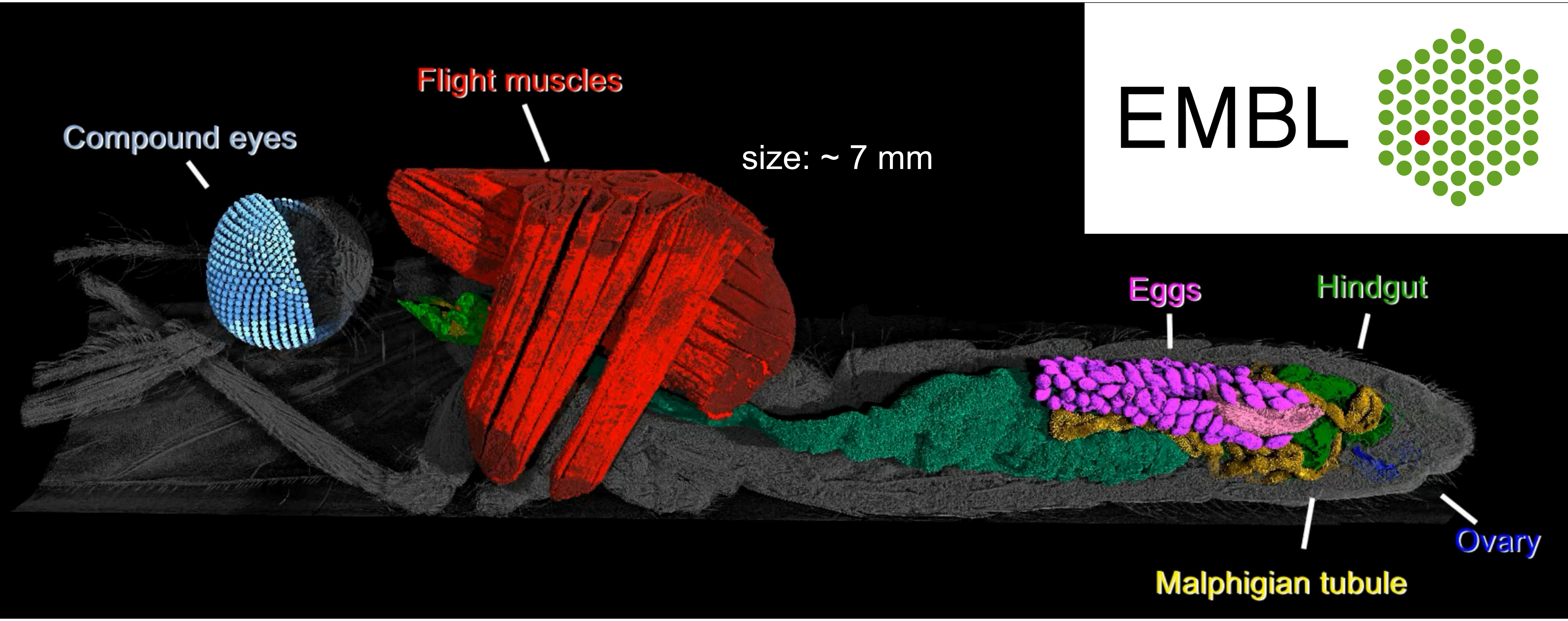

EMBL

High Throughput Tomography 'HiTT' on P14 (PETRA III)

3D X-ray tomography of a mosquito
(*Anopheles stephensi*)

Nedal Darif, Jonas Albers,
Matthew Lawson, Liz Duke

***Plasmodium berghei* infected *Anopheles stephensi* midgut**

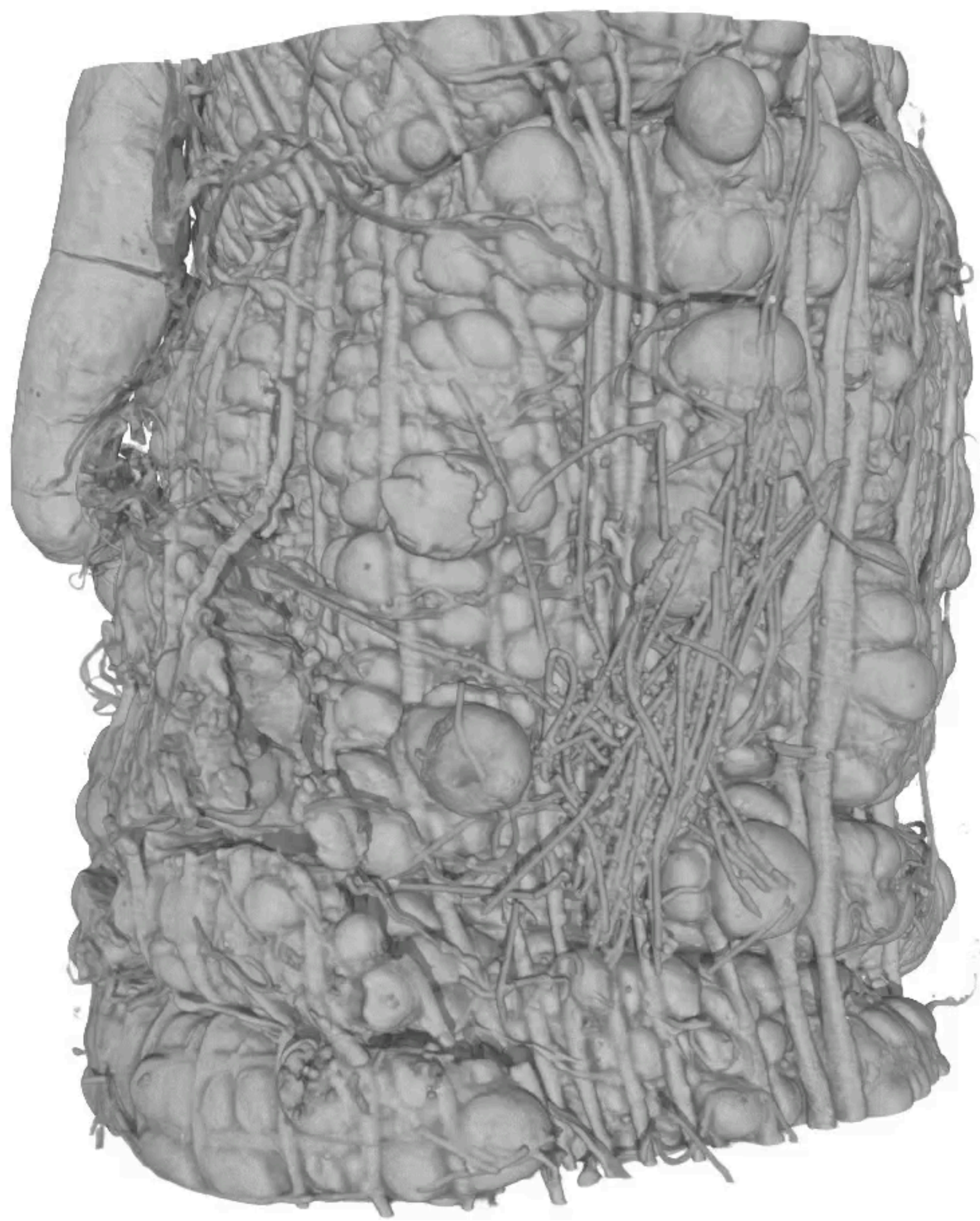

Visualize Catalysts in Action

Methane often wasted during oil production:

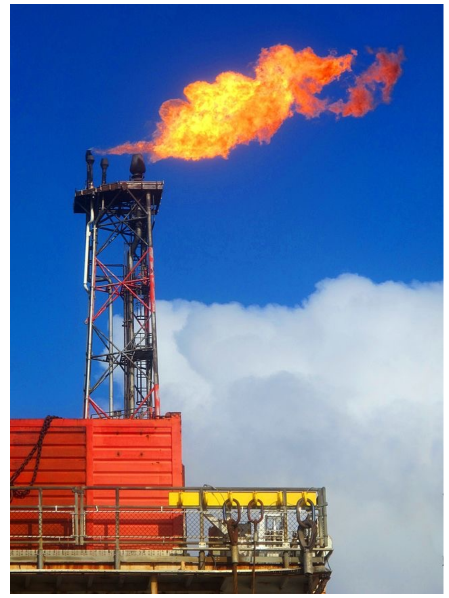

First step to convert methane into liquid fuels (syngas production):

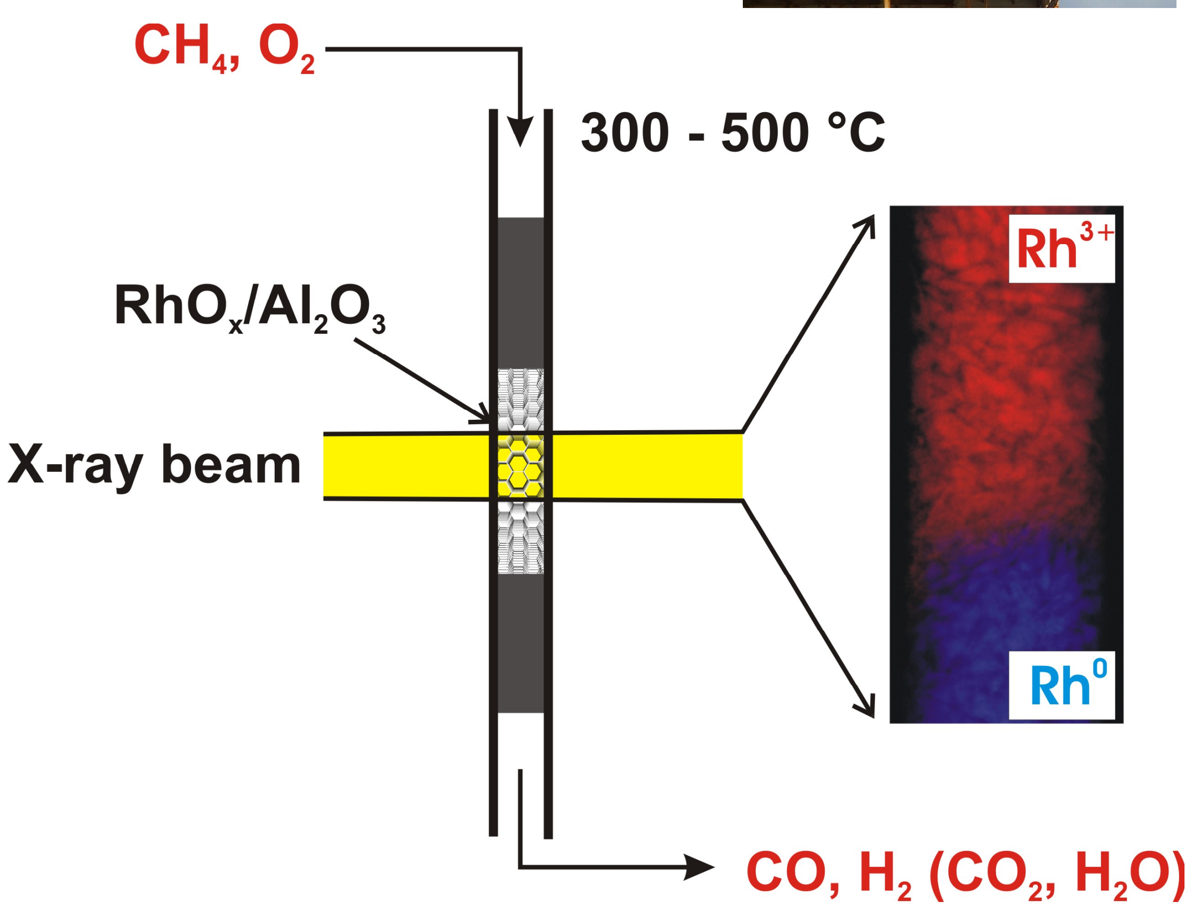


JPCBFK

VOLUME 110
JUNE 15, 2006
NUMBER 23
http://pubs.acs.org/JPCB

THE JOURNAL OF PHYSICAL CHEMISTRY B

2D-Mapping of a Heterogeneous Catalyst inside a Fixed-Bed Reactor by X-Ray Absorption Spectroscopy (see page XXXX)

CONDENSED MATTER, MATERIALS, SURFACES, INTERFACES, & BIOPHYSICAL CHEMISTRY

PUBLISHED WEEKLY BY THE AMERICAN CHEMICAL SOCIETY

Grunwaldt, et al.,
J. Chem. Phys. B **110,** 8674 (2006)

Visualize Catalysts in Action

Methane often wasted during oil production:

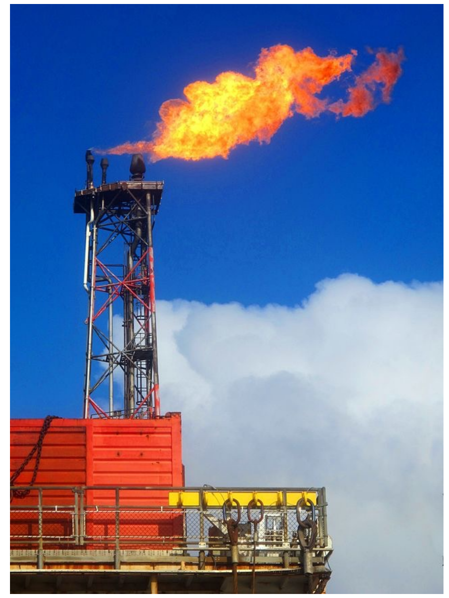

First step to convert methane into liquid fuels (syngas production):

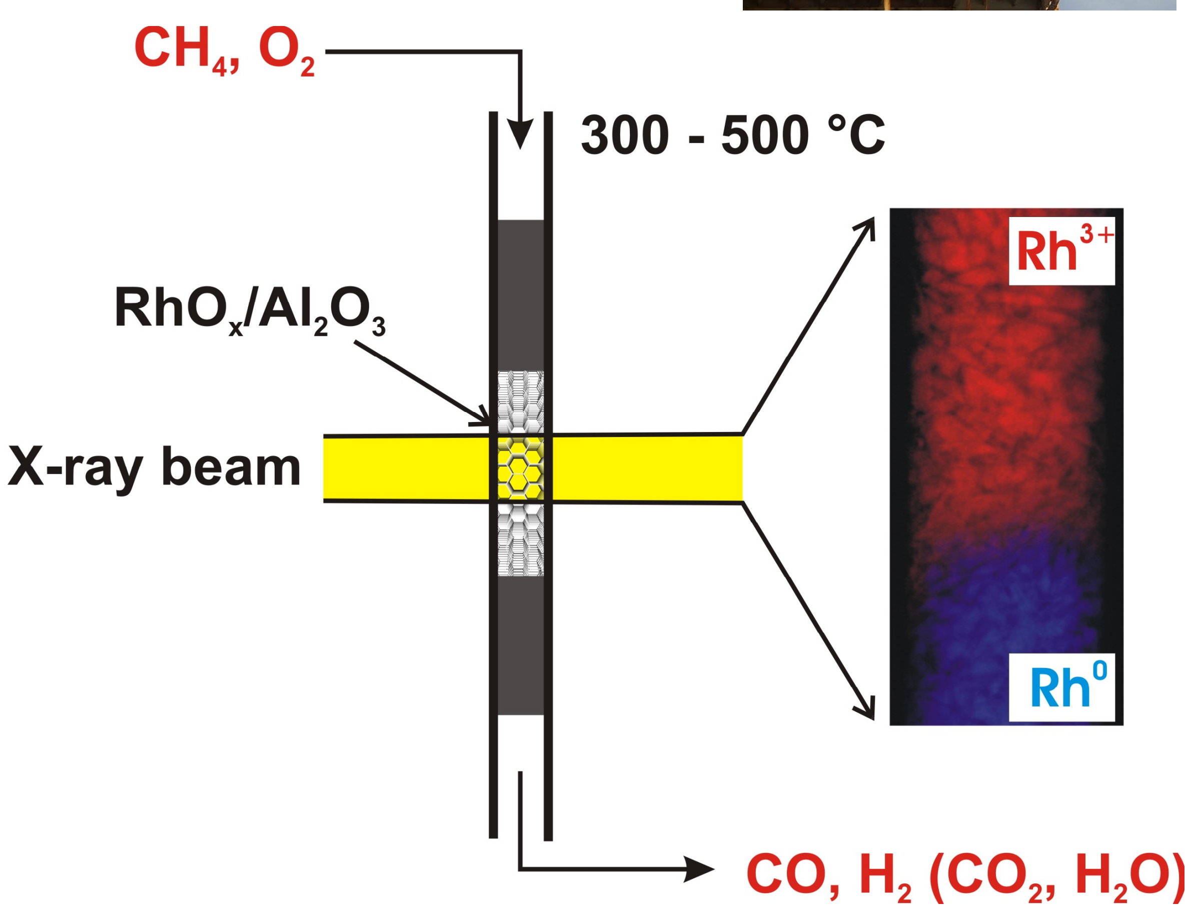

Grunwaldt, et al.,
J. Chem. Phys. B **110,** 8674 (2006)

Combustion of methane:

$$CH_4 + 2O_2 \longrightarrow CO_2 + 2H_2O$$

(exothermal: -801,7kJ/mol)

reforming of methane to H_2:

$$CH_4 + H_2O \xrightarrow{Rh} CO + 3H_2$$

(endothermal: 206.1kJ/mol)

$$CH_4 + CO_2 \xrightarrow{Rh} 2CO + 2H_2$$

(endothermal: 247,5kJ/mol)

potentially other reaction:
direct partial oxidation:

$$2CH_4 + O_2 \xrightarrow{Rh} 2CO + 8H_2$$

(exothermal: -35,5kJ/mol)

X-Ray Absorption: Lambert-Beer Law

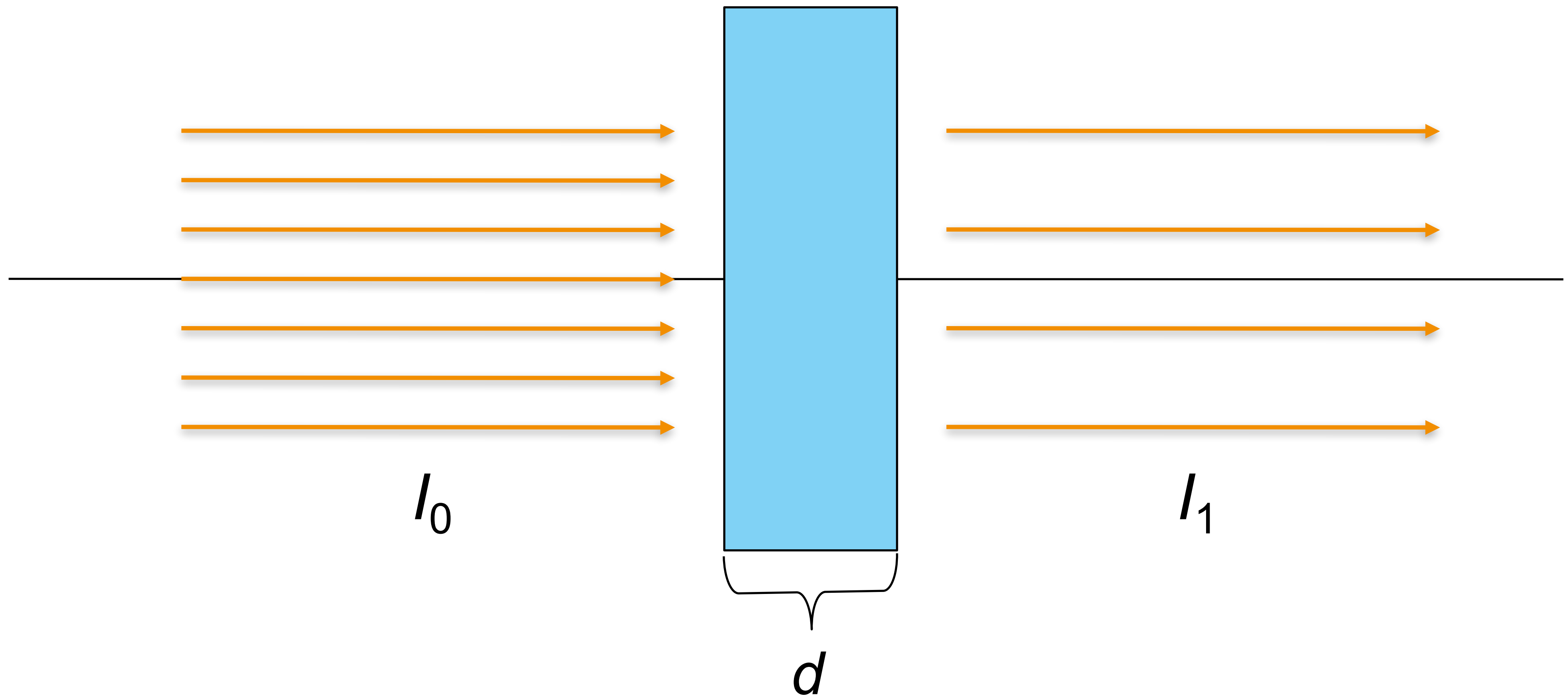

$$I_1(E) = I_0(E) \cdot \exp\left[-\mu(E)d\right]$$

$\mu(E)$: linear attenuation coefficient

$$\mu(E) \cdot d = \ln\left(\frac{I_0}{I_1}\right)$$

Photo Absorption

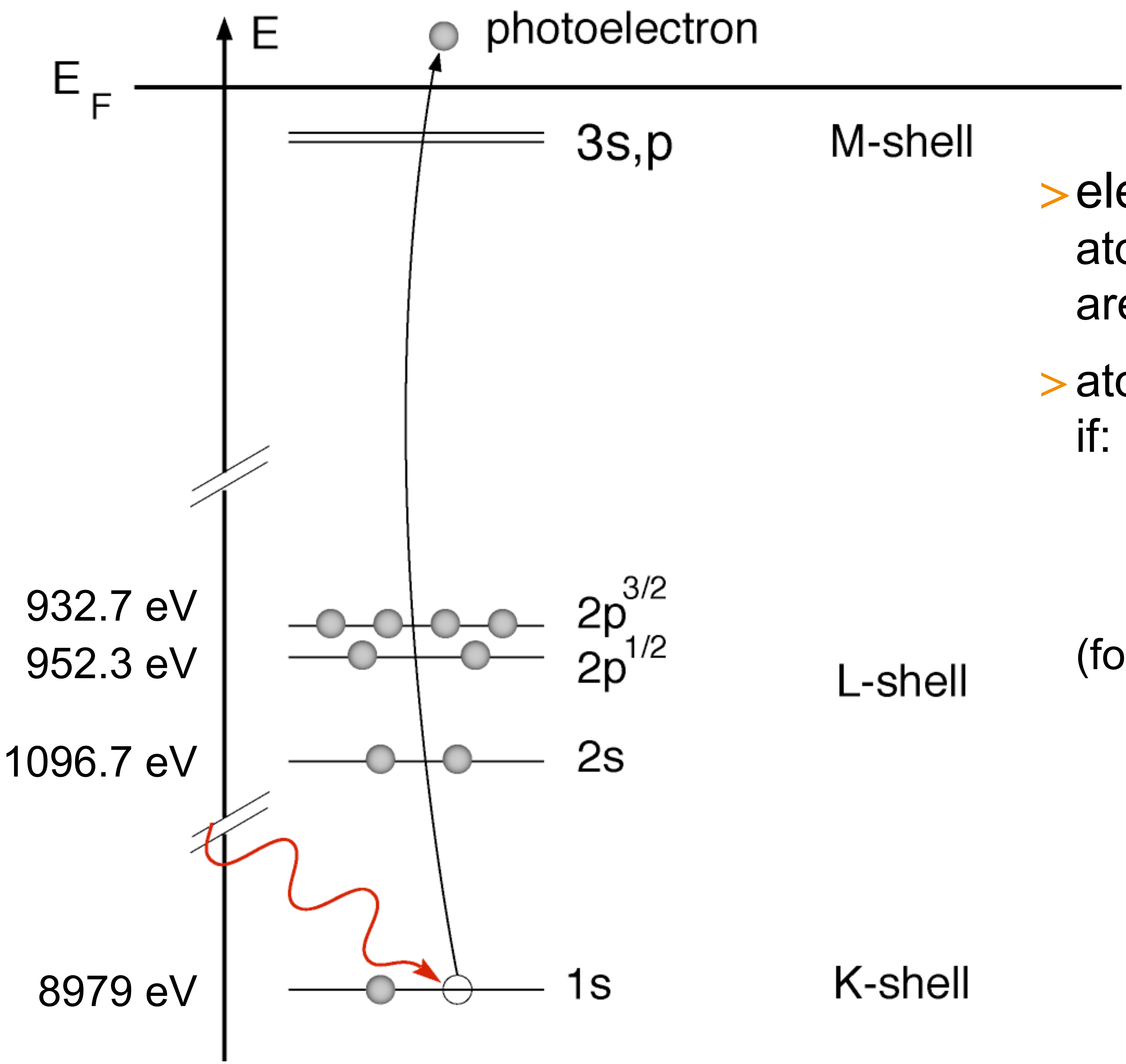

- electrons populate specific atomic states: binding energies are atom specific: K, L, M
- atom can absorb x-ray photon if:

$$E_{photon} > E_{ionization}$$

(follows from Pauli principle)

Example: Absorption in Cu & Ag

μ(E): linear attenuation coefficient

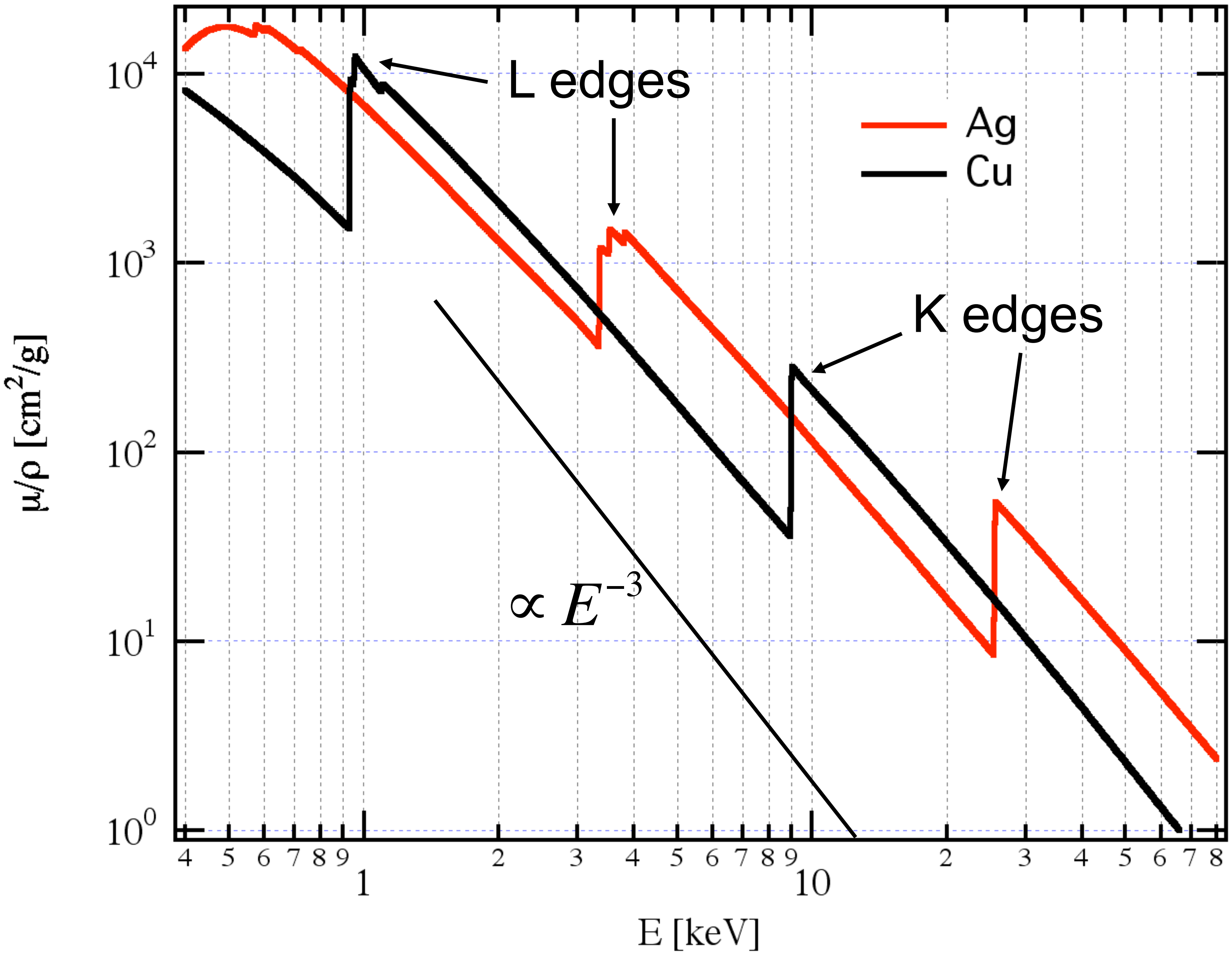

- mainly atomic effect
- strong dependence on x-ray energy:

$$\propto E^{-2.78}$$

- strong dependence on atomic number:

$$\propto Z^{2.7}$$

- largest contribution from inner shells

Example: Absorption in Cu

μ(E): linear attenuation coefficient

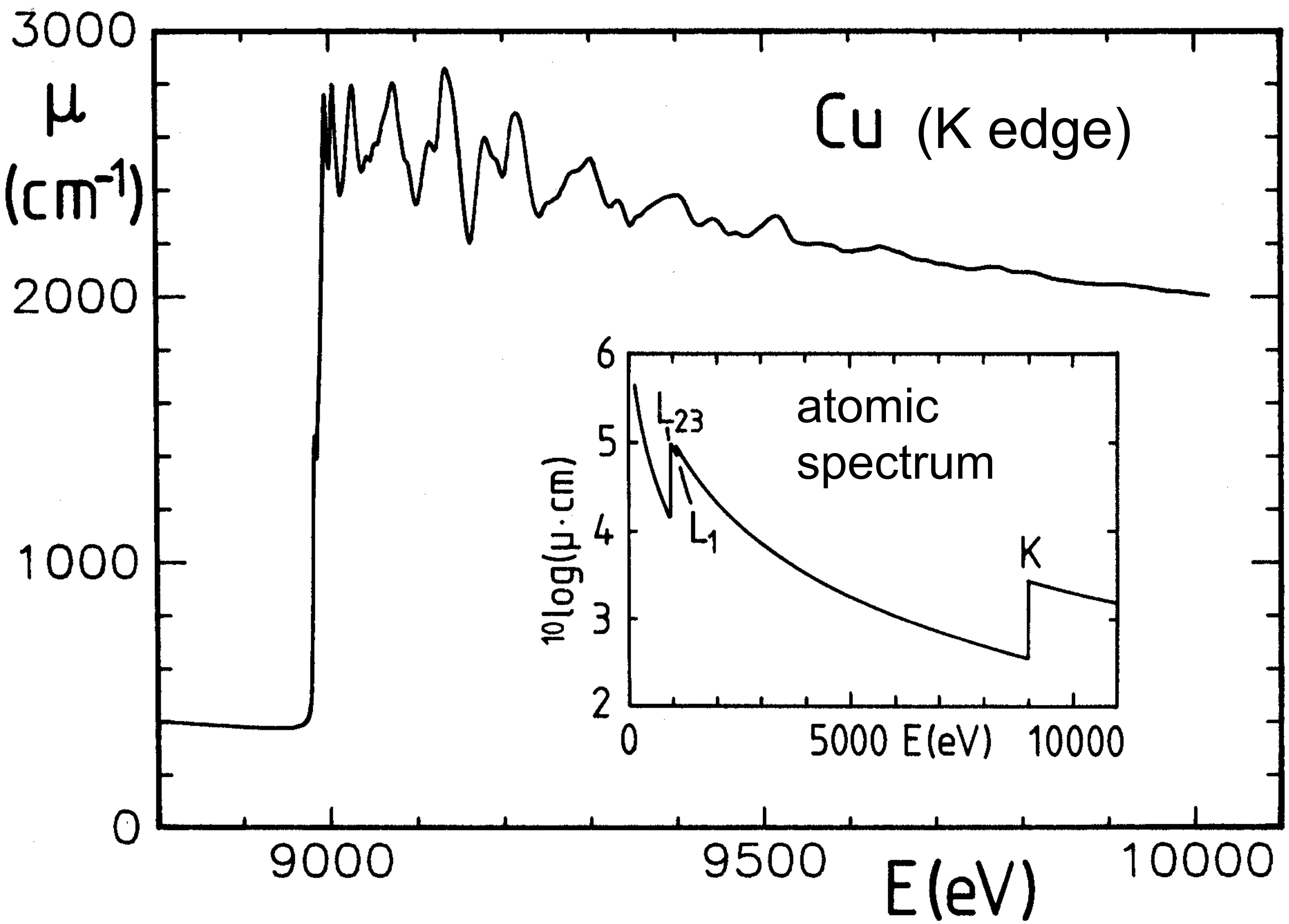

Metallic Cu:

mainly atomic effect

fine structure in solid:
X-ray Absorption Fine Stucture

X-ray Absorption Spectrum

Three characteristic features:

> Energy of absorption edge: oxidation state

> Near-edge region: (XANES: x-ray absorption near edge structure) local, projected density of states

> Extended fine structure: (EXAFS: extended x-ray absorption fine structure) local chemical environment of atomic species

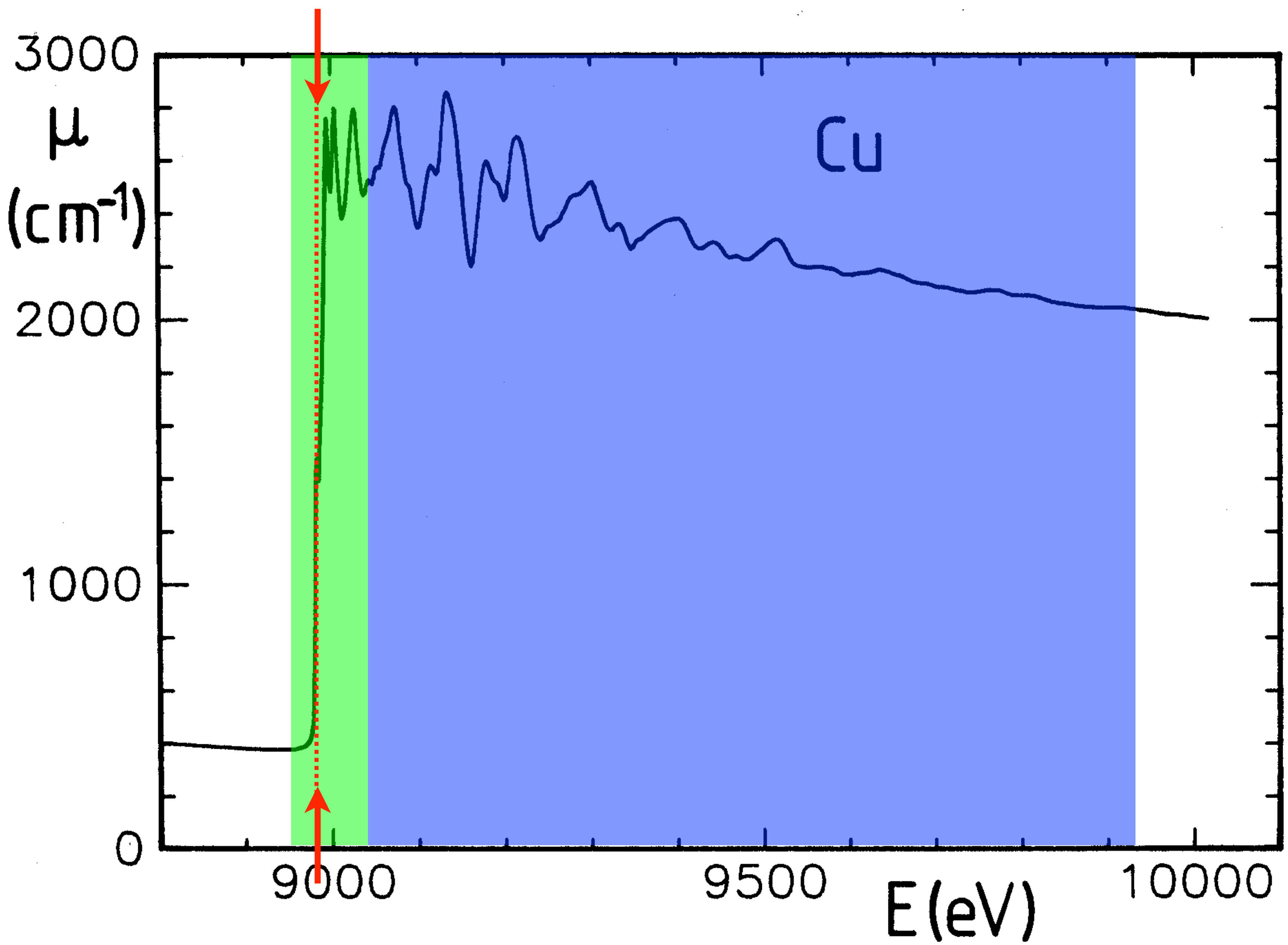

Energy of Absorption Edge

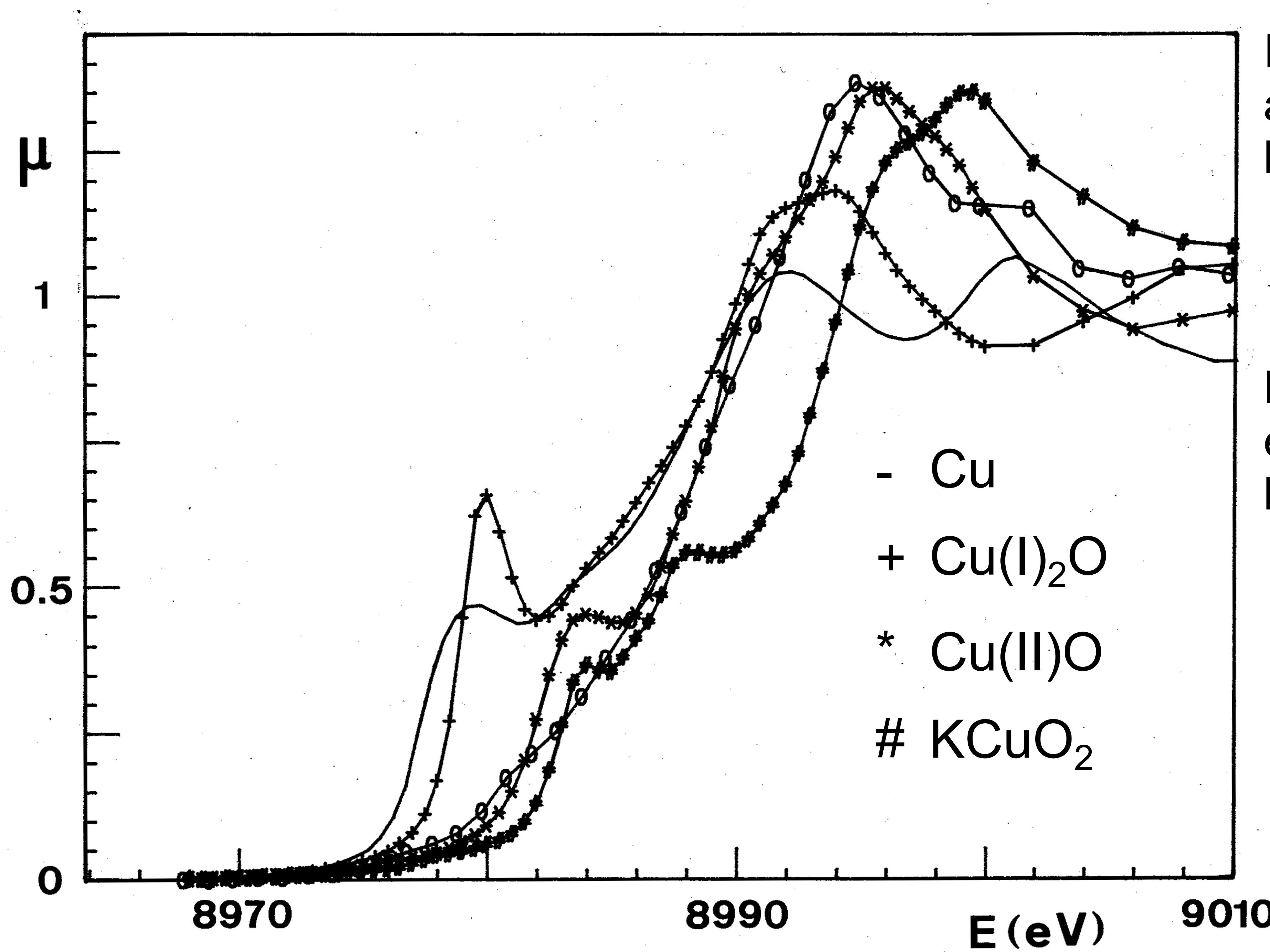

Increasing oxidation state: absorption edge shifts to higher x-ray energies

Reduced screening of electric field of nucleus by valence electrons:

other electrons more tightly bound!

Shape of Near-Edge Spectrum

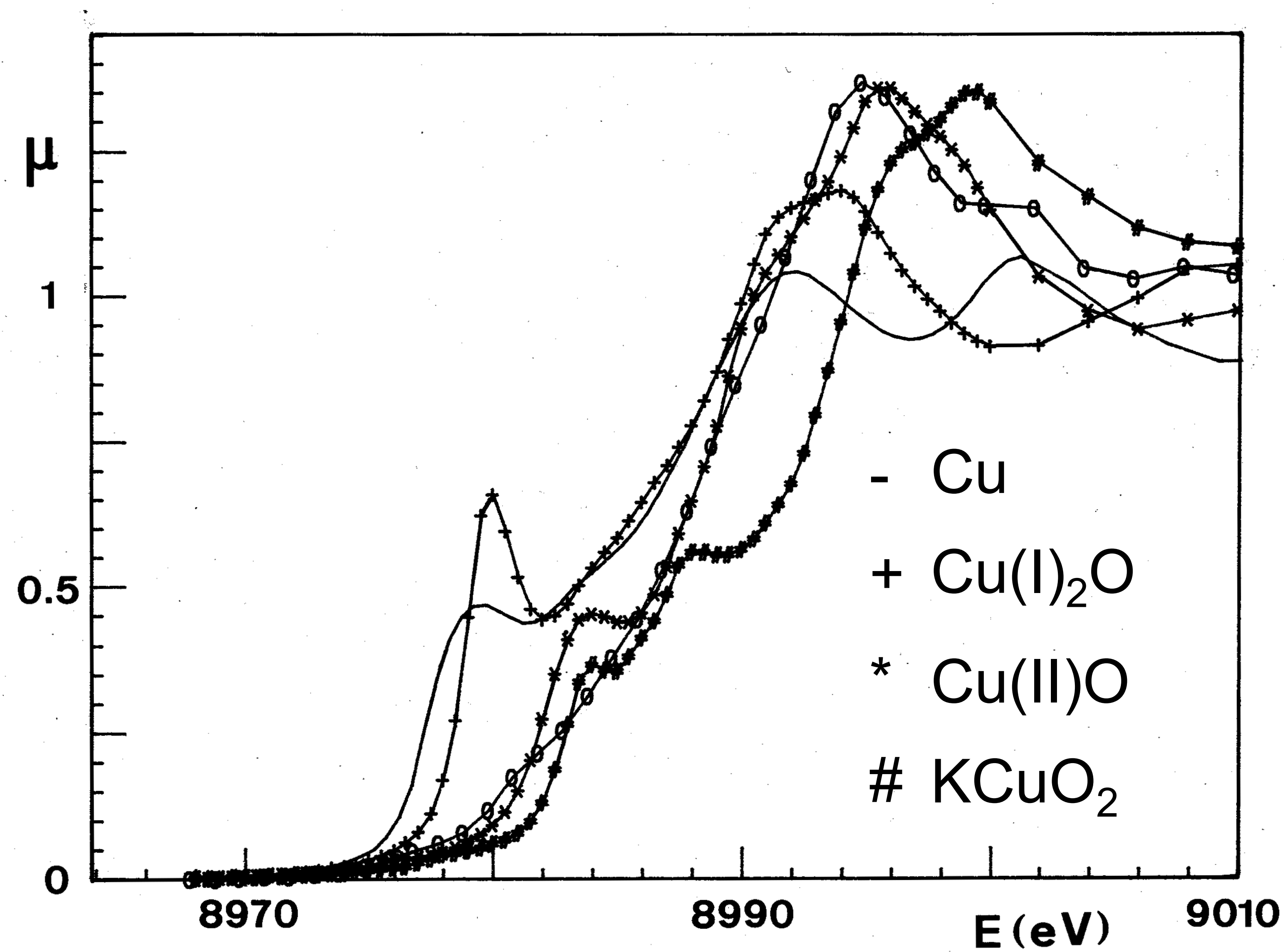

depends on density of states available to photoelectron

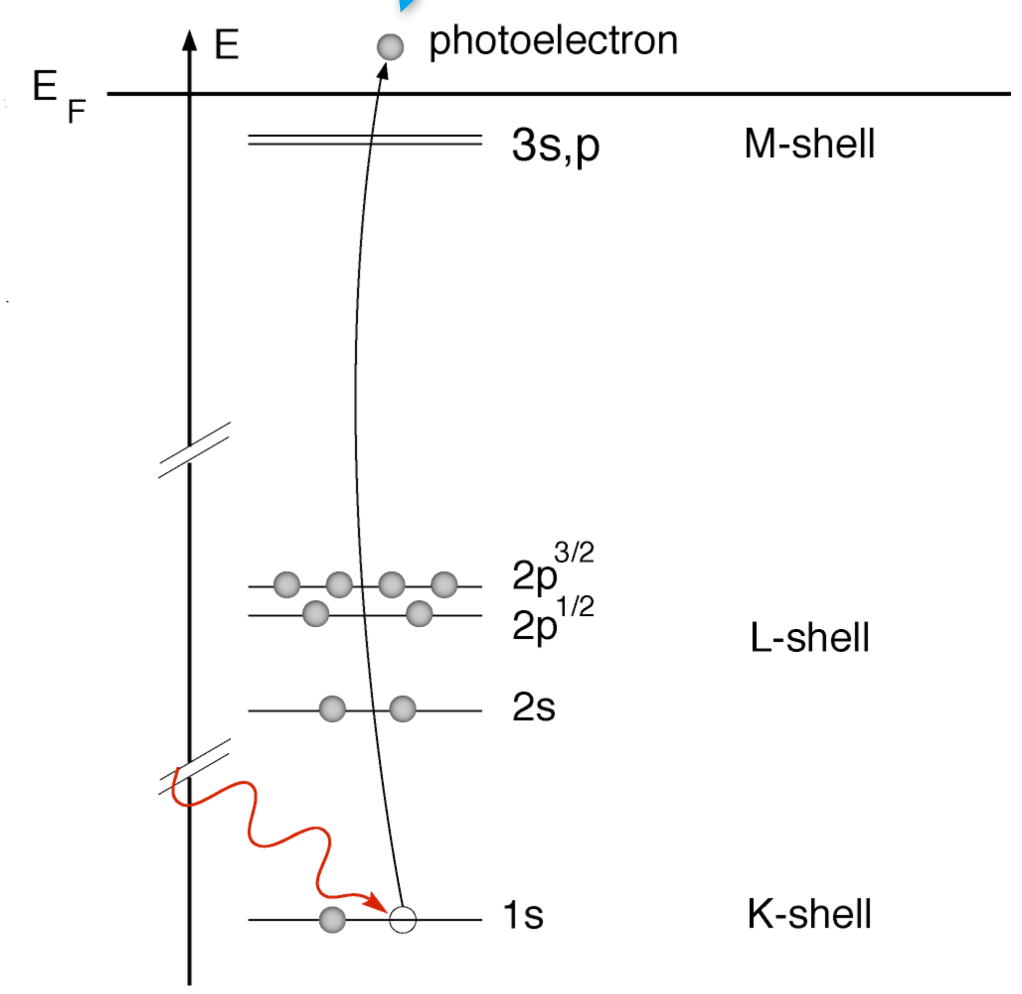

Shape of spectrum:

- can be modeled by methods in theoretical solid state physics
- can be used as „fingerprint“ to identify a given chemical environment

Visualize Catalysts in Action

Methane often wasted during oil production:

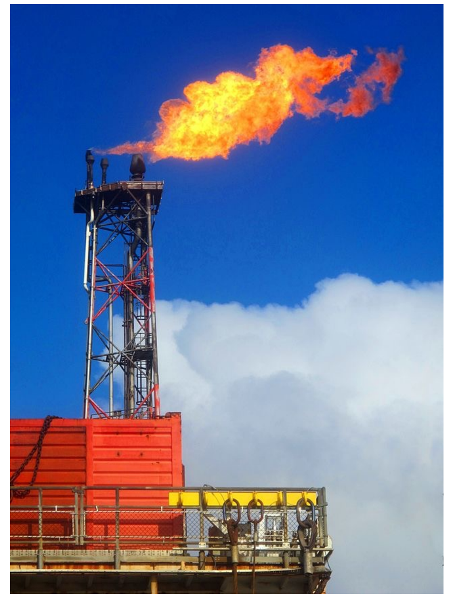

First step to convert methane into liquid fuels (syngas production):

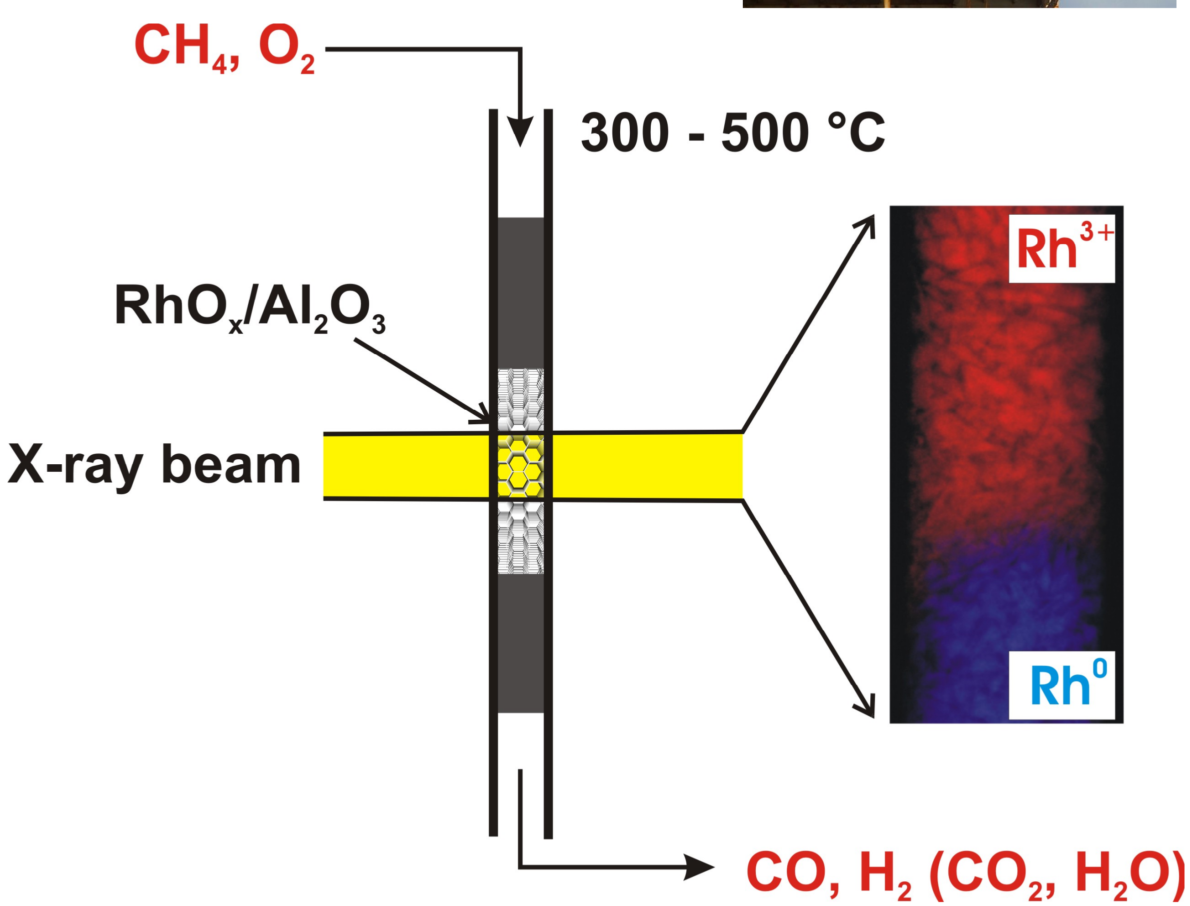

Grunwaldt, et al.,
J. Chem. Phys. B **110,** 8674 (2006)

Combustion of methane:

$$CH_4 + 2O_2 \longrightarrow CO_2 + 2H_2O$$

(exothermal: -801,7kJ/mol)

reforming of methane to H_2:

$$CH_4 + H_2O \xrightarrow{Rh} CO + 3H_2$$

(endothermal: 206.1kJ/mol)

$$CH_4 + CO_2 \xrightarrow{Rh} 2CO + 2H_2$$

(endothermal: 247,5kJ/mol)

potentially other reaction:
direct partial oxidation:

$$2CH_4 + O_2 \xrightarrow{Rh} 2CO + 8H_2$$

(exothermal: -35,5kJ/mol)

Visualize Catalysis

In-situ transmission imaging of catalyst bed inside chemical reactor

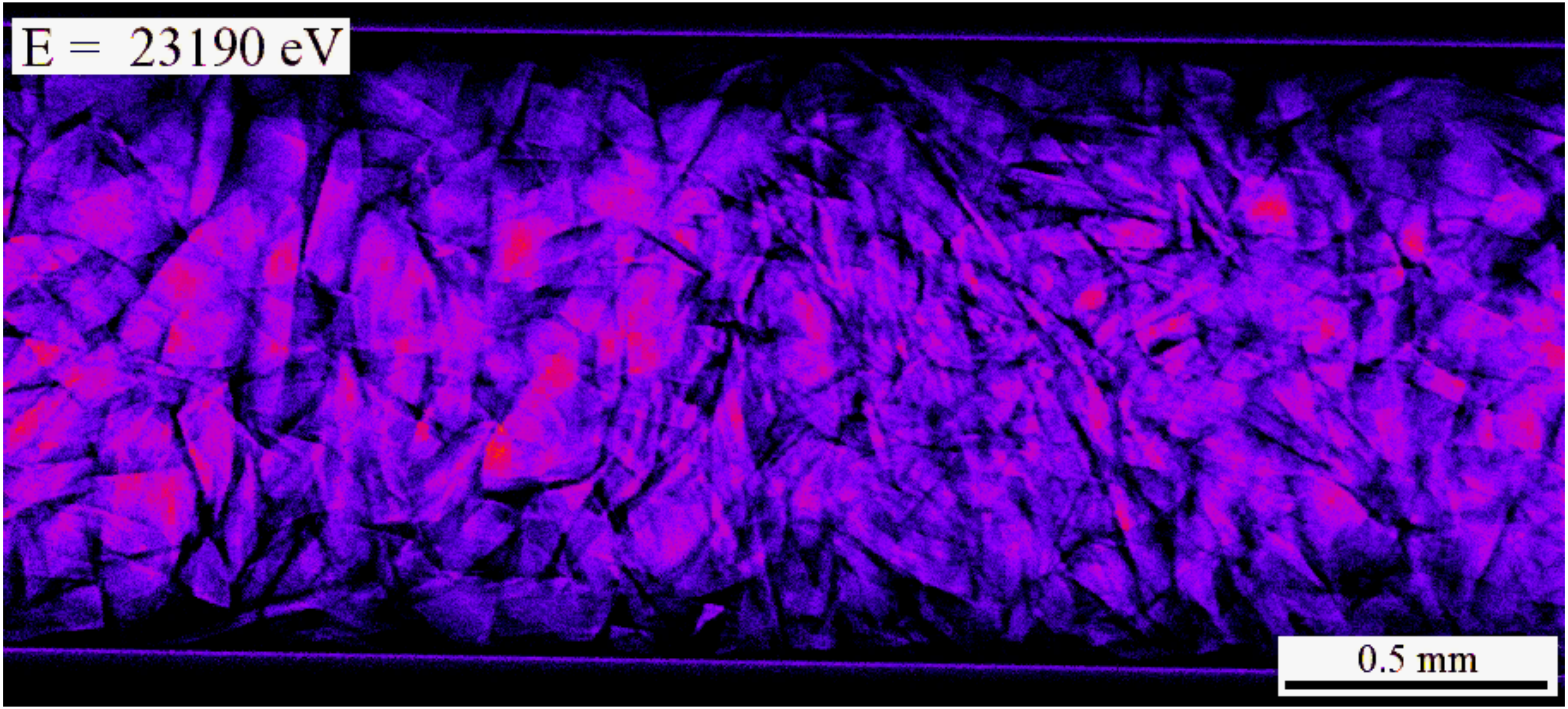

Grunwaldt, et al.,
J. Chem. Phys. B **110,** 8674 (2006)

Visualize Catalysis

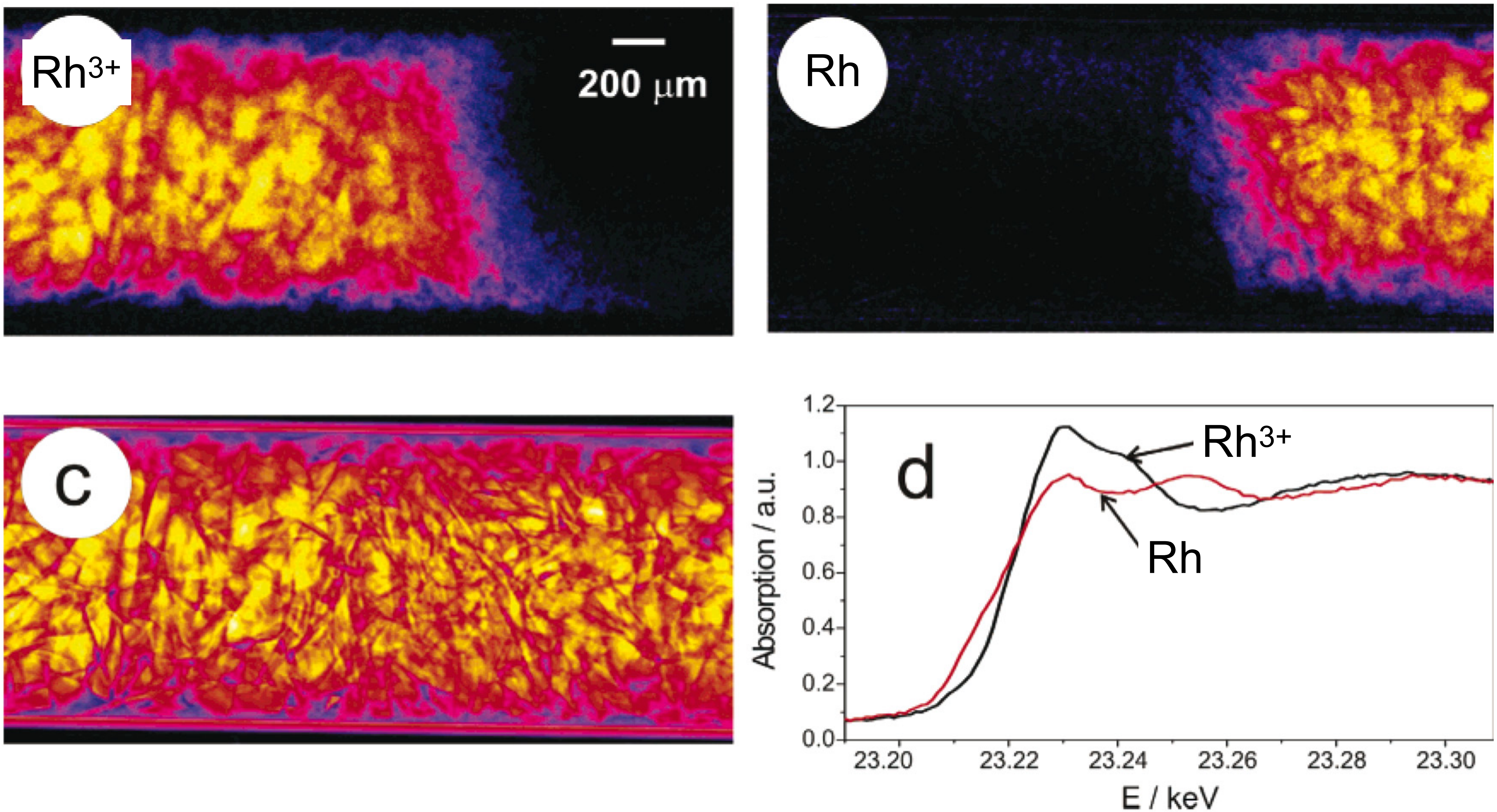

Grunwaldt, et al.,
J. Chem. Phys. B **110,** 8674 (2006)

Visualize Catalysis

$$2\ CH_4 + O_2 \rightarrow 2\ CO + 4\ H_2$$

direction of flow

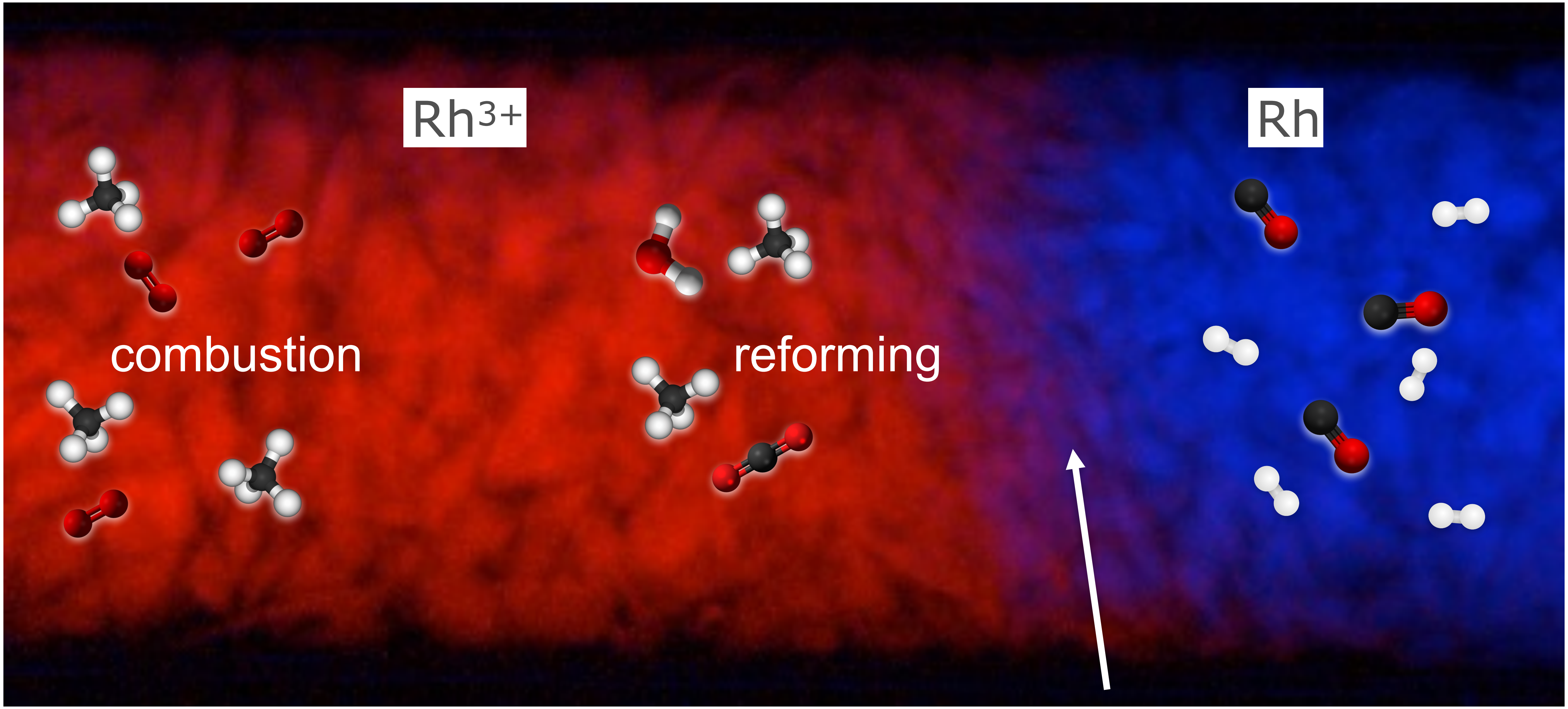

production of hydrogen
Rh is reduced!

Grunwaldt, et al.,
J. Chem. Phys. B **110,** 8674 (2006)

Scanning Microscopy and Tomography: Nanoprobe

X rays are focused onto the sample

raster scan sample through beam:

→ get x-ray analytical information locally and on nanoscale (resolution limited by focus size).

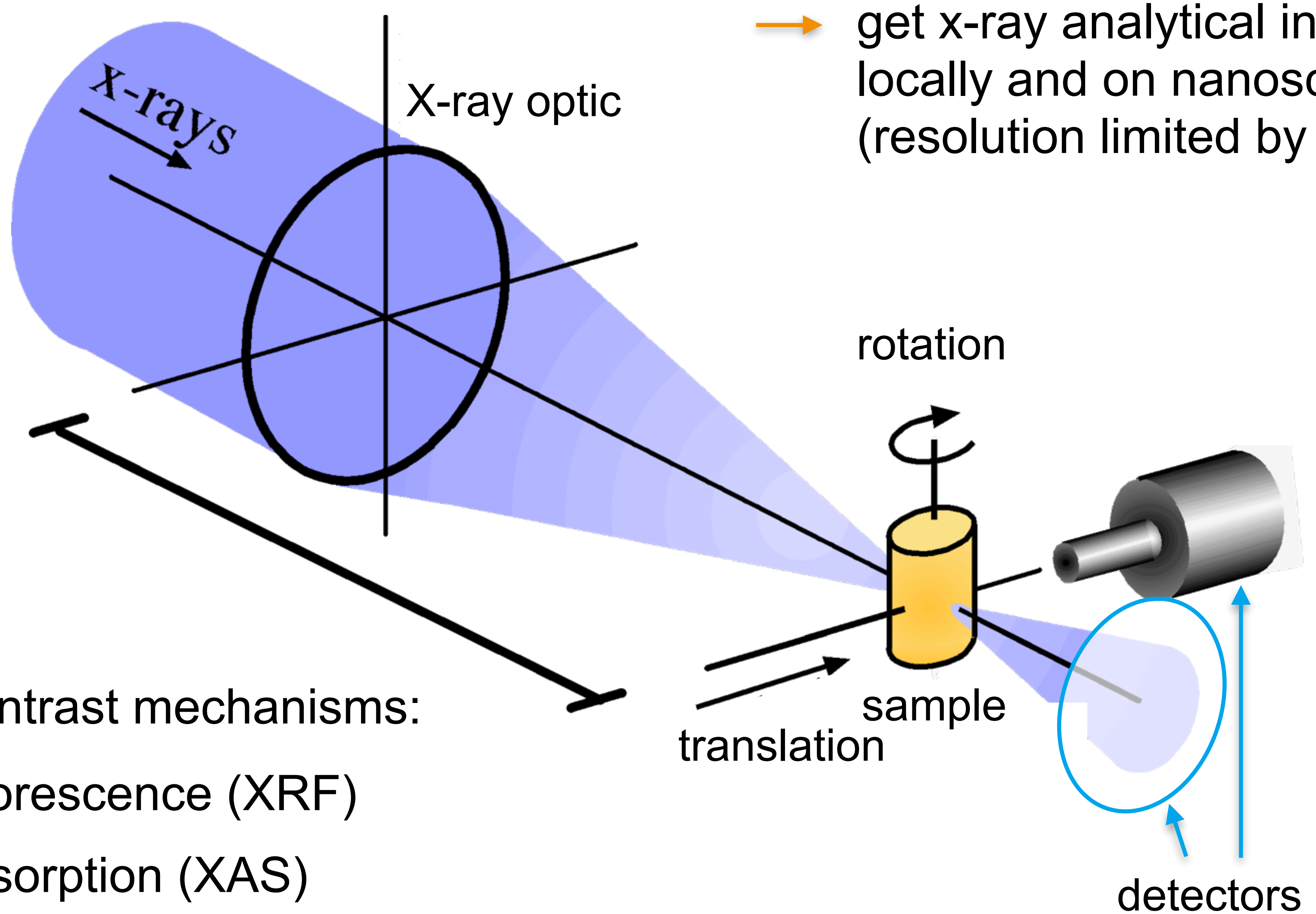

different contrast mechanisms:

- x-ray fluorescence (XRF)
- x-ray absorption (XAS)
- x-ray diffraction (XRD, SAXS, WAXS)
- maybe in future even IXS (RIXS)
- …

X-Ray Scanning Microscopy and Tomography

> Fluorescence microtomography

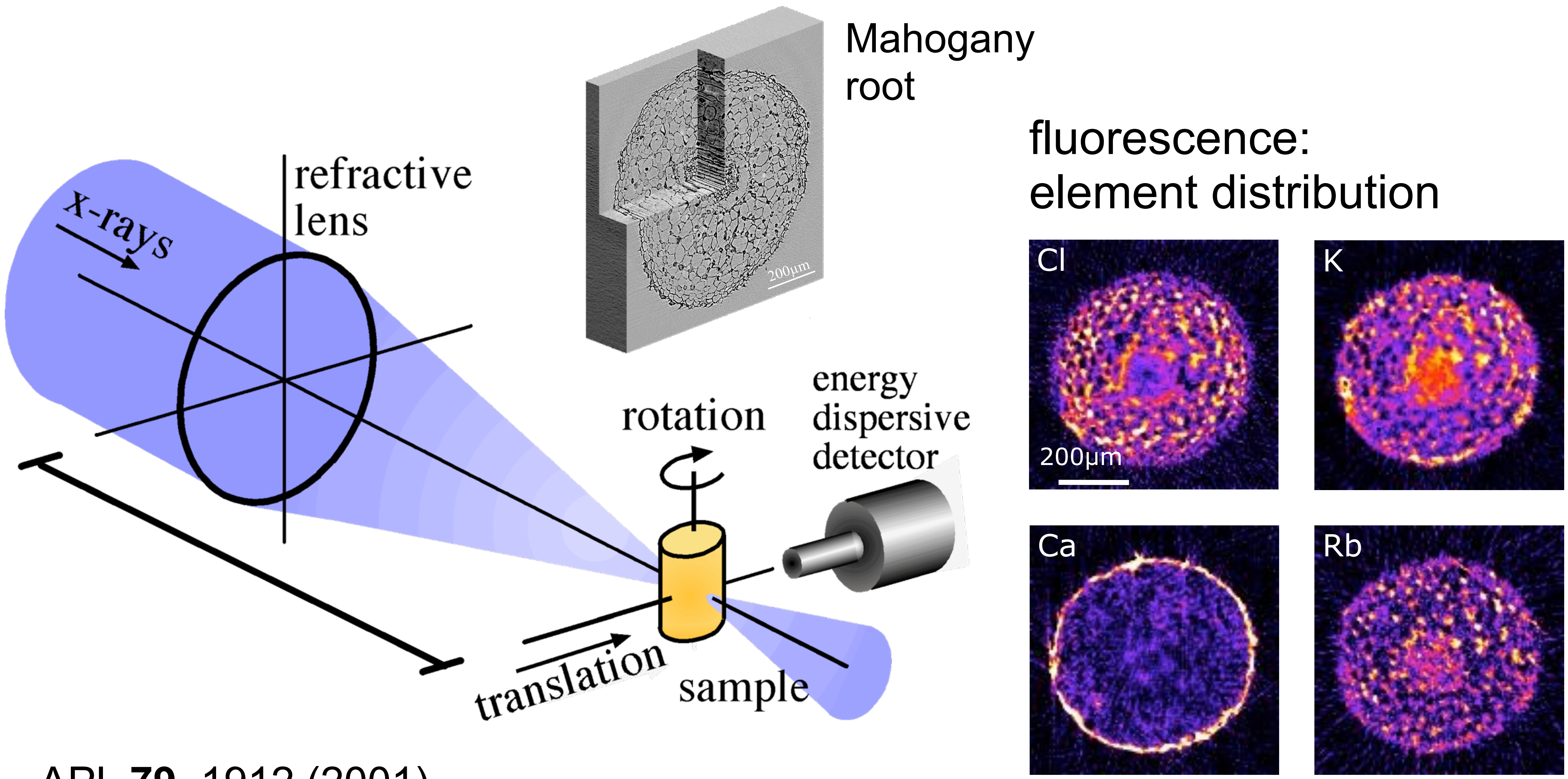

APL **79**, 1912 (2001).

X-Ray Scanning Microscopy and Tomography

- Fluorescence microt

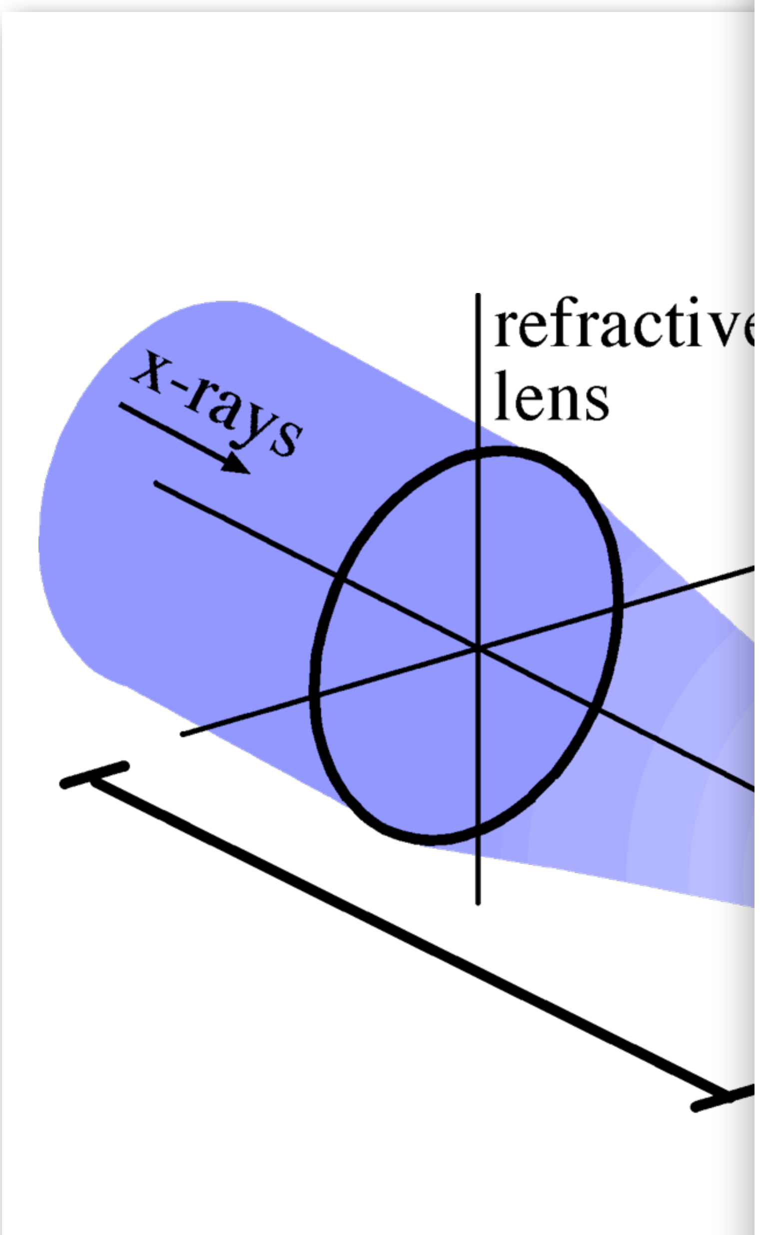

APL **79**, 1912 (2001).

Full fluorescence tomogram of zebra fish embryo

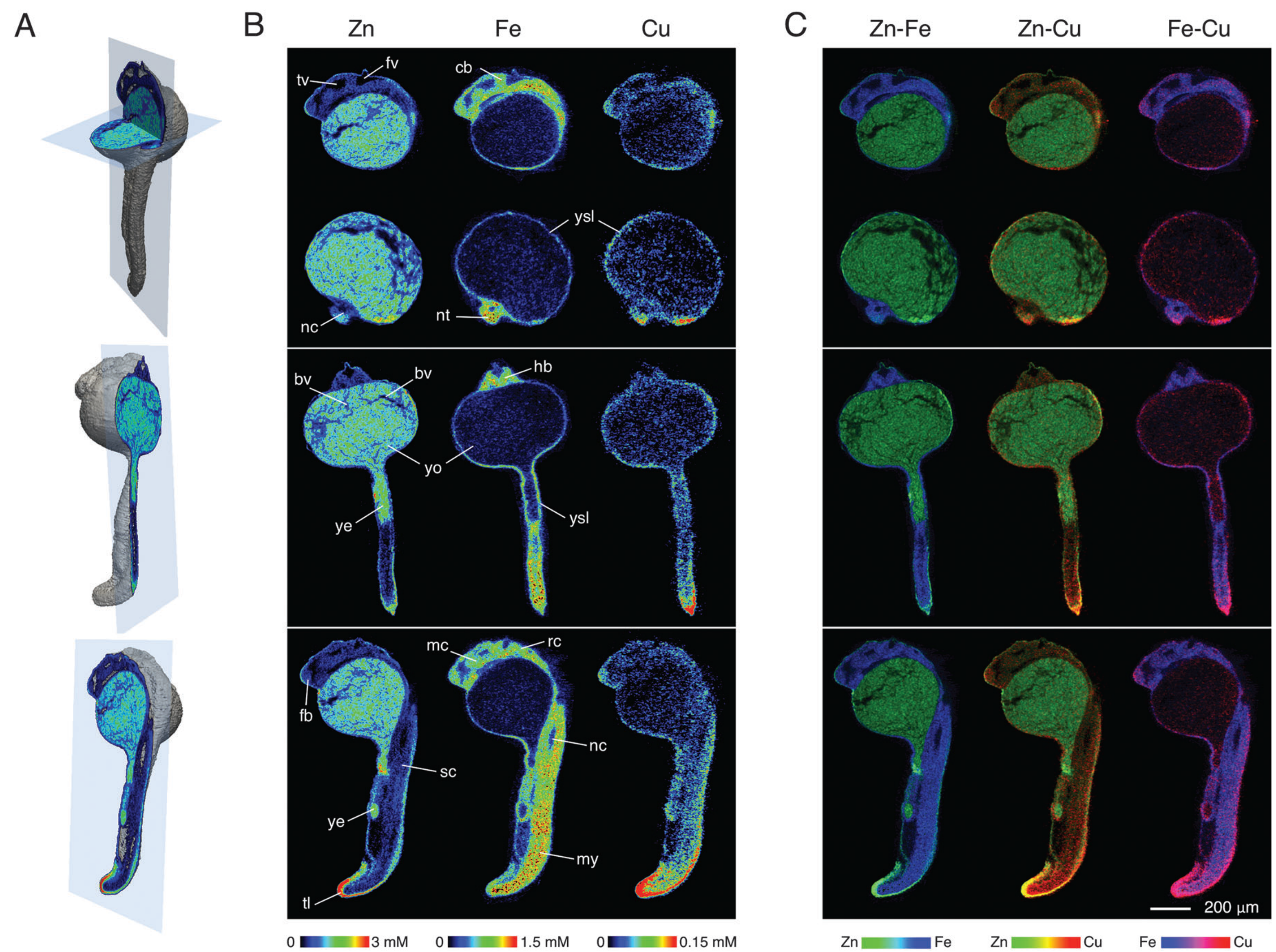

D. Bourassa, et al., Metallomics 6, 1648 (2014).

X-Ray Scanning Microscopy and Tomography

> Fluorescence microtomography
> Tomographic absorption spectroscopy (XANES tomography)

Absorption spectroscopic tomography
distribution of chemical states

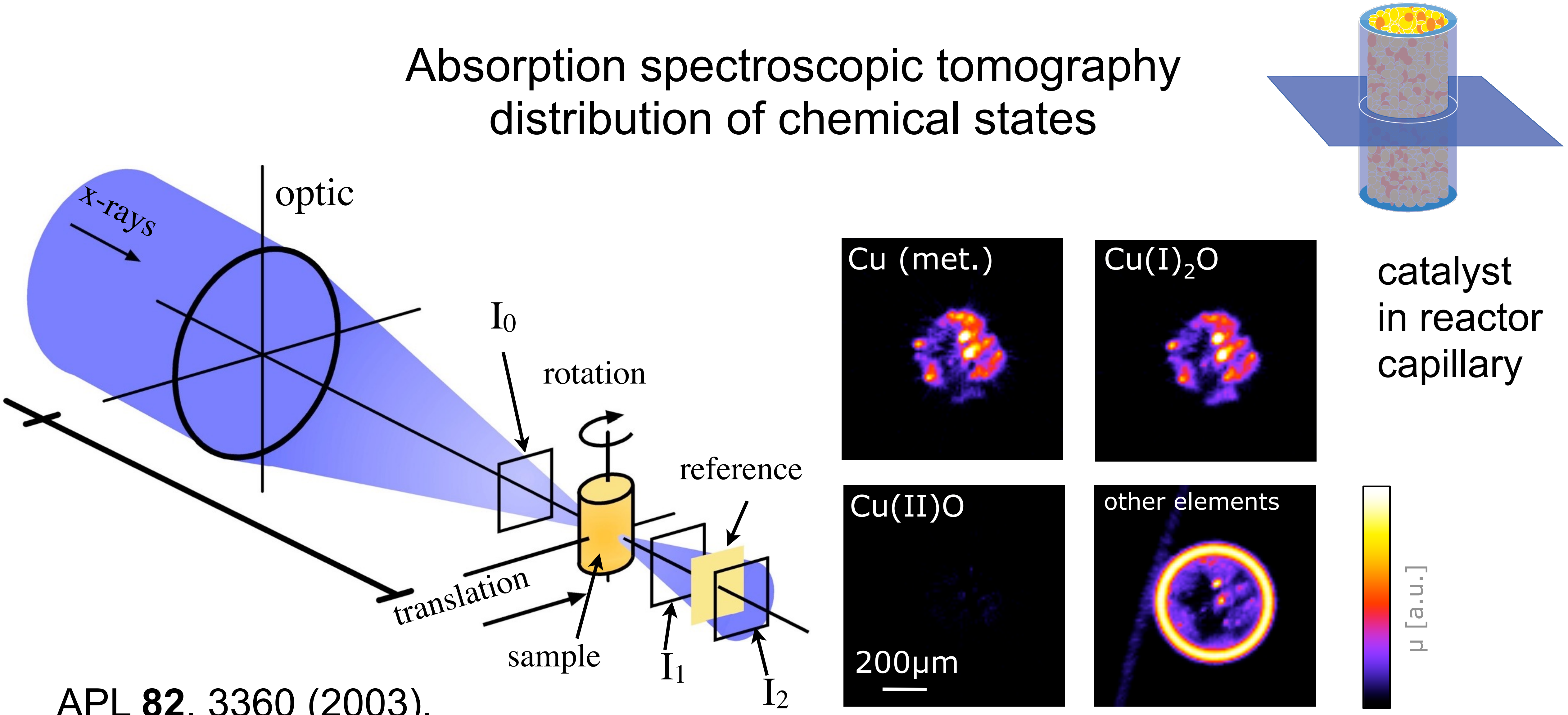

APL **82**, 3360 (2003).

X-Ray Scanning Microscopy and Tomography

- > Fluorescence microtomography
- > Tomographic absorption spectroscopy (XANES tomography)
- > Small-angle x-ray scattering tomography (SAXS tomography)

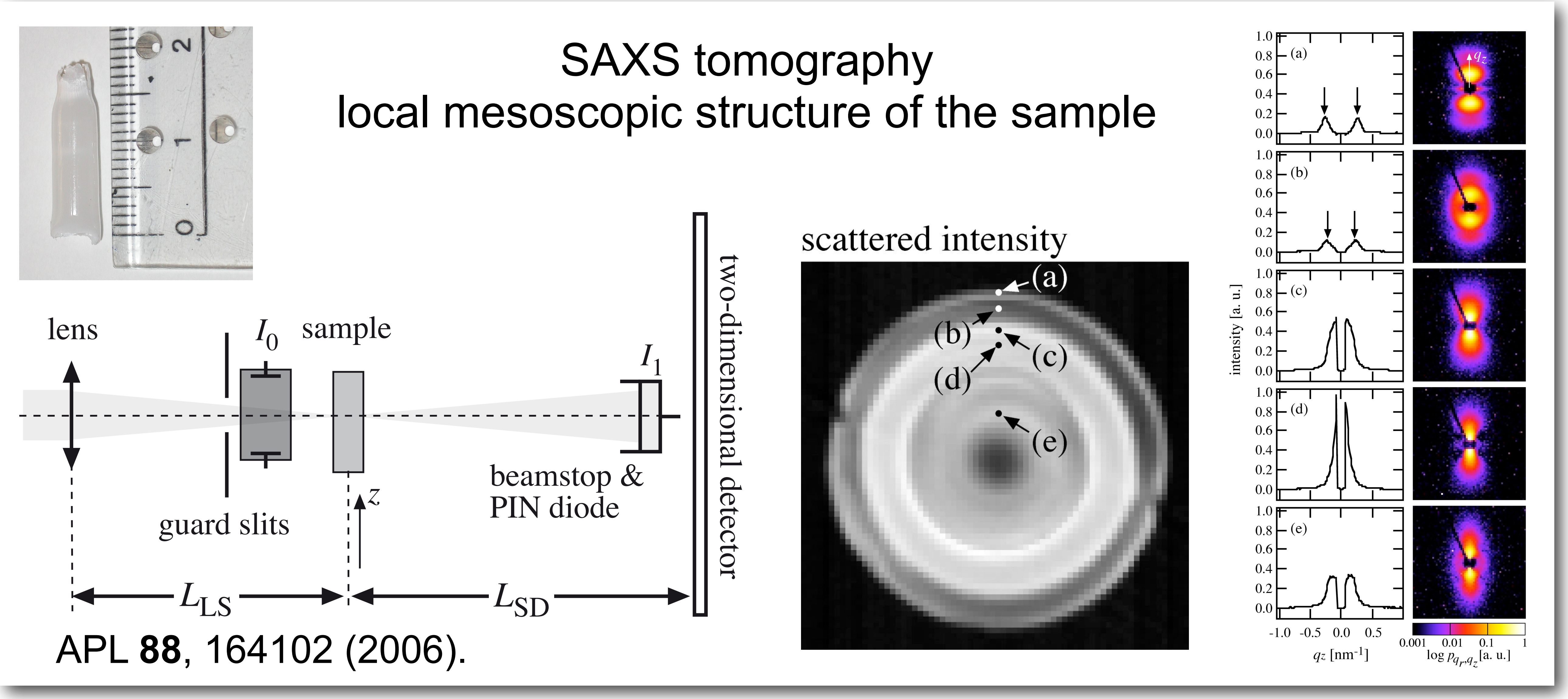

X-Ray Scanning Microscopy and Tomography

> Fluorescence microtomography
> Tomographic absorpti
> Small-angle x-ray sca

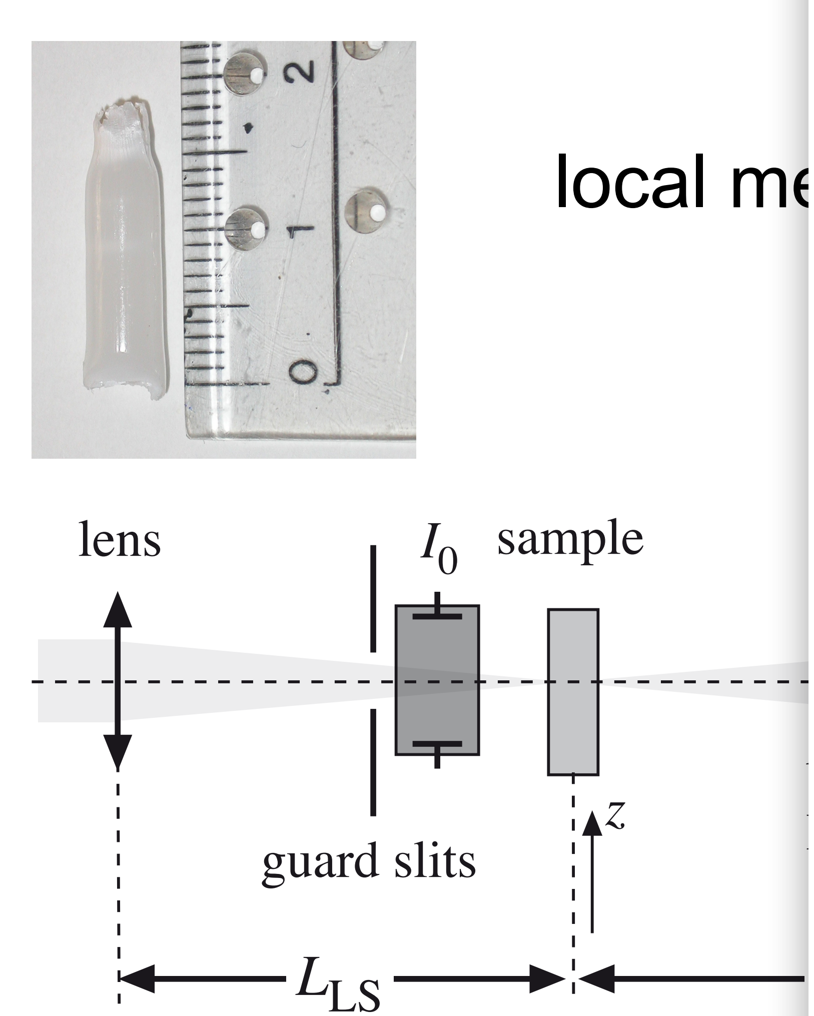

APL **88**, 164102 (2006).

Wide-Angle-X-Ray-Scattering (WAXS) Tomography

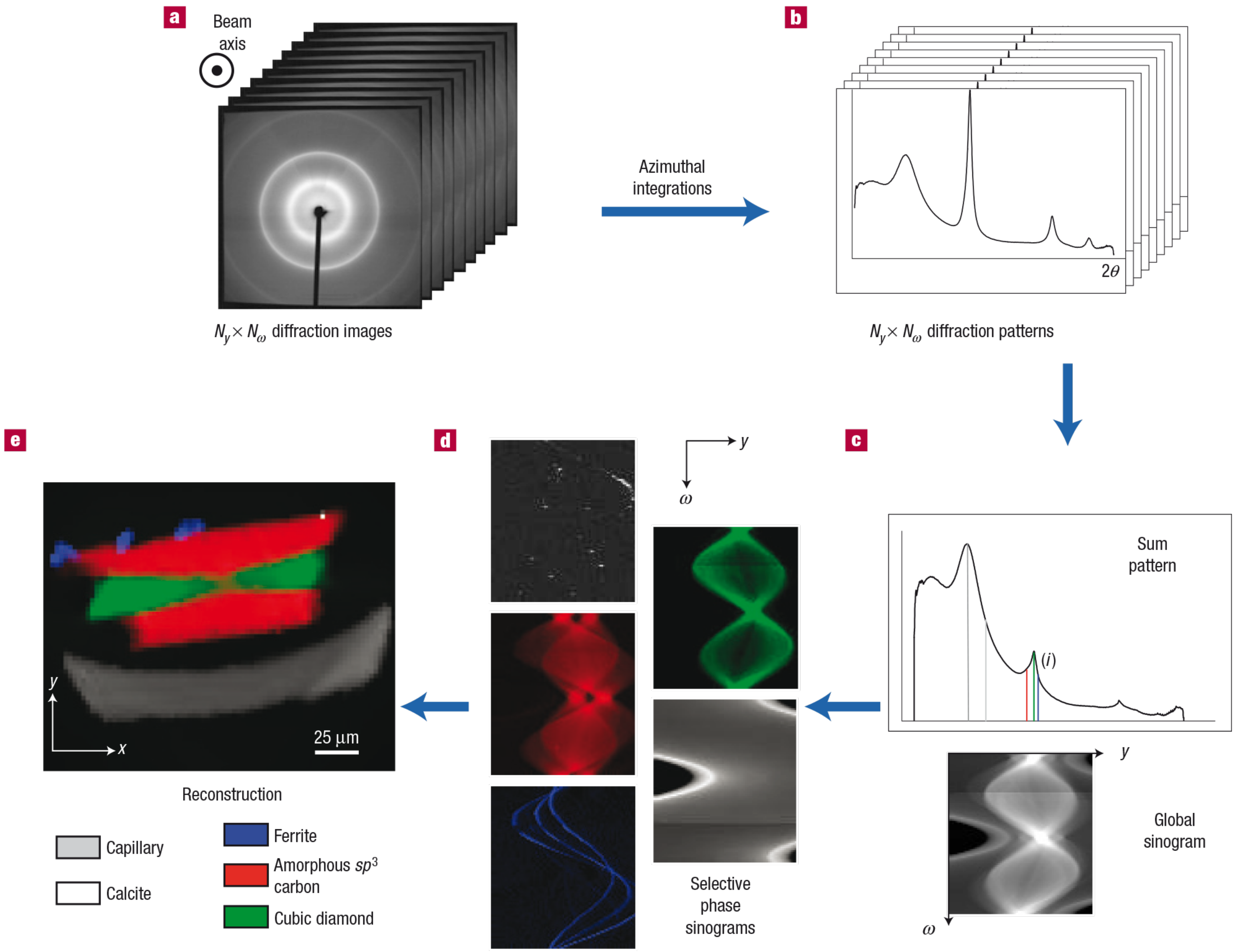

P. Bleuet, et al., Nat. Materials **7**, 468 (2008).

Scanning Microscopy with Hard X-Rays

Source is imaged onto the sample to create an intensive micro-/nanobeam:

Focus size and shape determined by:

- source size
- demagnification L_2/L_1
- diffraction limit
- aberrations

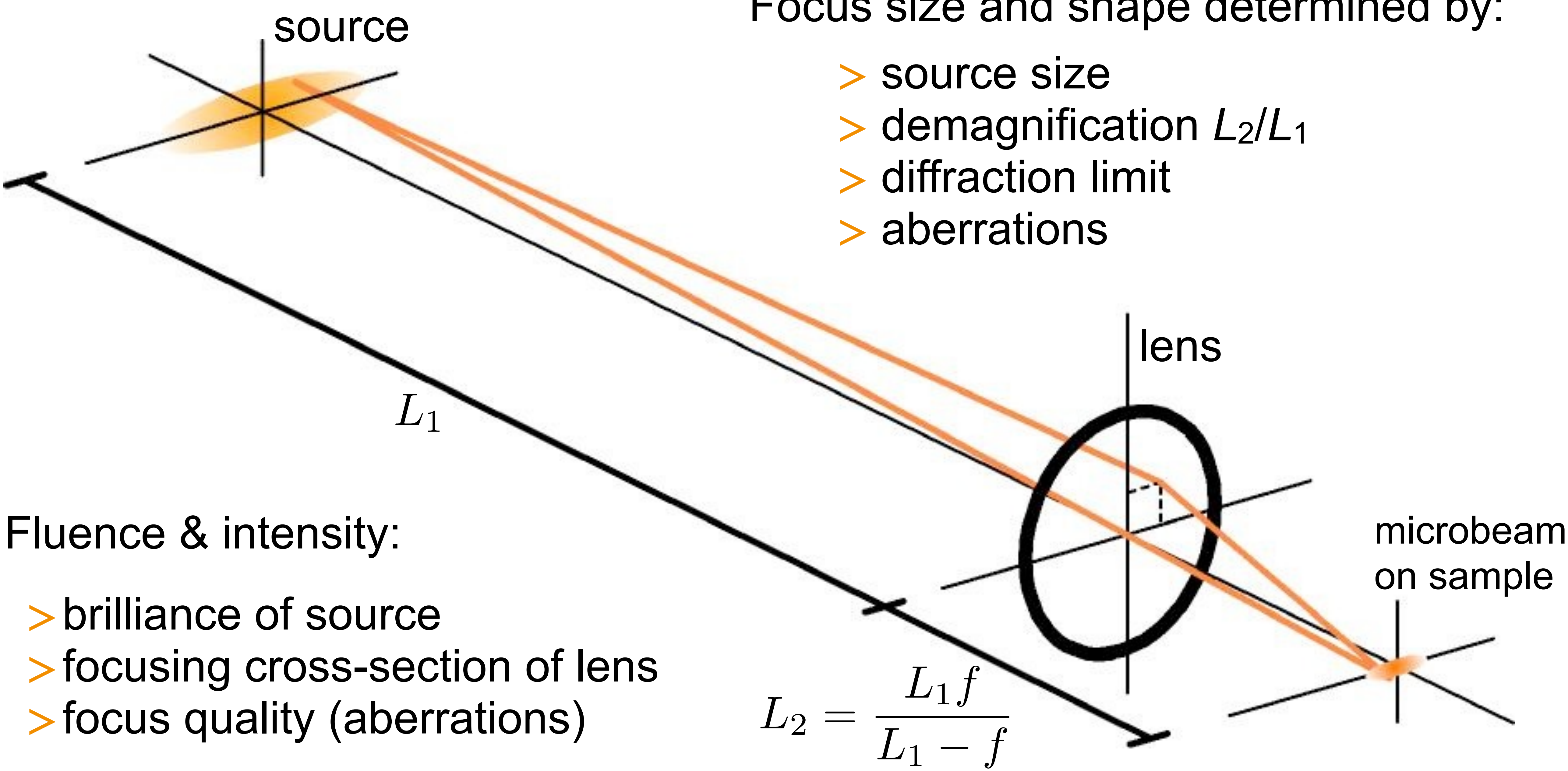

$$L_2 = \frac{L_1 f}{L_1 - f}$$

Fluence & intensity:

- brilliance of source
- focusing cross-section of lens
- focus quality (aberrations)

Spectral Brightness

10000x more light per decade (since 1965)

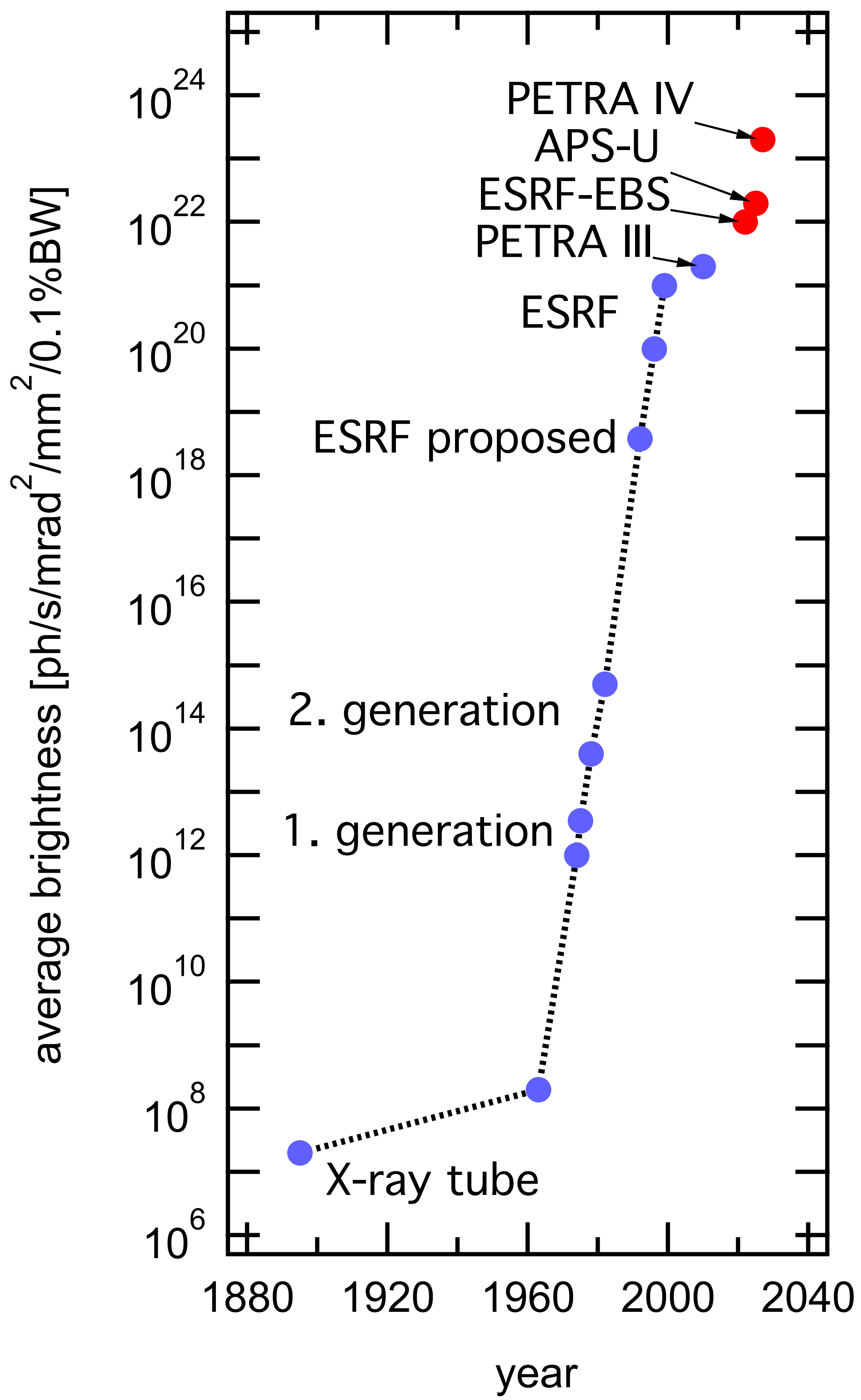

Spectral brightness:

$$B_{\mathrm{sp}} = \frac{F}{\Omega \cdot A \cdot \Delta E / E}$$

Flux per phase-space volume

coherent flux:

$$F_c \propto B_{\mathrm{sp}} \cdot \lambda^2 \cdot \frac{\Delta E}{E}$$

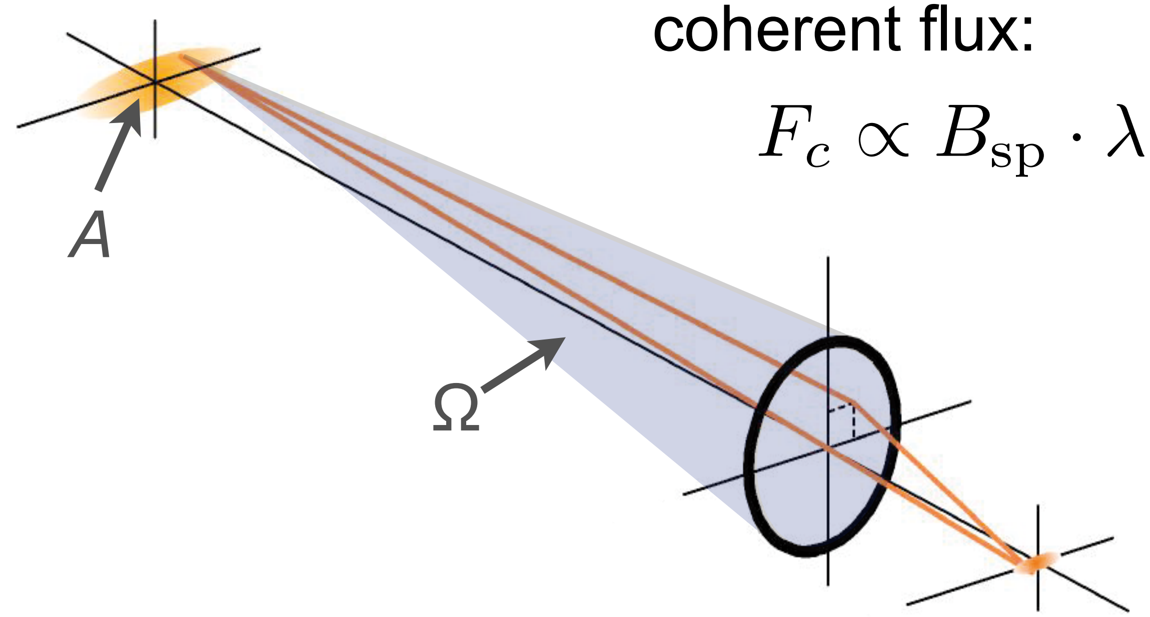

Improvements in brightness:

- faster measurements (time resolution)
- nano-imaging (spatial resolution)
- spectroscopy (energy resolution)

Fluorescence Tomography

Example: investigating the ion transport in plants

Fluorescence analysis of plants:

- > strong diffusion of elements
- > cell structure complicated and delicate

Difficult sample preparation

- > cryo sections
- > fracture surfaces

ideal:

nondestructive probe of
inner structures of sample

root of Mahogany tree

Fluorescence Tomography

Root of Mahogany tree

element distribution on virtual section through sample

Example:

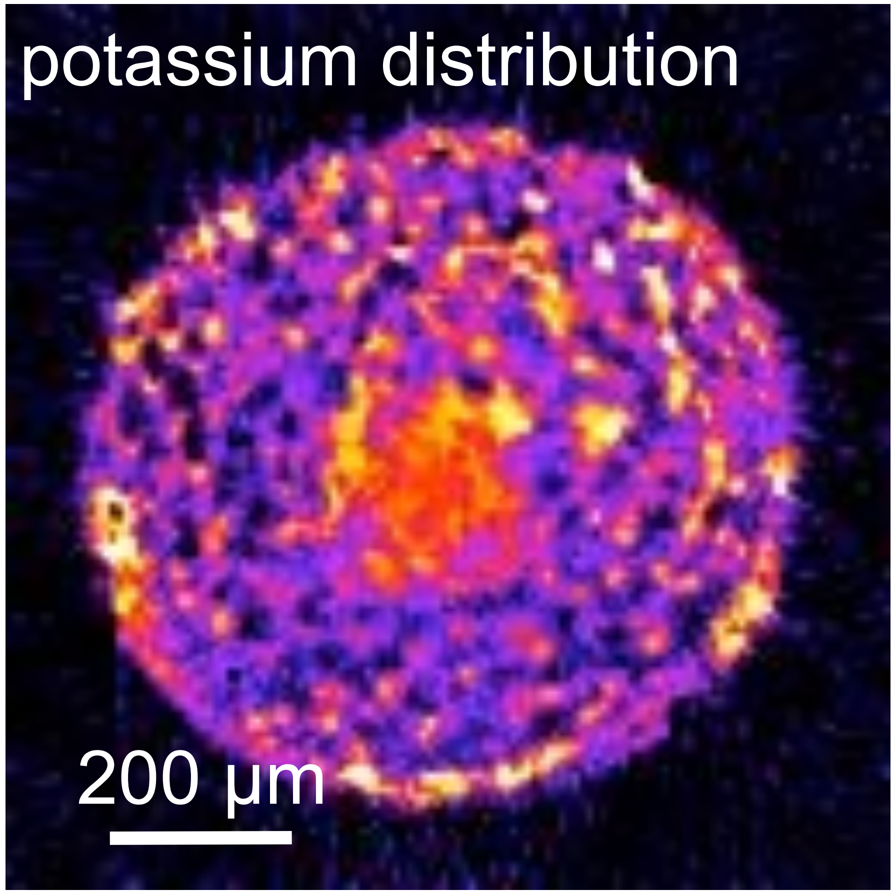

X-ray Fluorescence & Auger Process

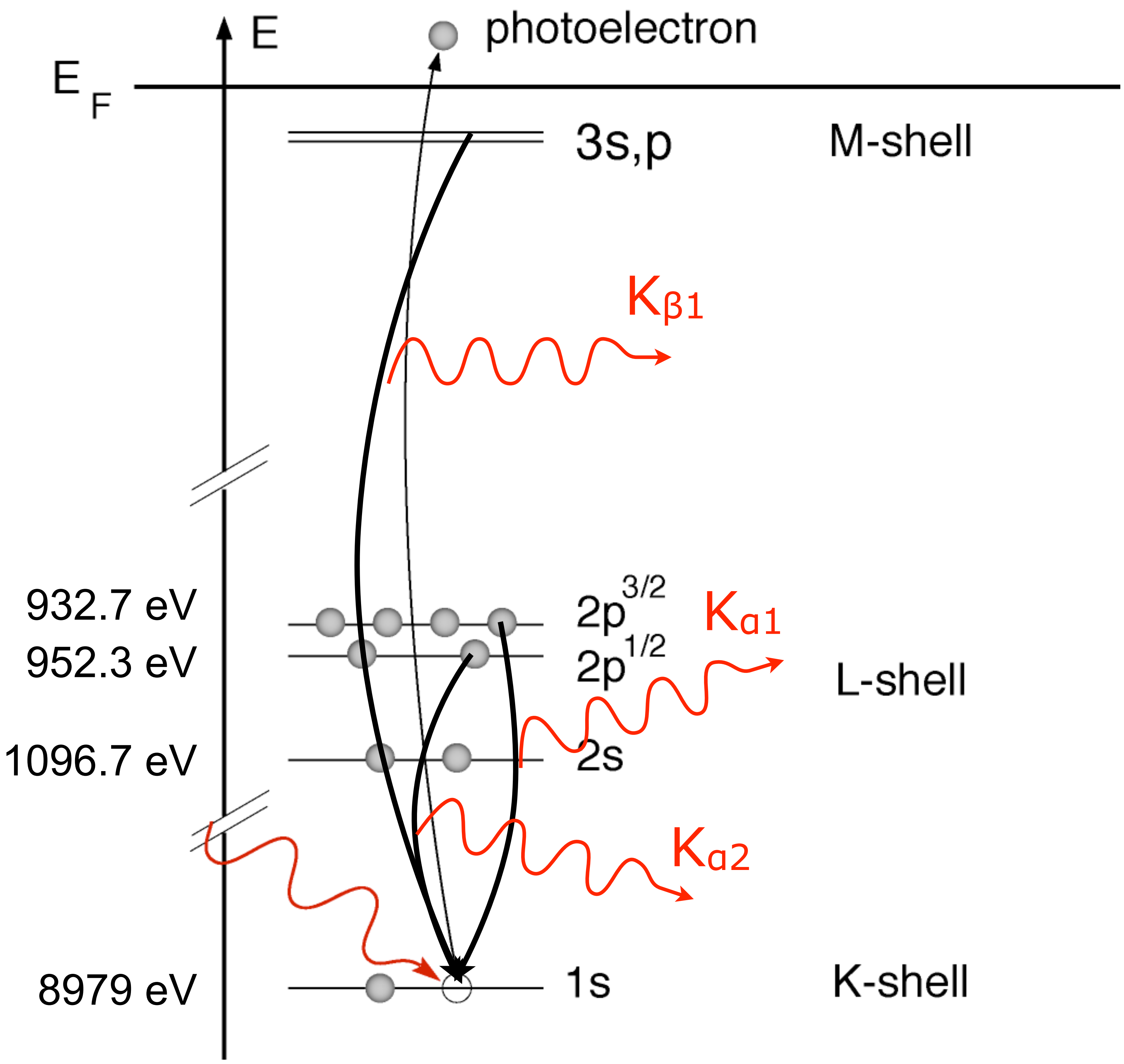

X-ray Absorption

leaves atom in excited state (core hole):

Secondary processes:

- fluorescence

X-ray Fluorescence & Auger Process

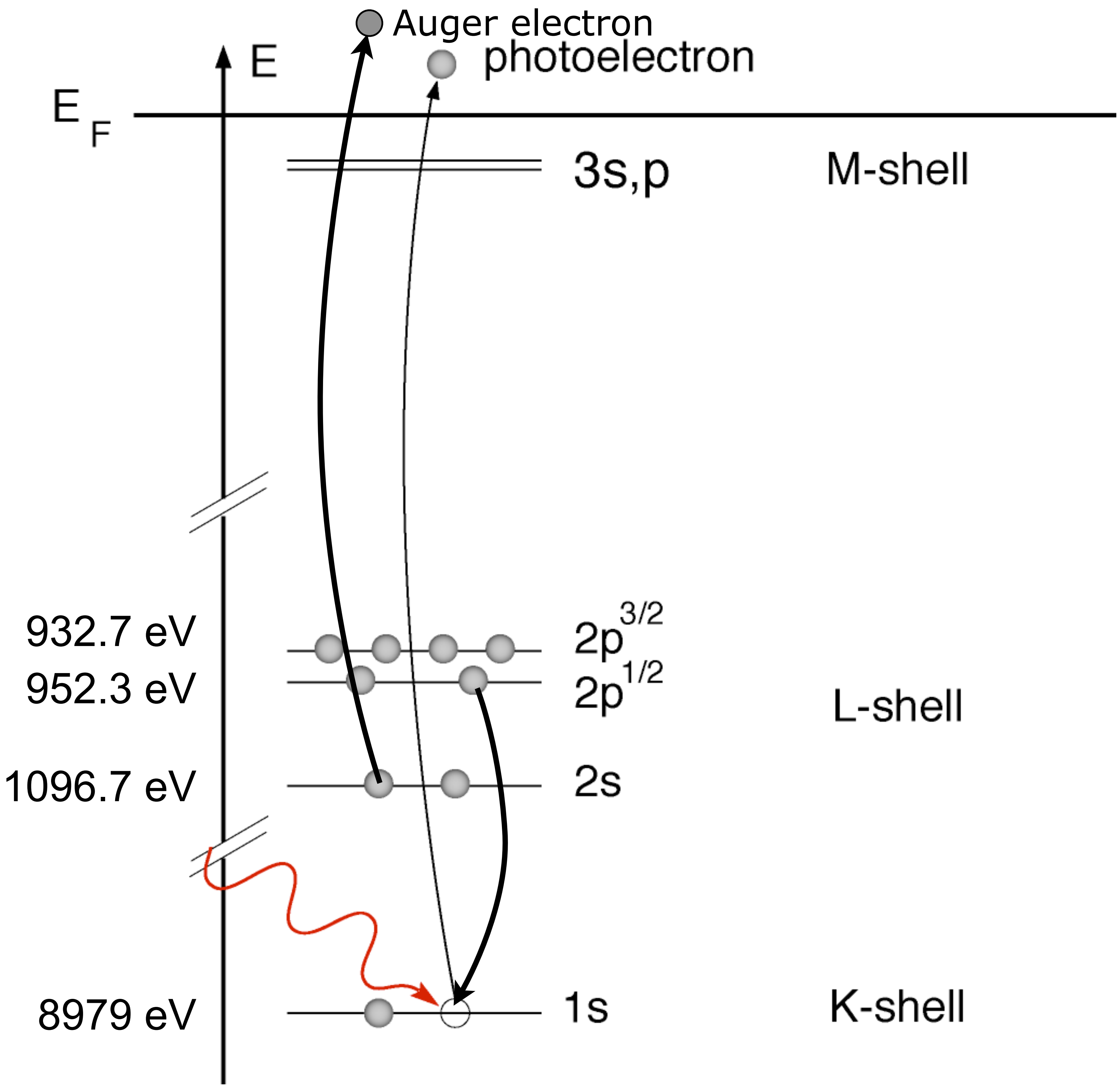

X-ray Absorption

leaves atom in excited state (core hole):

Secondary processes:

> fluorescence

Fluorescence Yield

$1 - \varepsilon =$ Auger yield

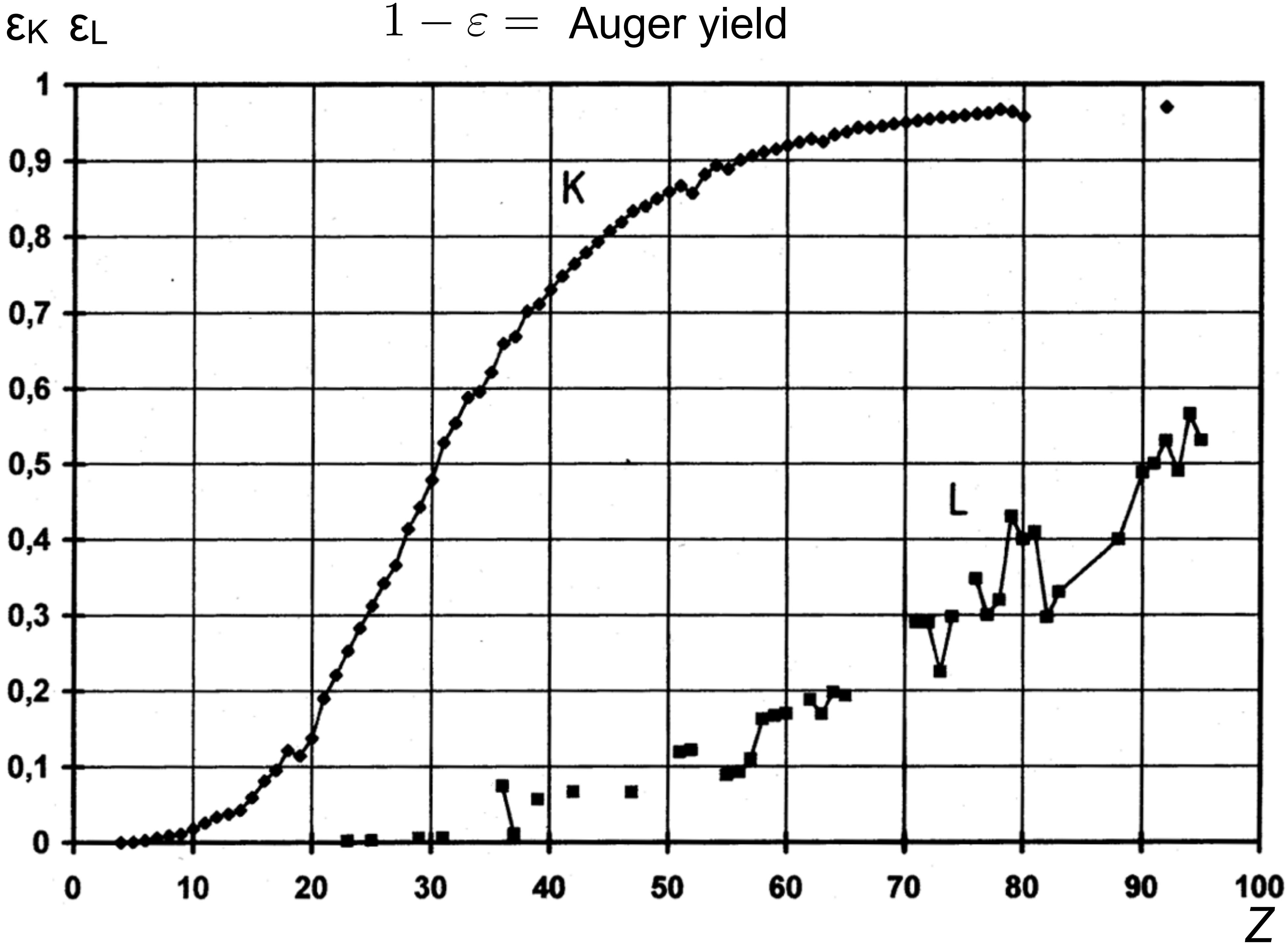

element specific

Fluorescence dominates at higher binding energies for core hole excitation (growing with atomic number Z)

Fluorescence Spectrum

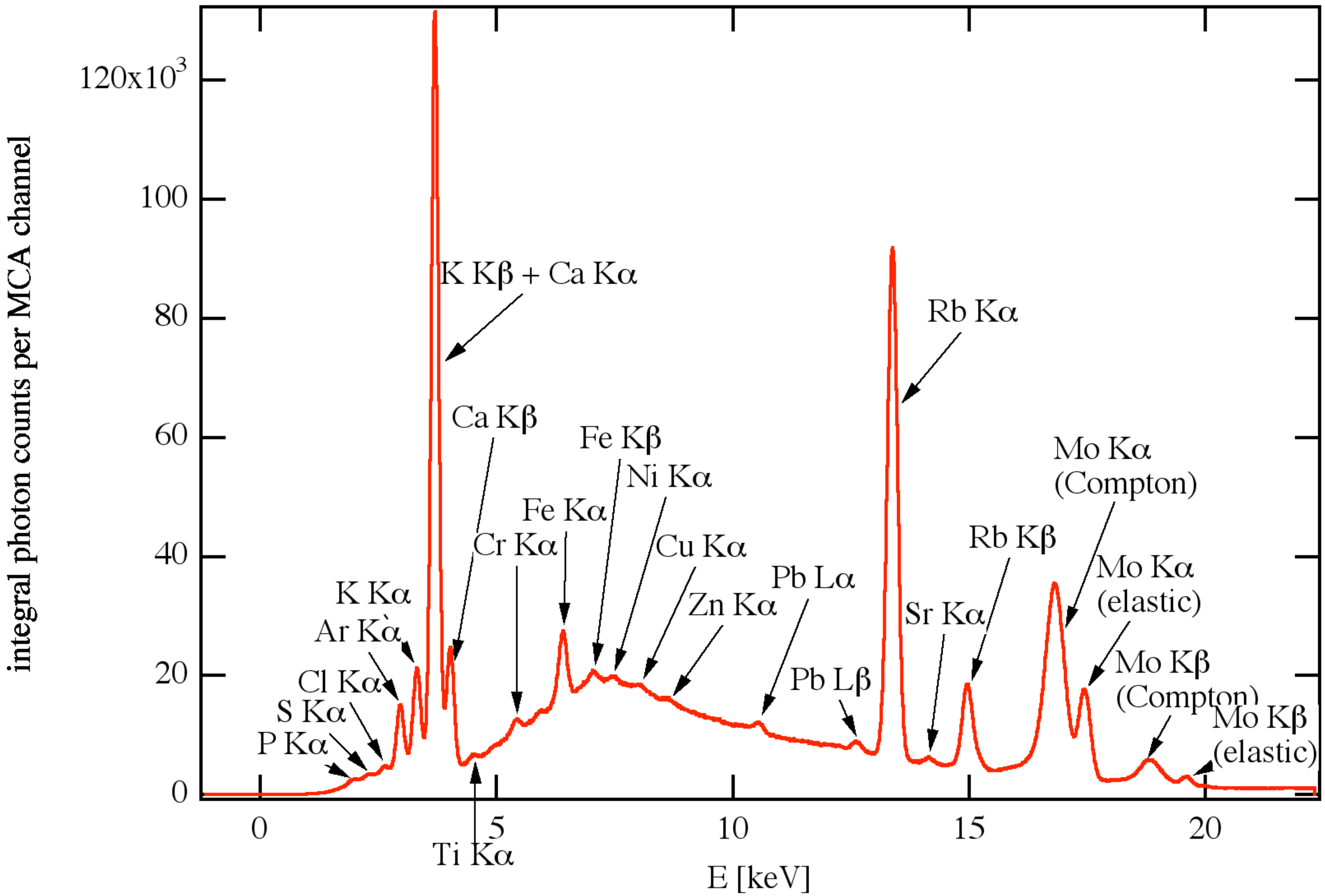

Illuminated atoms emit characteristic fluorescence radiation!

Example spectrum excitation with X-ray tube:

Background due to scattered spectrum of X-ray tube

Limitation of detection limits by background!

Excitation with Monochromatic Synchrotron Radiation

Example: undulator radiation (Si 111 monochrom.): 19.5 keV

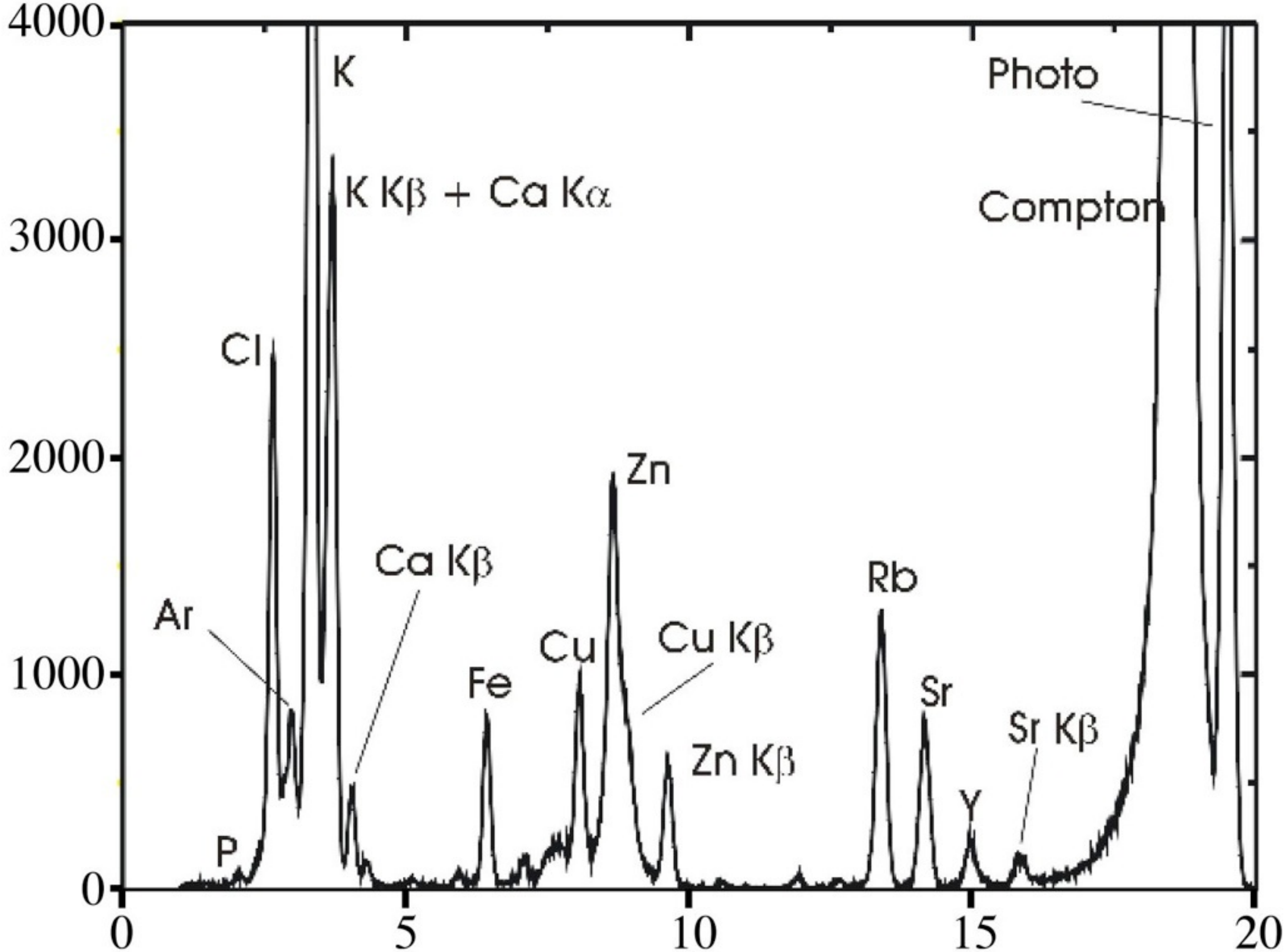

No background due to scattered radiation at fluorescence energy

High signal-to-background ratio!!

very low detection limits possible (ppb-level)!

Scanning Probe: Fluorescence Microtomography

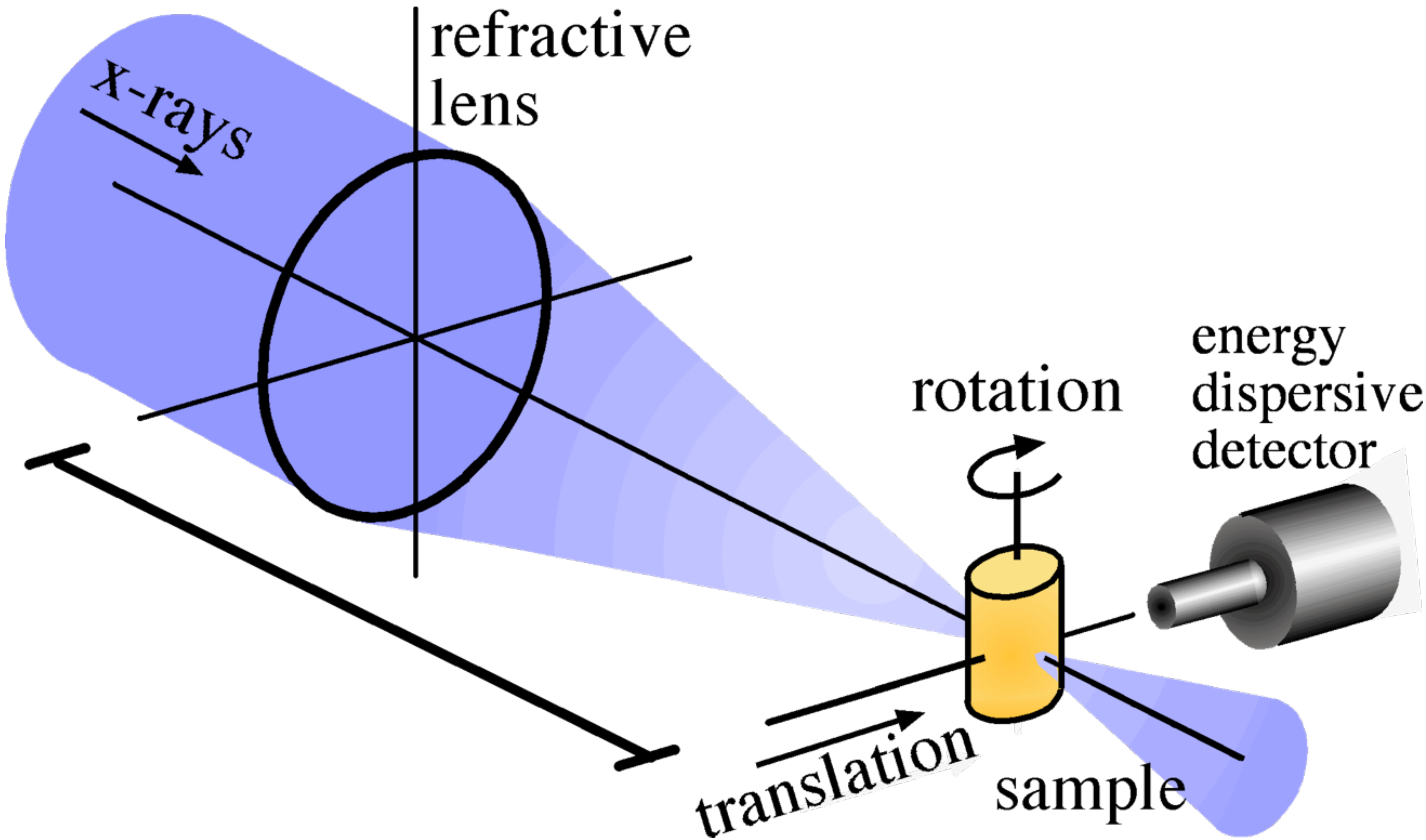

Fluorescence Microtomography

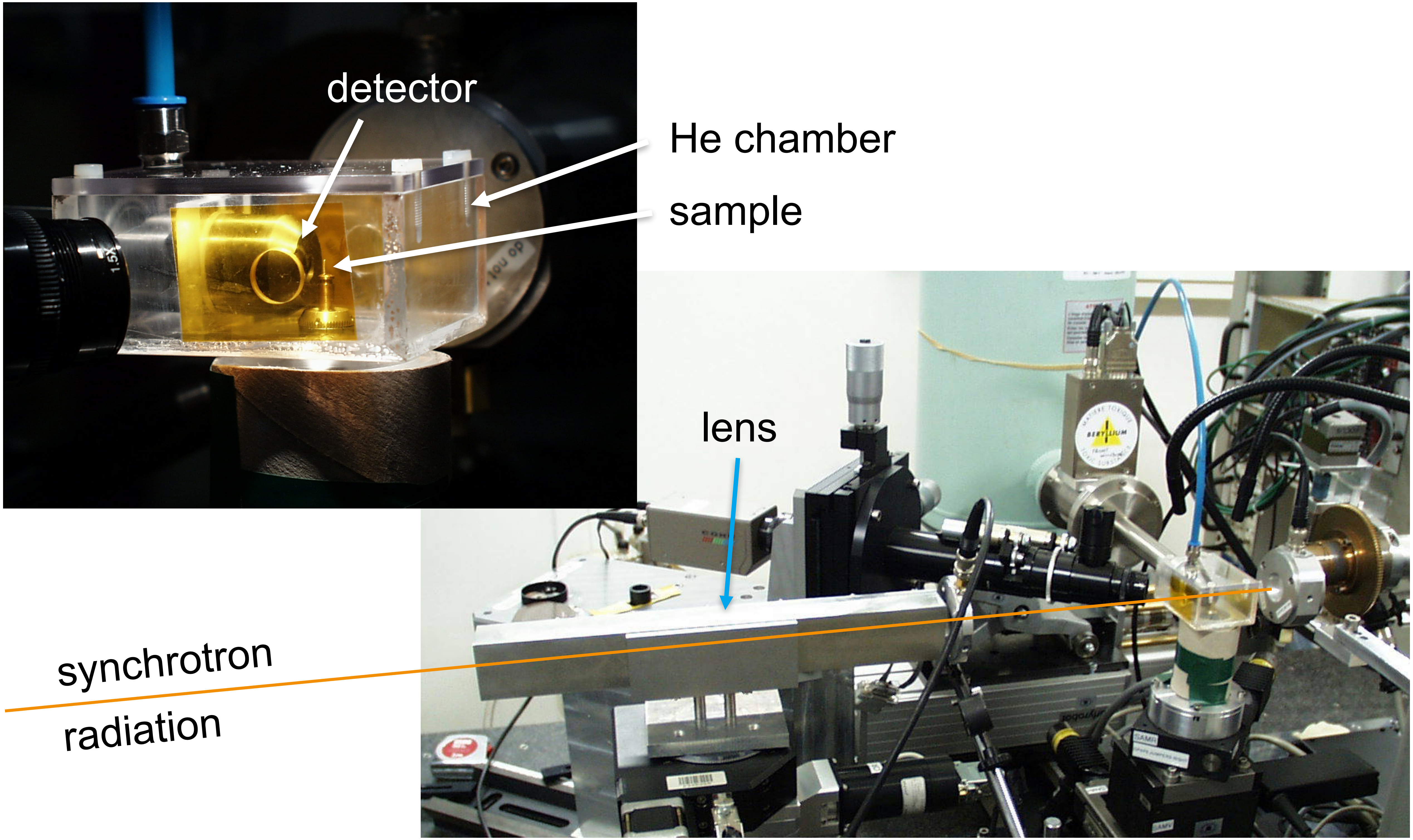

Fluorescence Tomography: Measured Data

Sinograms:

Cl Kα | K Kα | Rb Kα

152 rotations

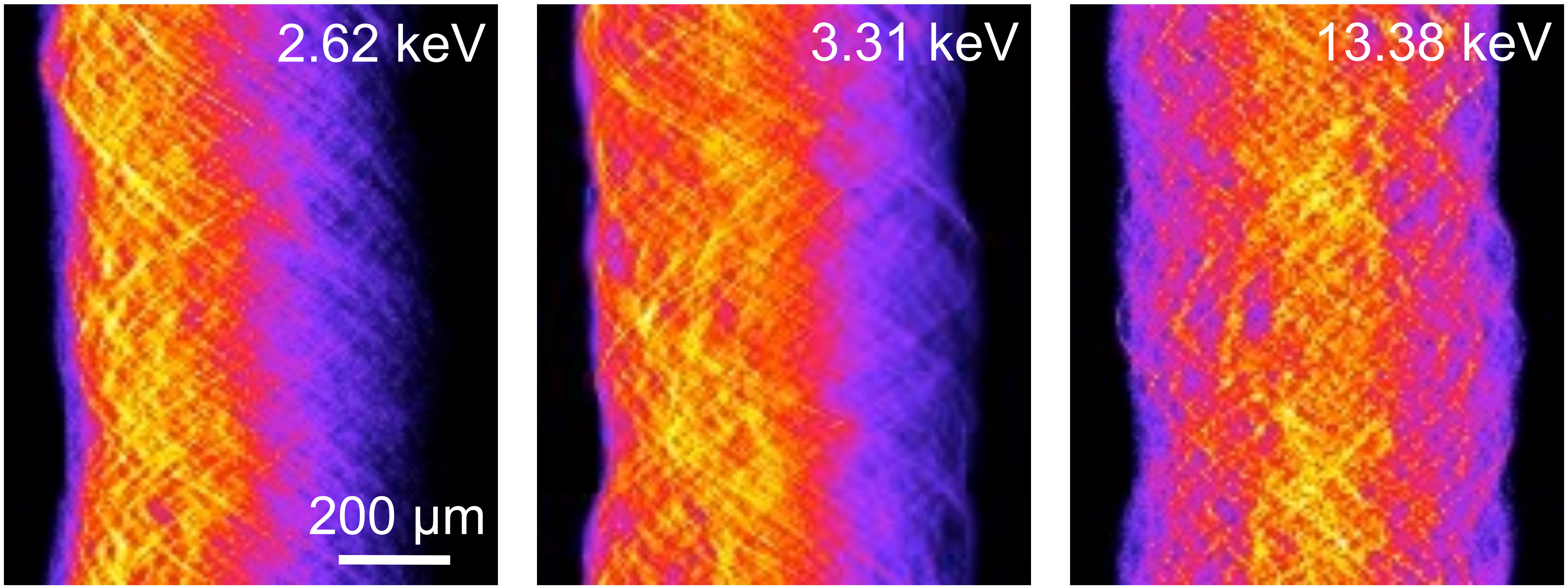

$0^\circ - 360^\circ, \delta\varphi = 2.38^\circ$

translations: 128, 6µm

experimental parameters:

- energy: 19.5 keV
- refractive lens (Al): *N* = 150, f = 45.4 cm, m = 1/127
- beam size: 1.5 x 6µm^2, flux: 1.1 · 10^{10} ph/s

Fluorescence Tomography: Measured Data

Sinograms:

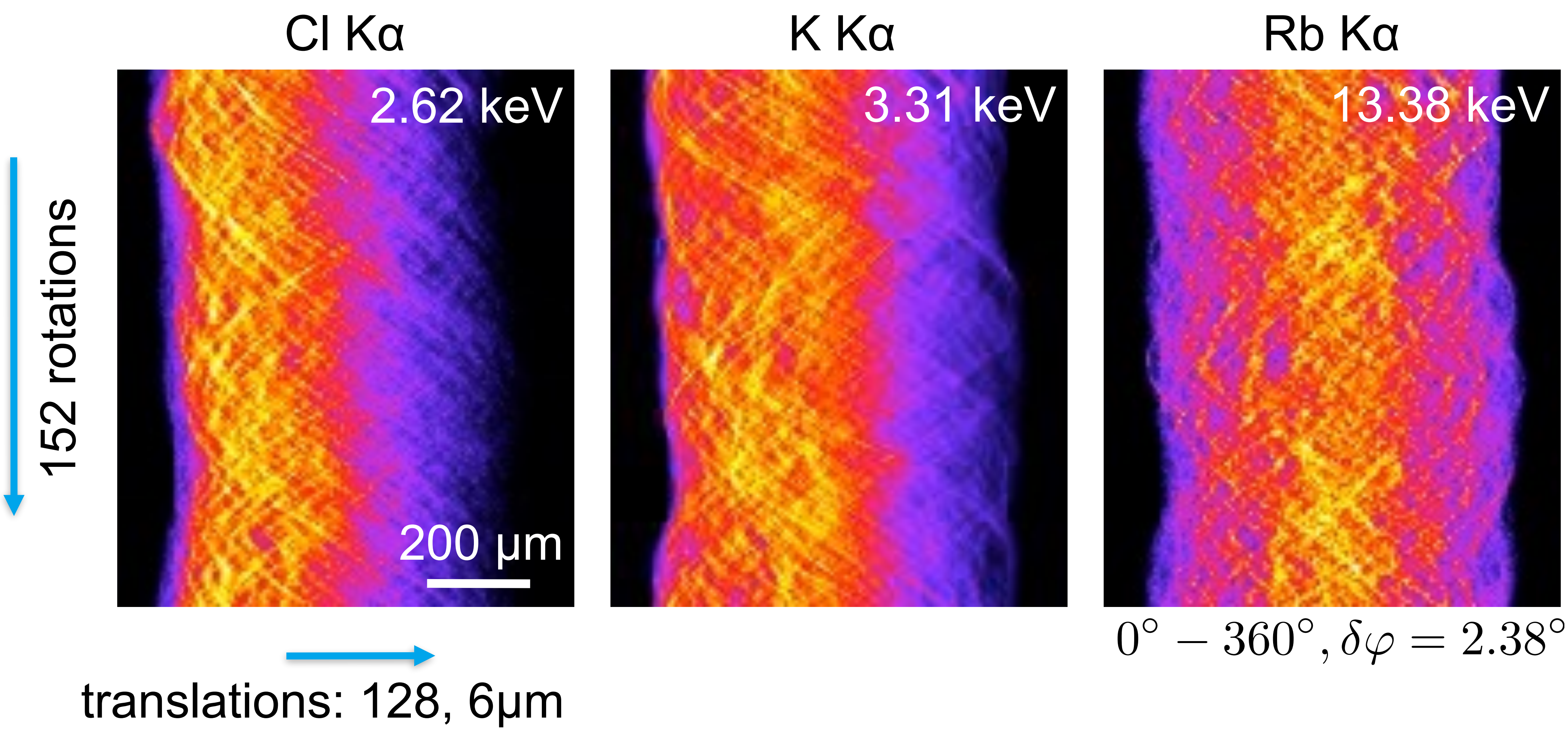

Symmetry:

$$I_{i\nu}(-r, \varphi + \pi) = I_{i\nu}(r, \varphi)$$

only holds (approx.) for Rb!
Absorption of fluorescence radiation: asymmetry in sinogram.

Fluorescence Tomography: Model

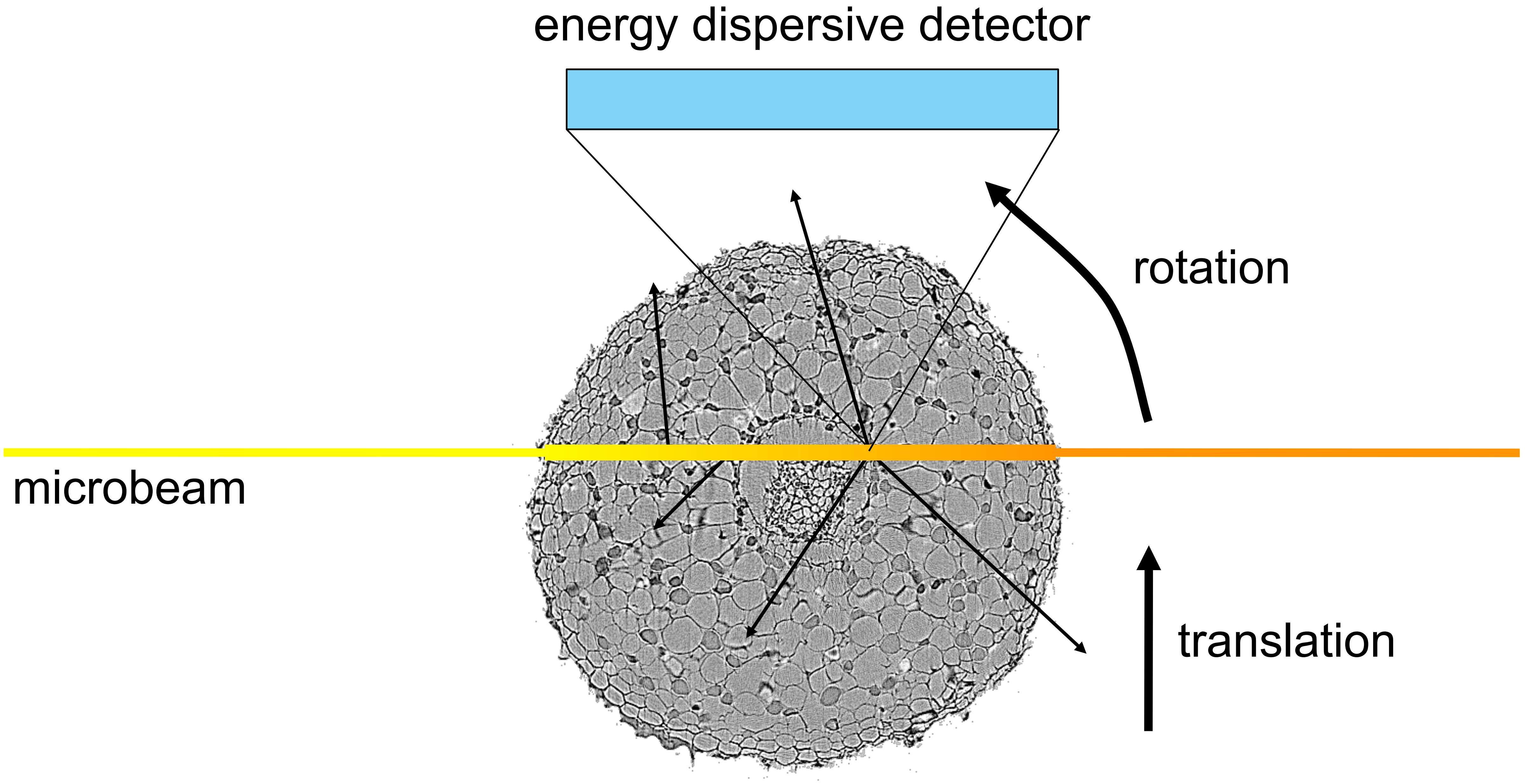

$$I_{i\nu}(r,\varphi) = I_0 \int ds \left[e^{-\int_{-\infty}^{s} ds' \mu_0(x,y)} \cdot p_{i\nu}(x,y) \cdot \int d\gamma e^{-\int dr' \mu_{i\nu}(x,y)} \right]$$

Absorption Correction

Example: potassium distribution in Mahogany root

Disregarding attenuation of fluorescence:

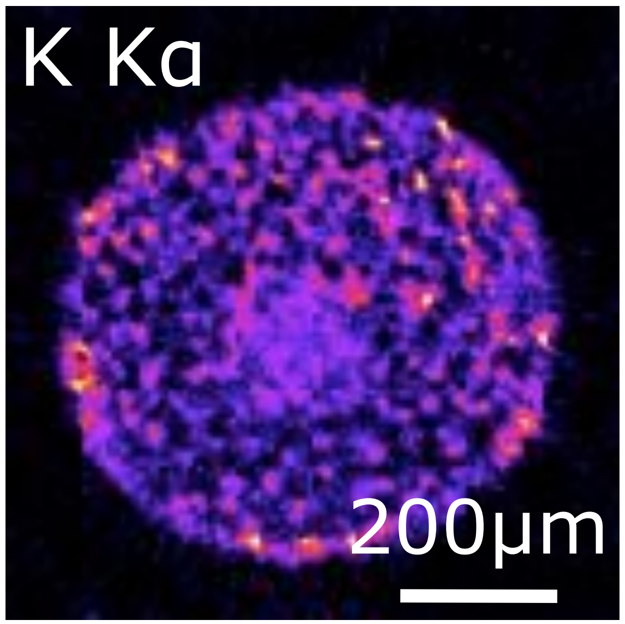

$$\mu_{\mathrm{K\,K}\alpha} = 0$$

simple tomographic model

reconstructed sinogram

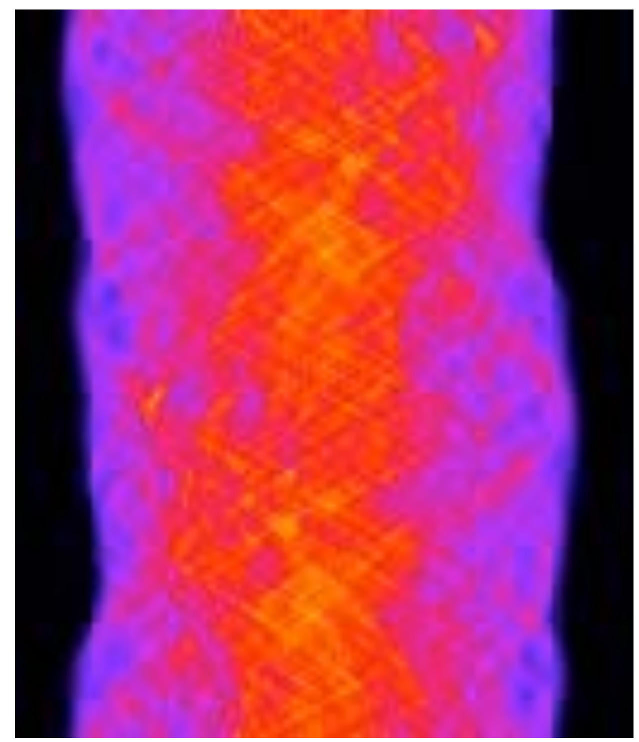

measured sinogram

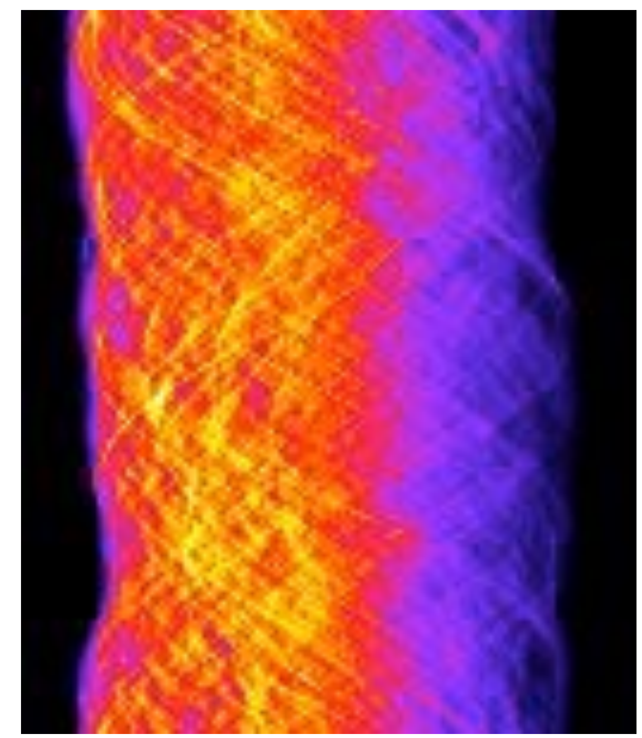

C. Schroer, Appl. Phys. Lett. **79**, 1912 (2001).

Absorption Correction

Example: potassium distribution in Mahogany root

Accounting for attenuation of fluorescence:

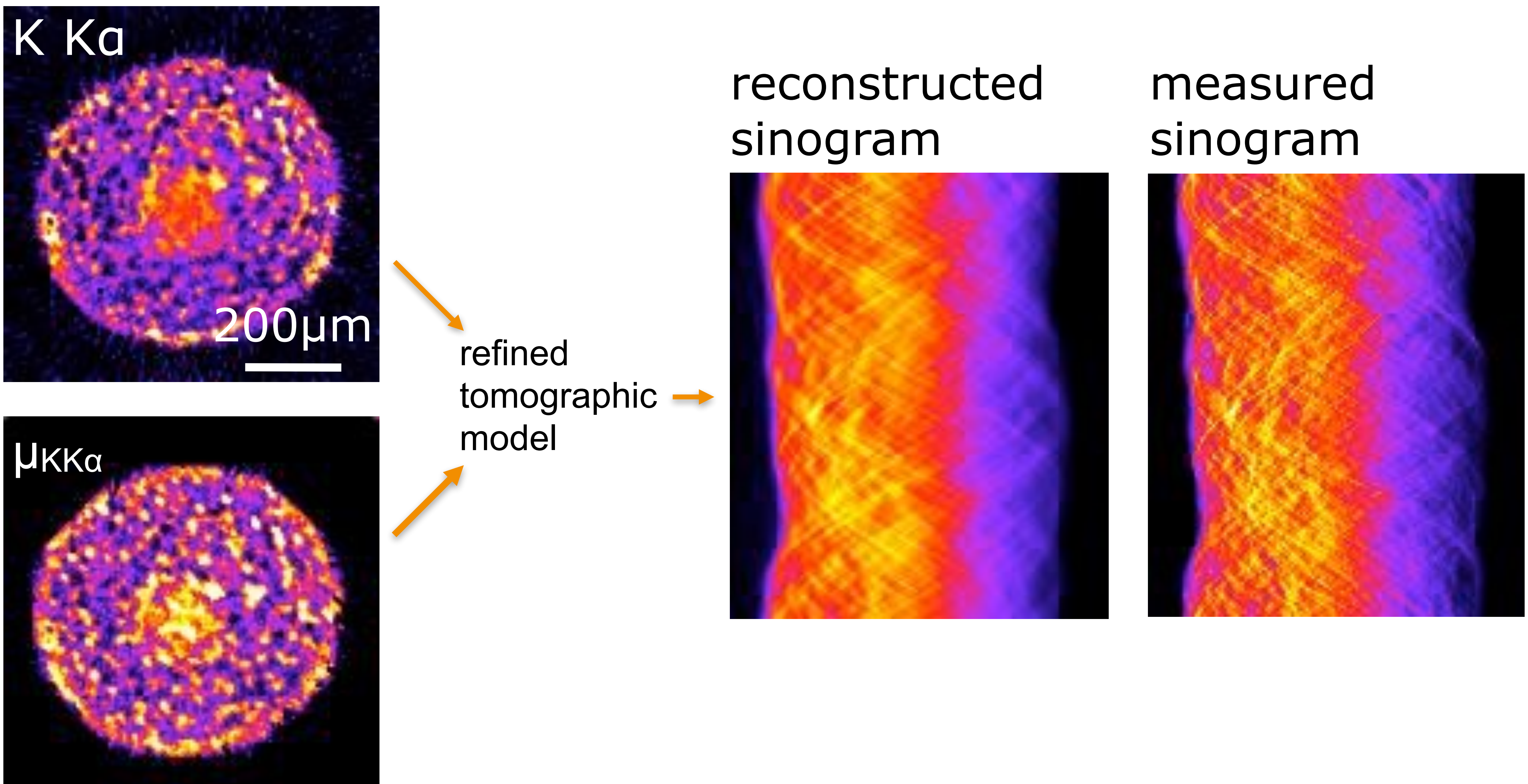

C. Schroer, Appl. Phys. Lett. **79**, 1912 (2001).

Fluorescence Tomography

root of Mahogany tree

pixel size: 6 µm

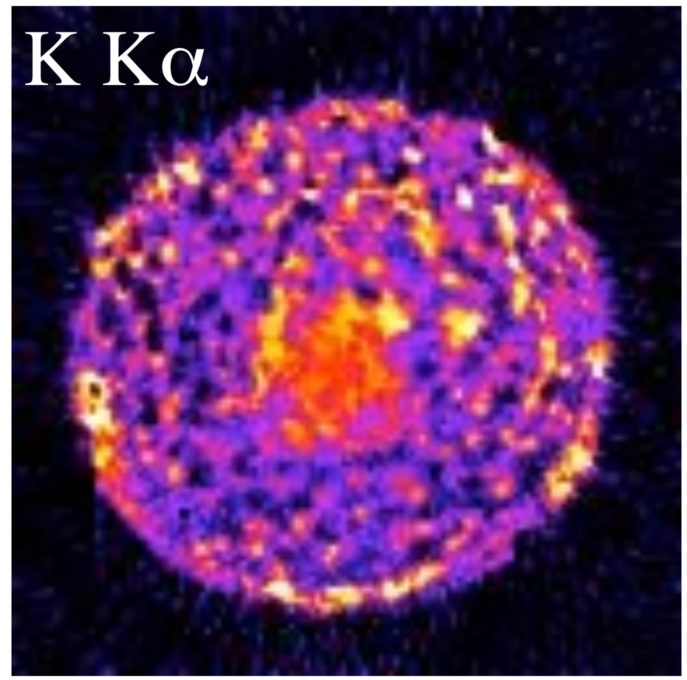

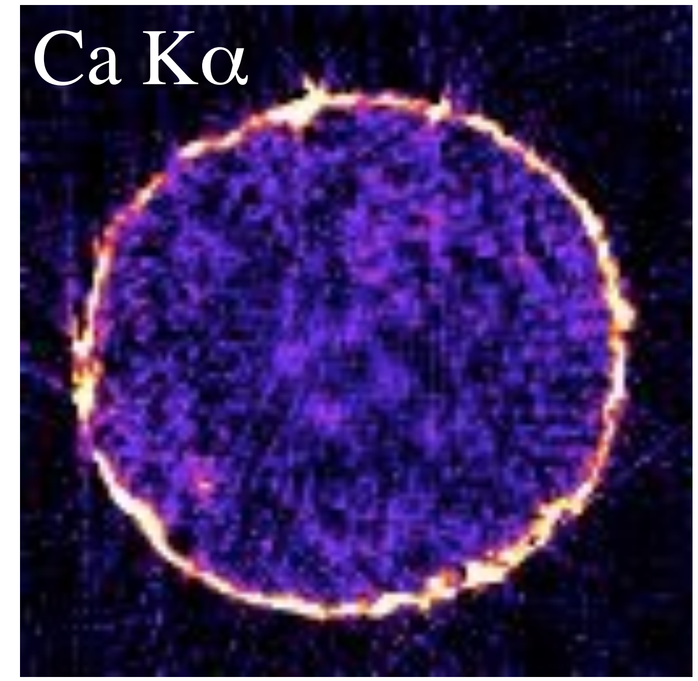

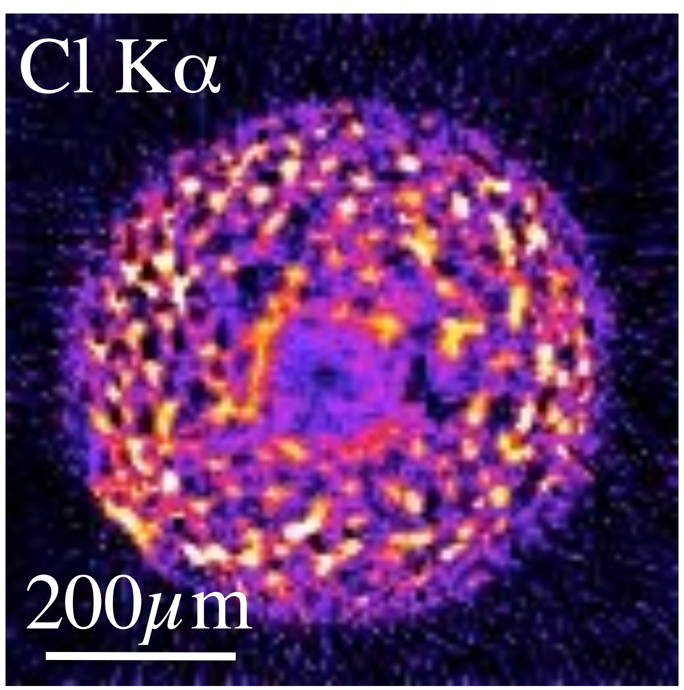

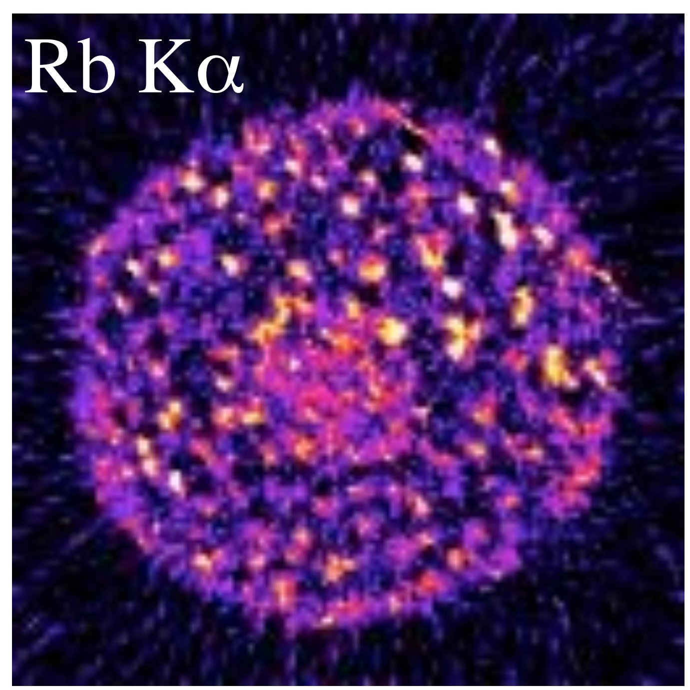

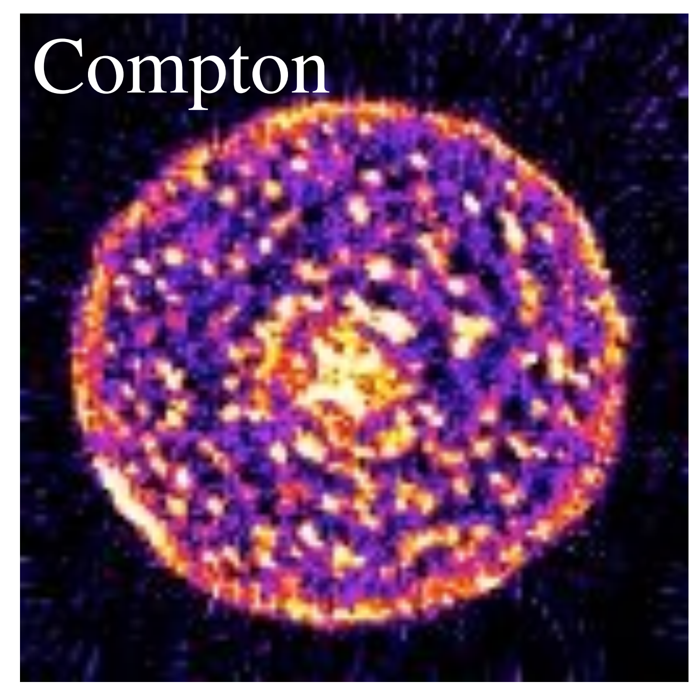

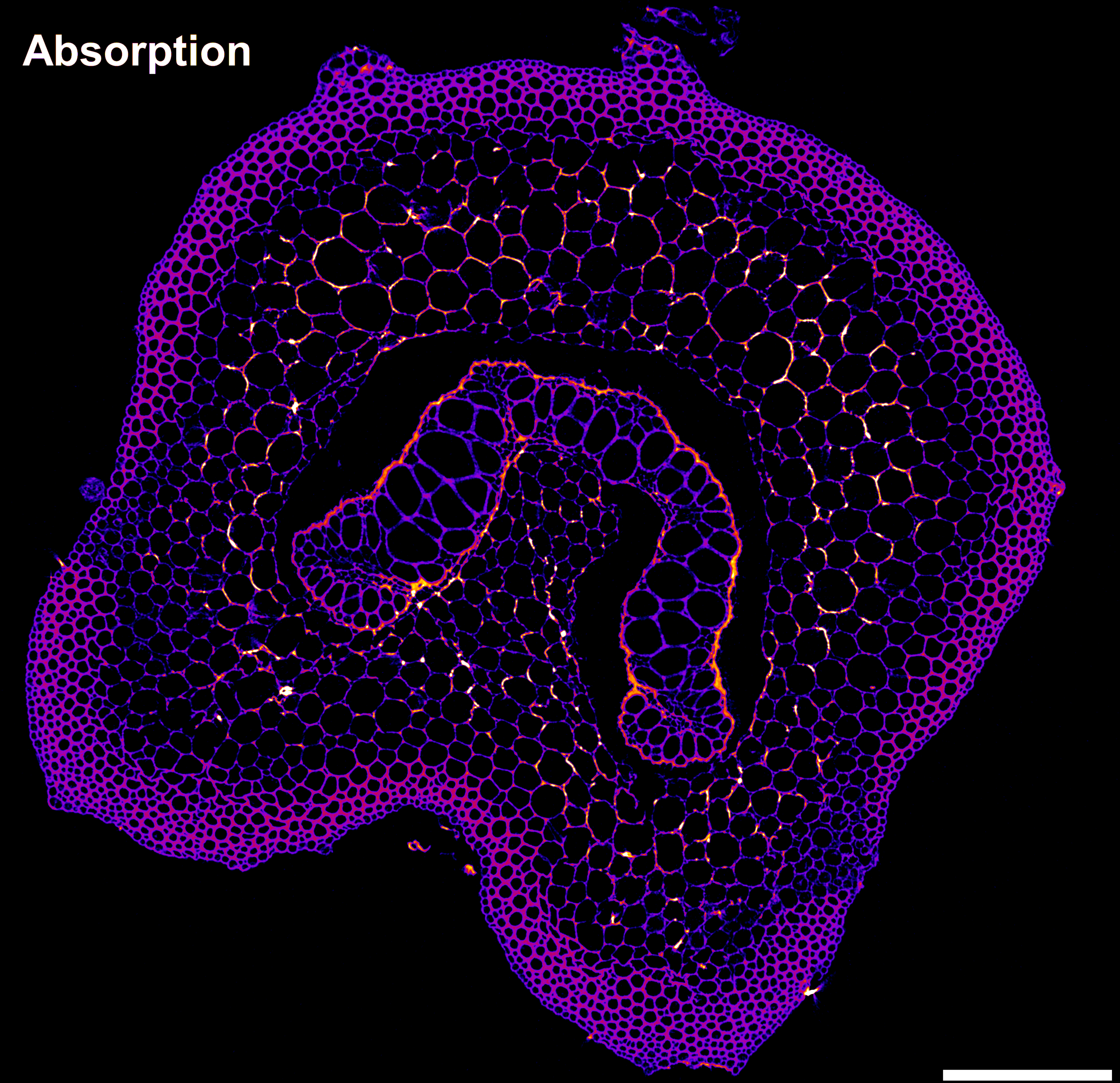

Pteris vittata rachis (As hyperaccumulator)

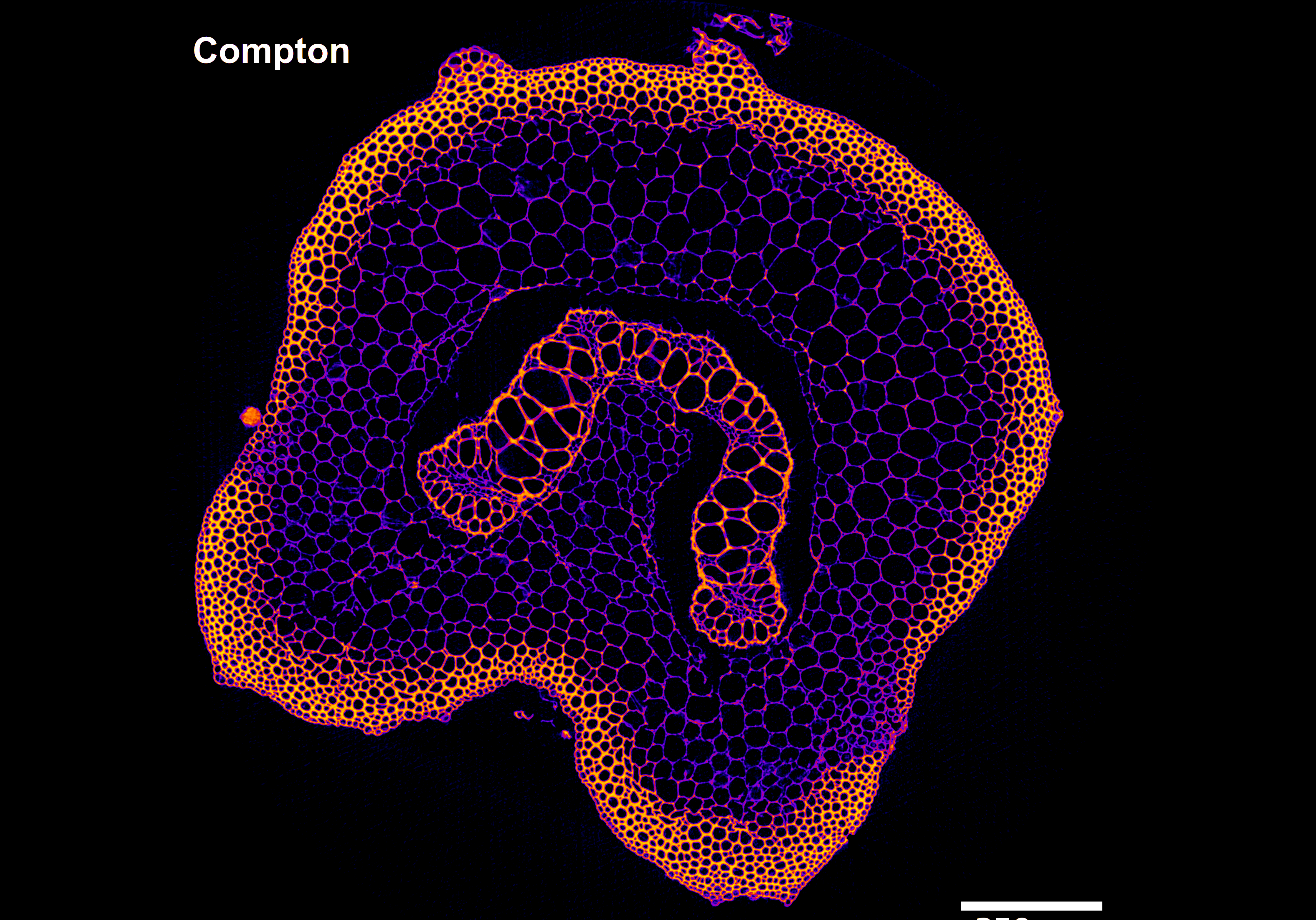

Pteris vittata rachis (As hyperaccumulator)

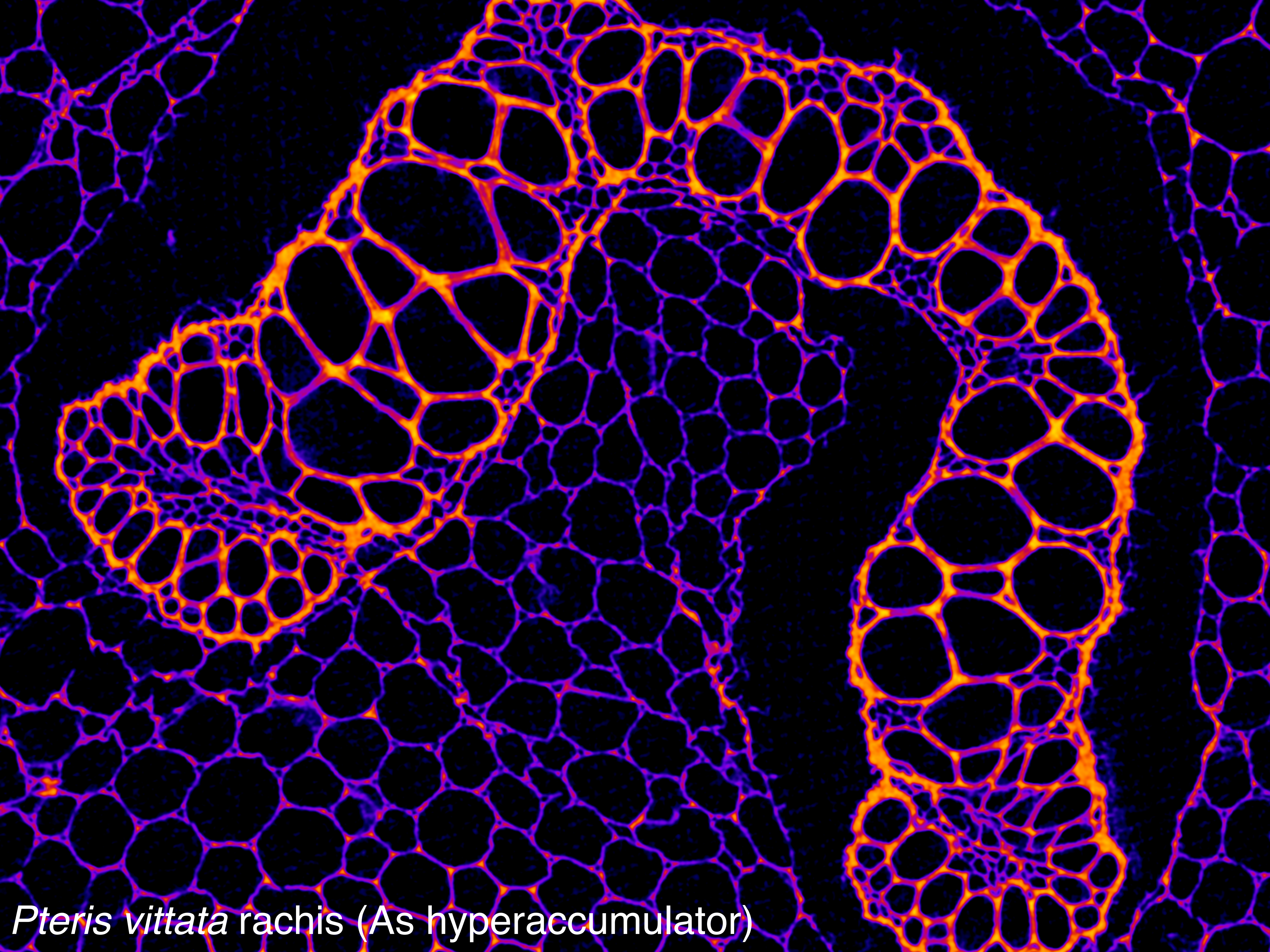
Pteris vittata rachis (As hyperaccumulator)

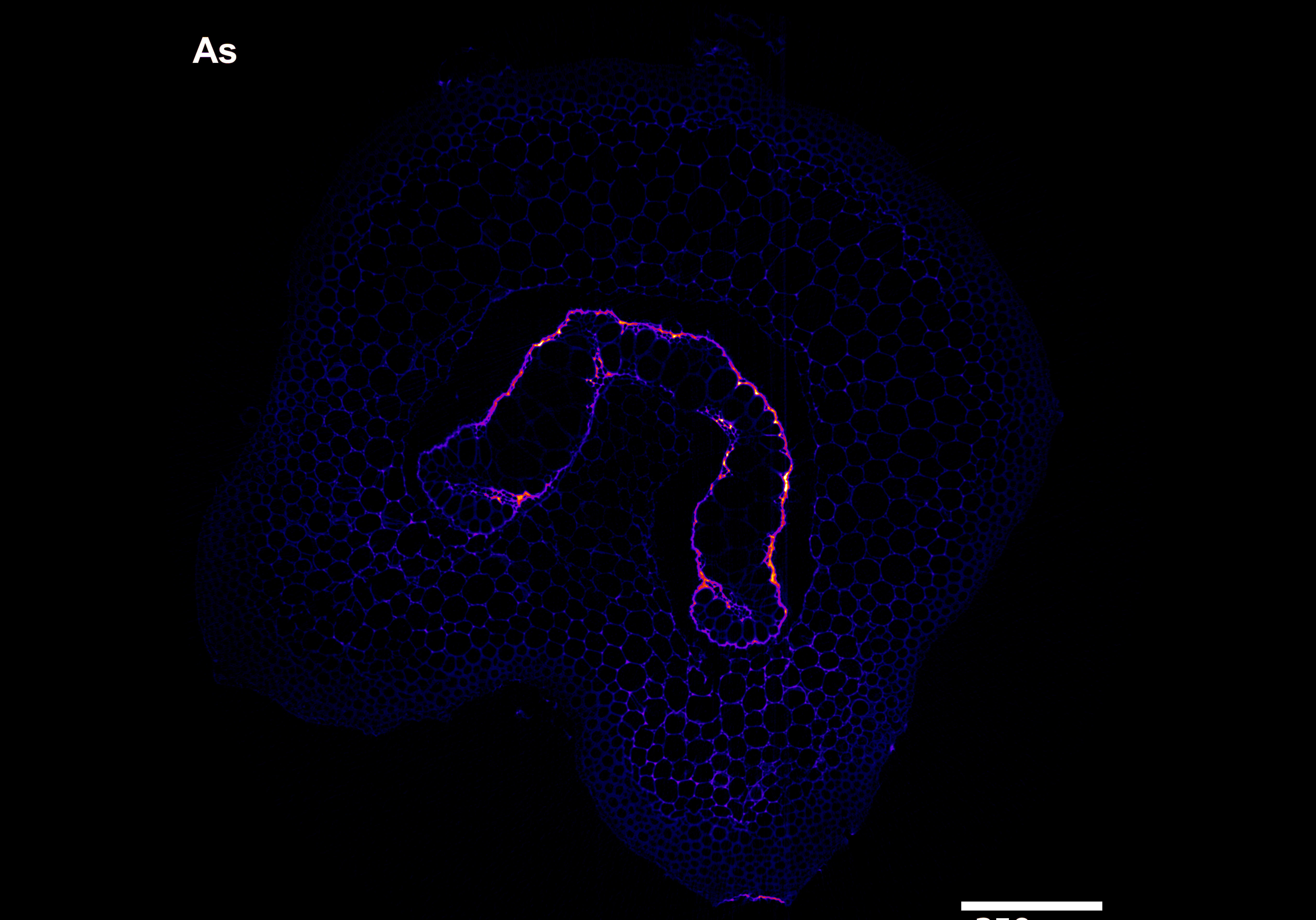

Pteris vittata rachis (As hyperaccumulator)

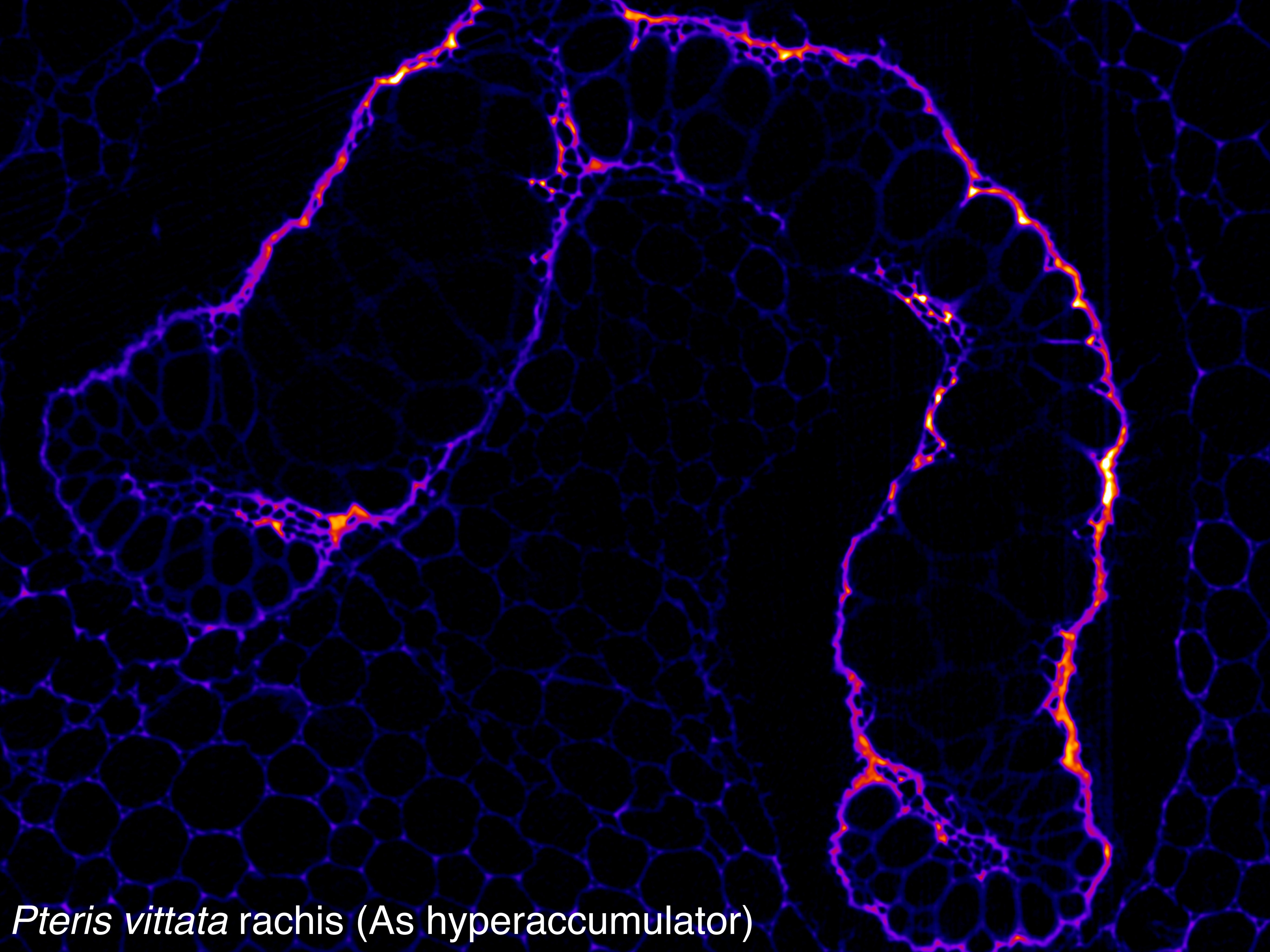

Pteris vittata rachis (As hyperaccumulator)

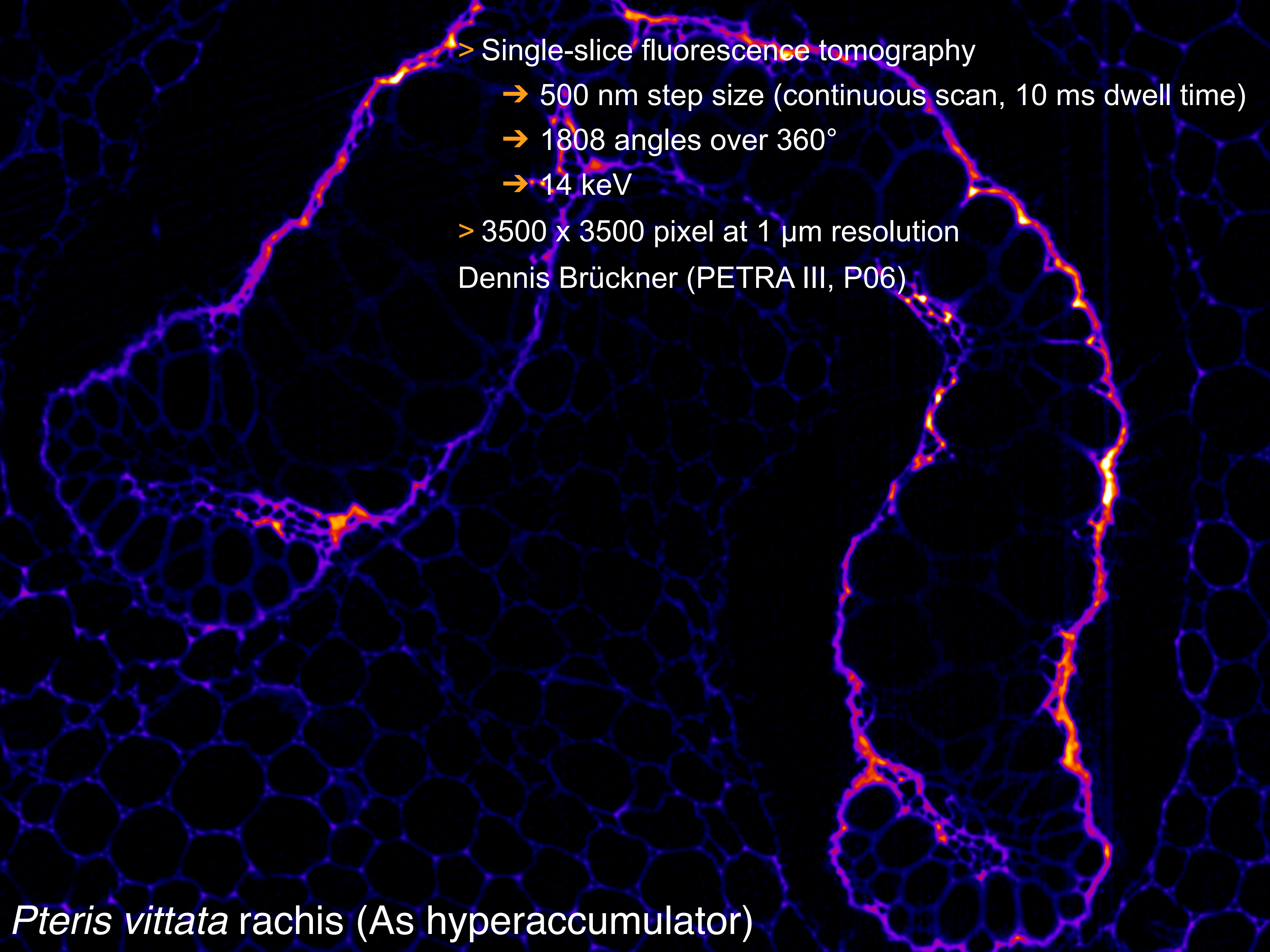
> Single-slice fluorescence tomography
➔ 500 nm step size (continuous scan, 10 ms dwell time)
➔ 1808 angles over 360°
➔ 14 keV
> 3500 x 3500 pixel at 1 µm resolution
Dennis Brückner (PETRA III, P06)
Pteris vittata rachis (As hyperaccumulator)

SAXS Tomography: Local Nanostructure

SAXS: Small-Angle X-ray Scattering

Investigating the local nanostructure on a virtual section through sample

Sample:

Non-destructive investigation
of inner structure of sample

virtual section

reconstructed SAXS
cross section at each point
on the virtual section

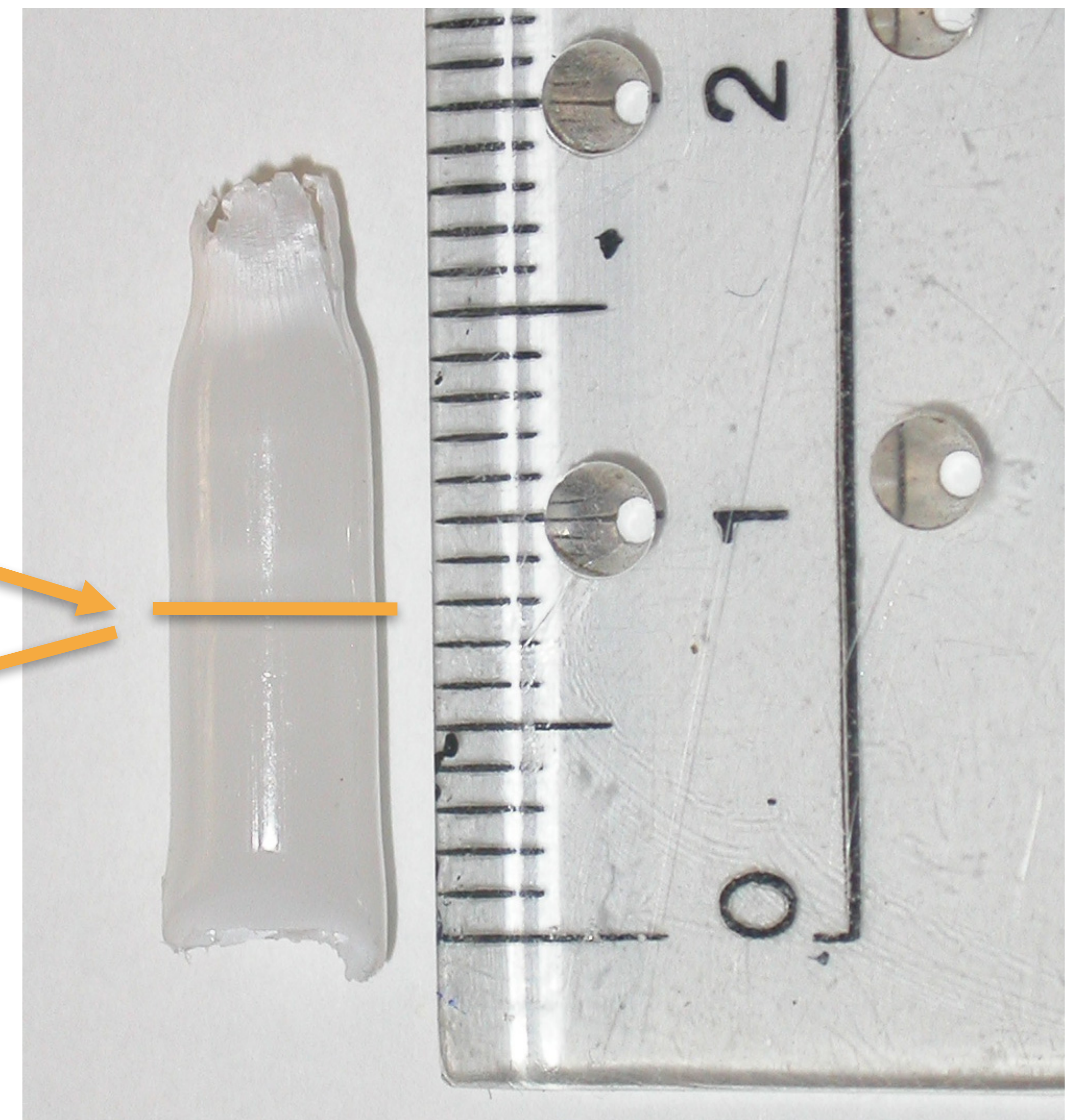

polyethylene rod

C. Schroer, et al., Appl. Phys. Lett. **88**, 164102 (2006)

Tomographic Small-Angle X-Ray Scattering

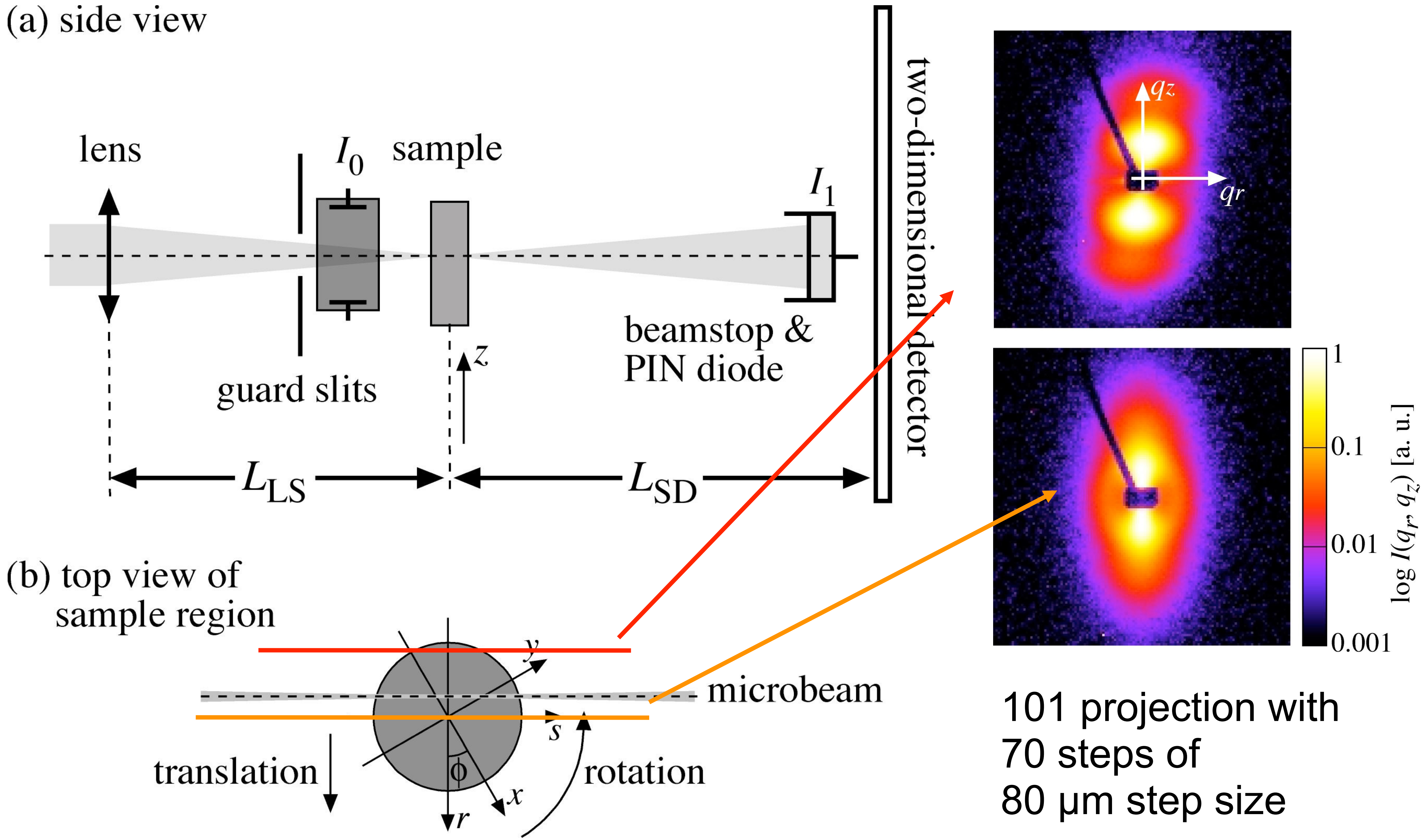

101 projection with
70 steps of
80 µm step size

SAXS Tomography

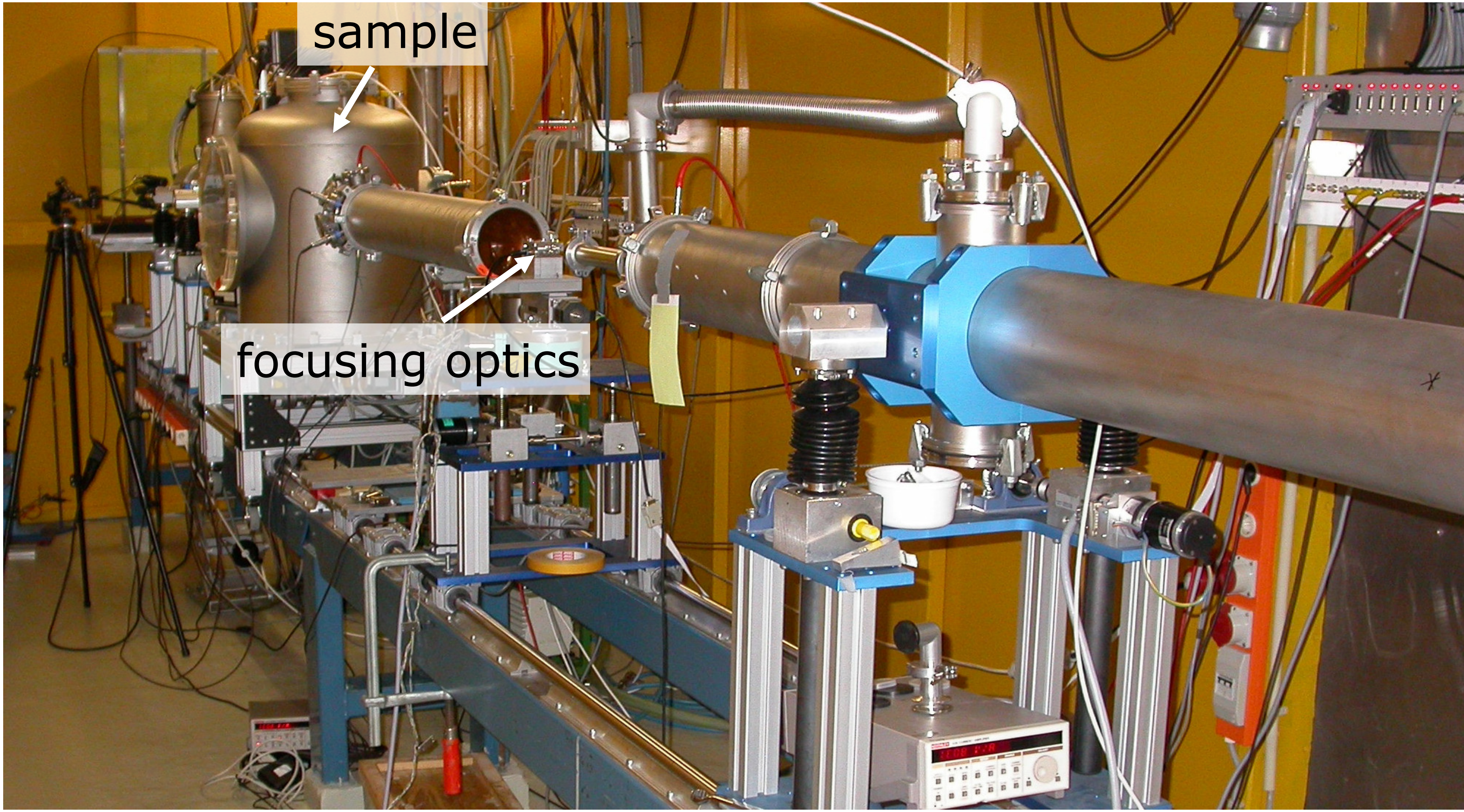

SAXS Tomography

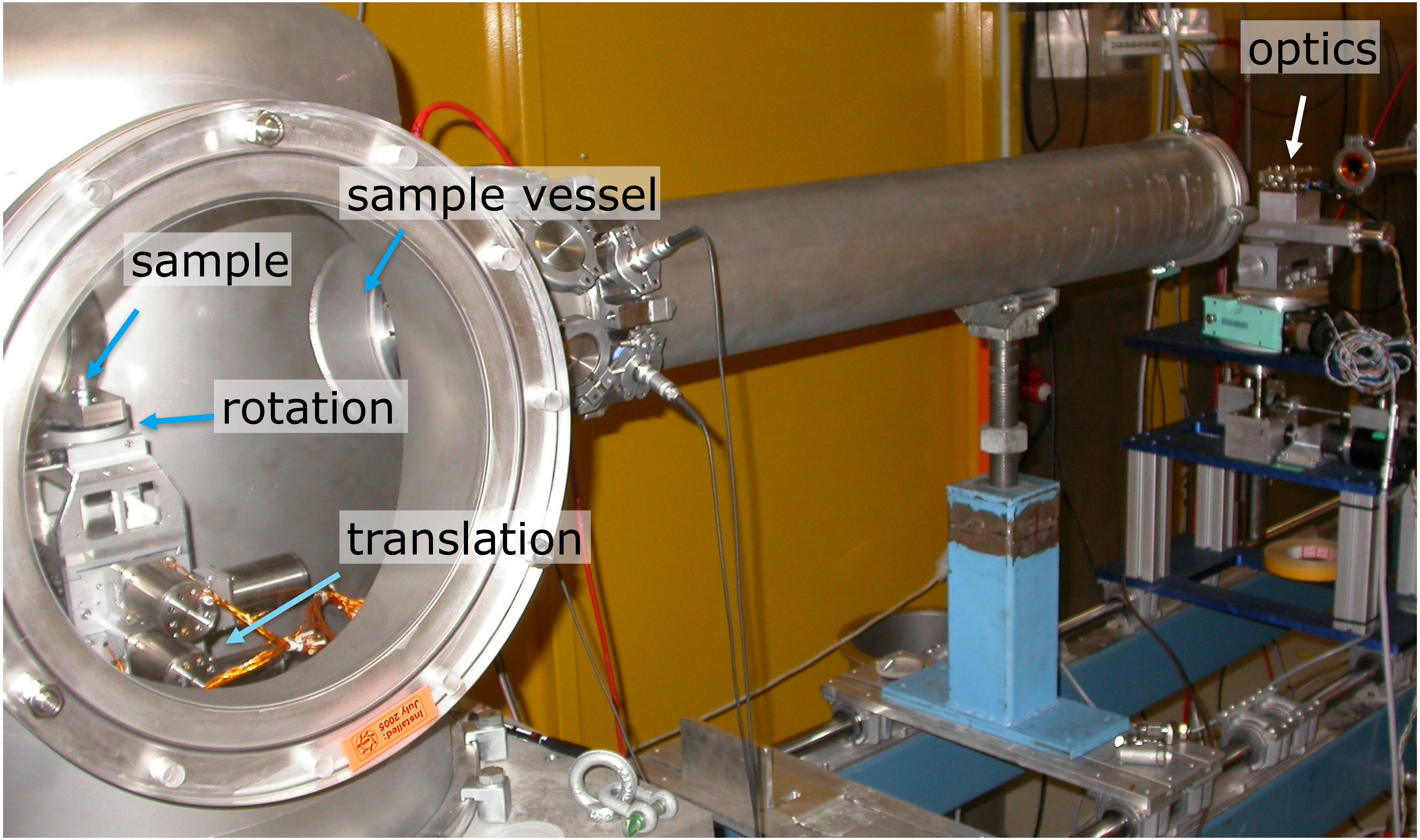

SAXS Tomography

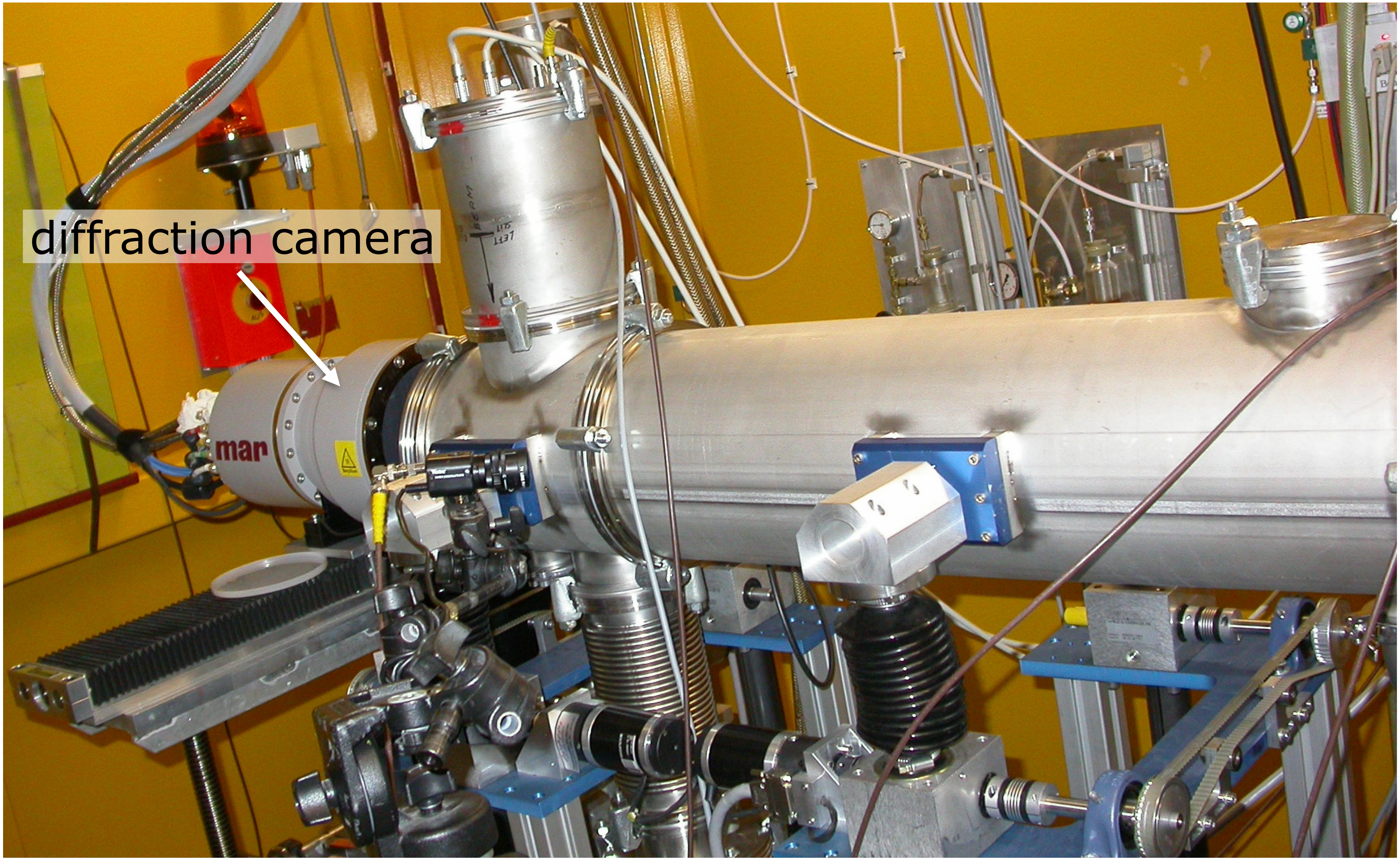

SAXS Tomography

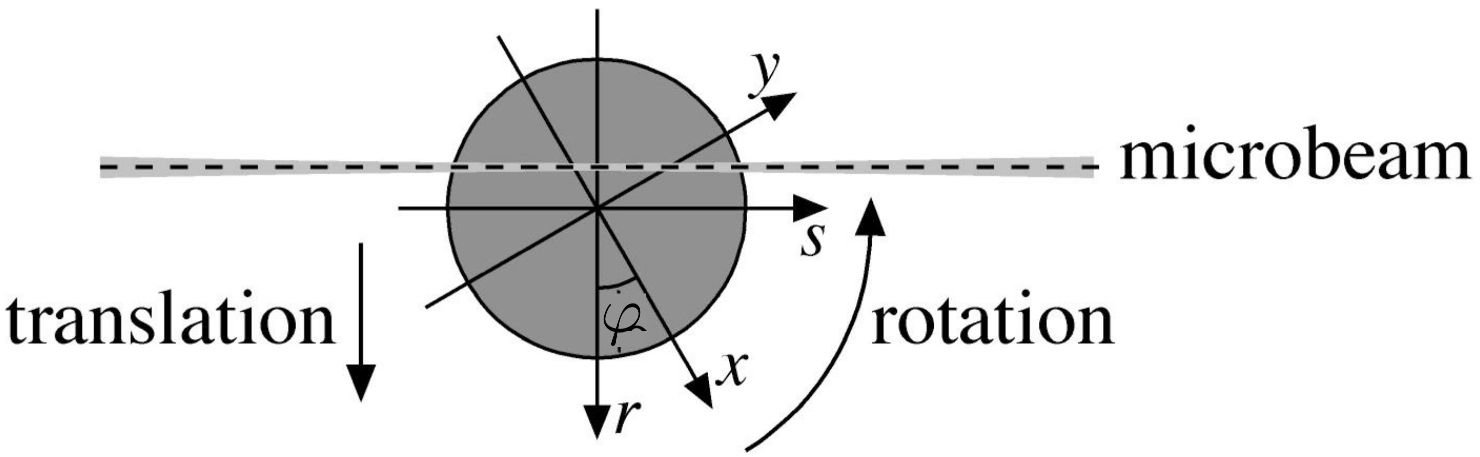

Transmitted beam:

$$I_1(r,\varphi) = I_0 \exp\left\{ -\int ds' \mu\left[x(s',r), y(s',r)\right] \right\}$$

Standard tomography:

homogeneous density (polyethylene):

$$\rho = \left[0.88 \pm 0.04\right] \mathrm{g/cm}^3$$

attenuation

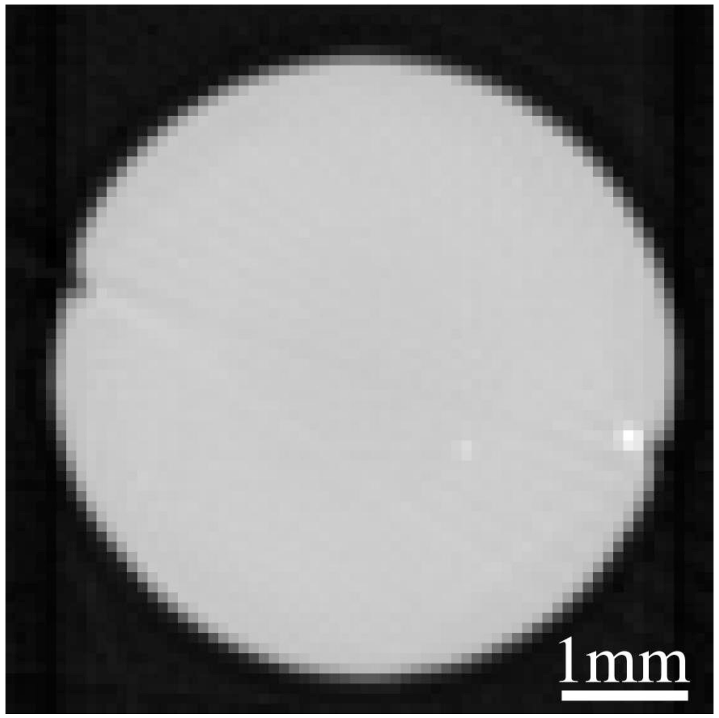

C. Schroer, et al., Appl. Phys. Lett. **88**, 164102 (2006)

SAXS Tomography

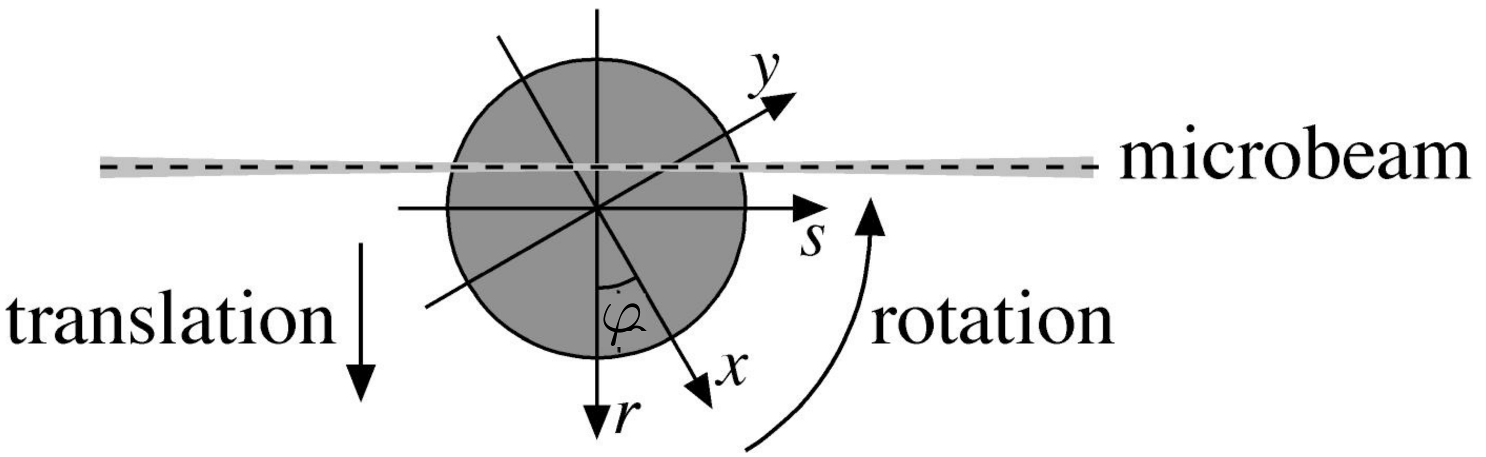

scattered signal:

$$I_{\vec{q}}(r,\varphi) = I_0 \int ds\ f(\varphi,s,r)p_{\vec{q},\varphi}(x,y)g(\varphi,s,r)$$

attenuation of primary beam:

$$f(\varphi,s,r) = \exp\left\{-\int_{-\infty}^{s} ds'\ \mu(x,y)\right\}$$

attenuation of scattered beam

$$g(\varphi,s,r) = \exp\left\{-\int_{s}^{\infty} ds'\ \mu(x,y)\right\}$$

Diffraction signal in forward direction:

$$I_1(r,\varphi) = I_0(r,\varphi)\cdot f(\varphi,s,r)\cdot g(\varphi,s,r)$$ independent of *s*

C. Schroer, et al., Appl. Phys. Lett. **88**, 164102 (2006)

SAXS Tomography

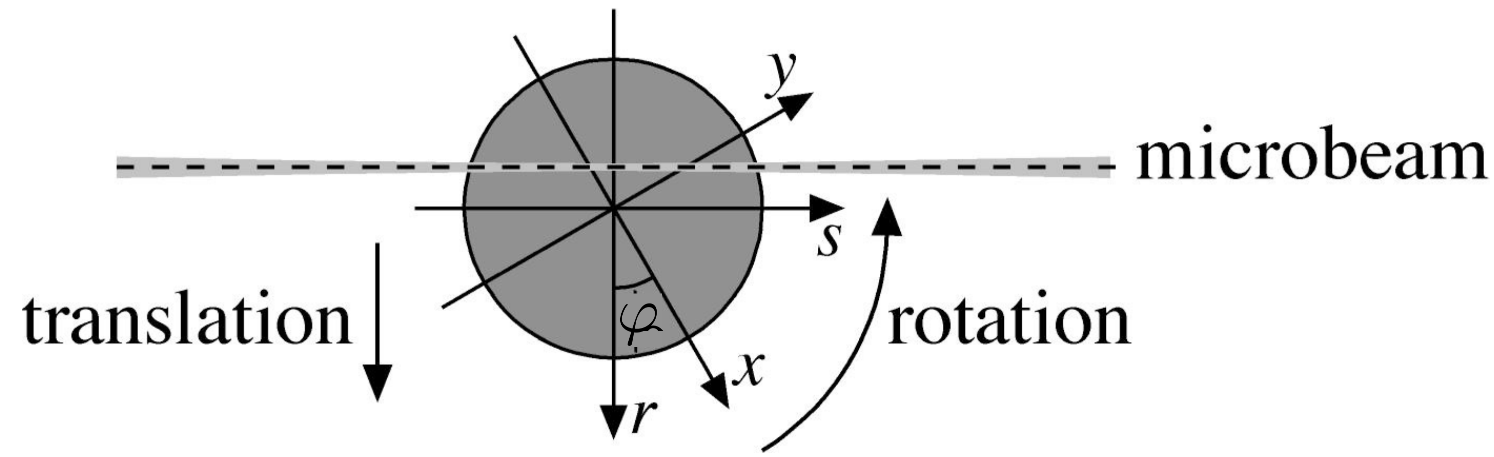

scattered signal:

$$I_{\vec{q}}(r,\varphi) = I_1 \int ds\, p_{\vec{q},\varphi}(x,y)$$

tomography works only if $p_{\vec{q},\varphi}(x,y)$ is independent φ

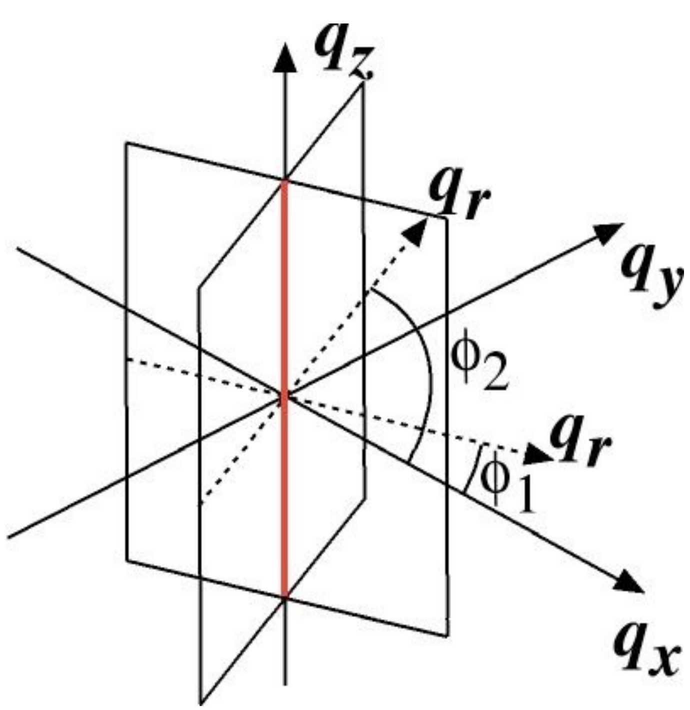

general case: $p_{\vec{q},\varphi}(x,y)$ complicated function

reconstruction only for $q_r = 0$
(q along rotation axis)

C. Schroer, et al., Appl. Phys. Lett. **88**, 164102 (2006)

SAXS Tomography

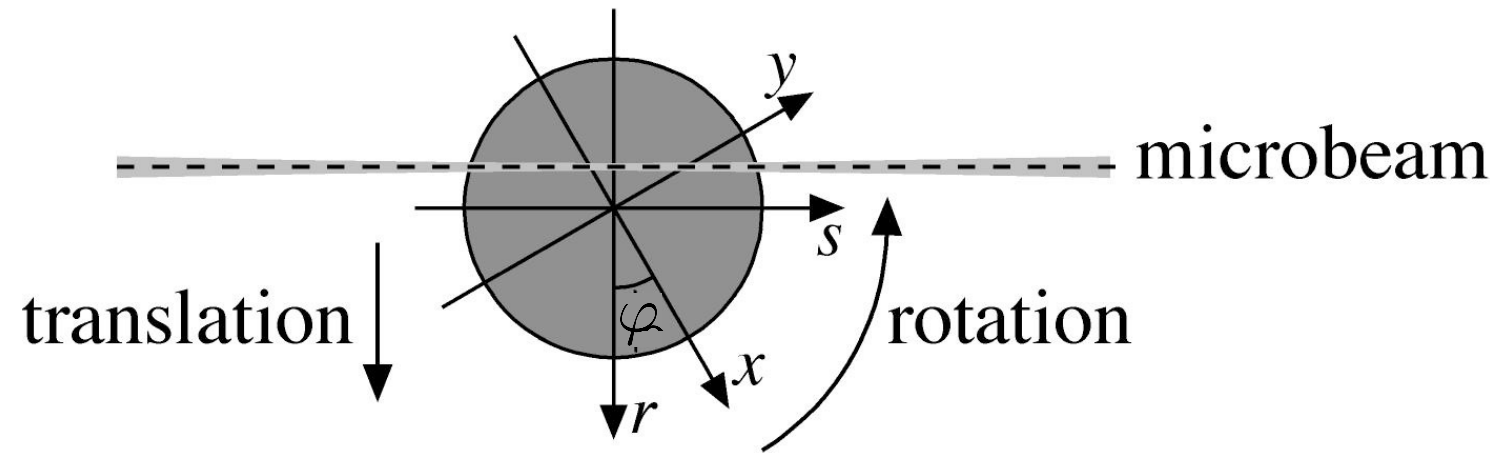

scattered signal:

$$I_{\vec{q}}(r,\varphi) = I_1 \int ds\, p_{\vec{q},\varphi}(x,y)$$

tomography works only if $p_{\vec{q},\varphi}(x,y)$ is independent φ

special case: $p_{\vec{q},\varphi}(x,y)$ has rotation symmetry

around rotation axis

reconstruction of full SAXS cross section
in the vicinity of $q = 0$

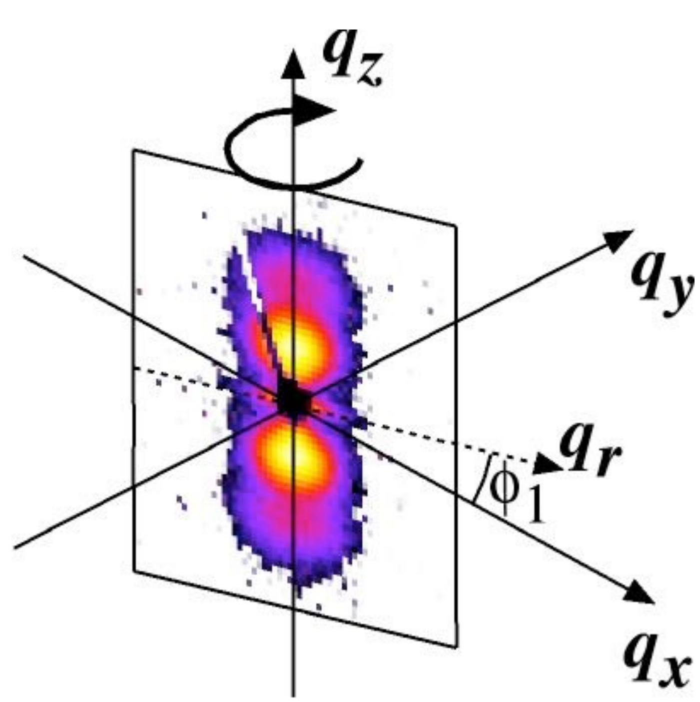

C. Schroer, et al., Appl. Phys. Lett. **88**, 164102 (2006)

SAXS Tomography

reconstruction:

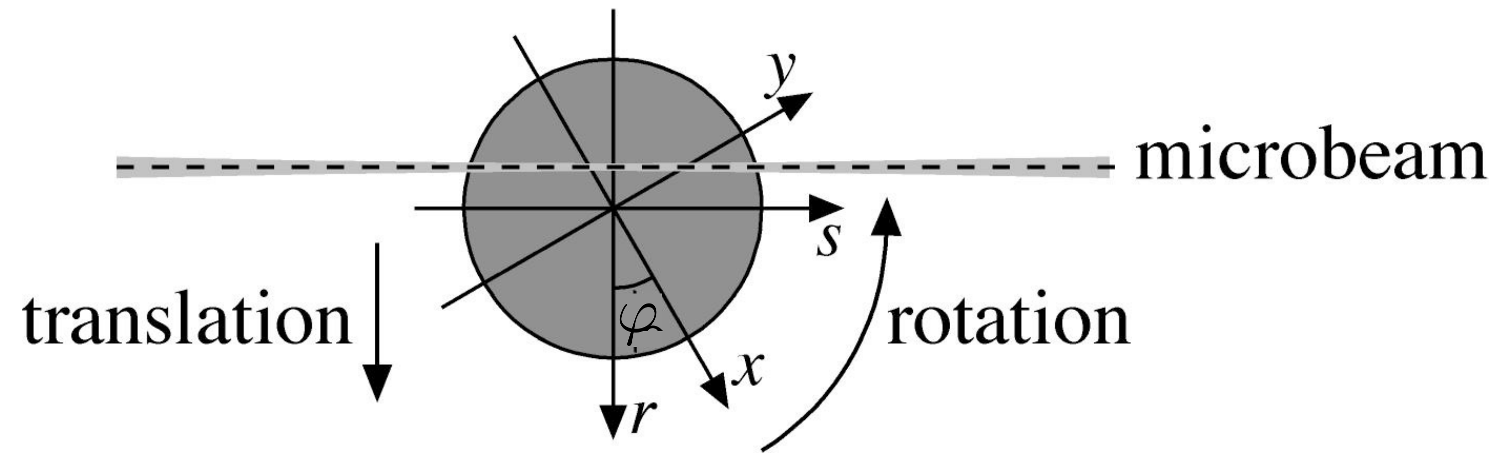

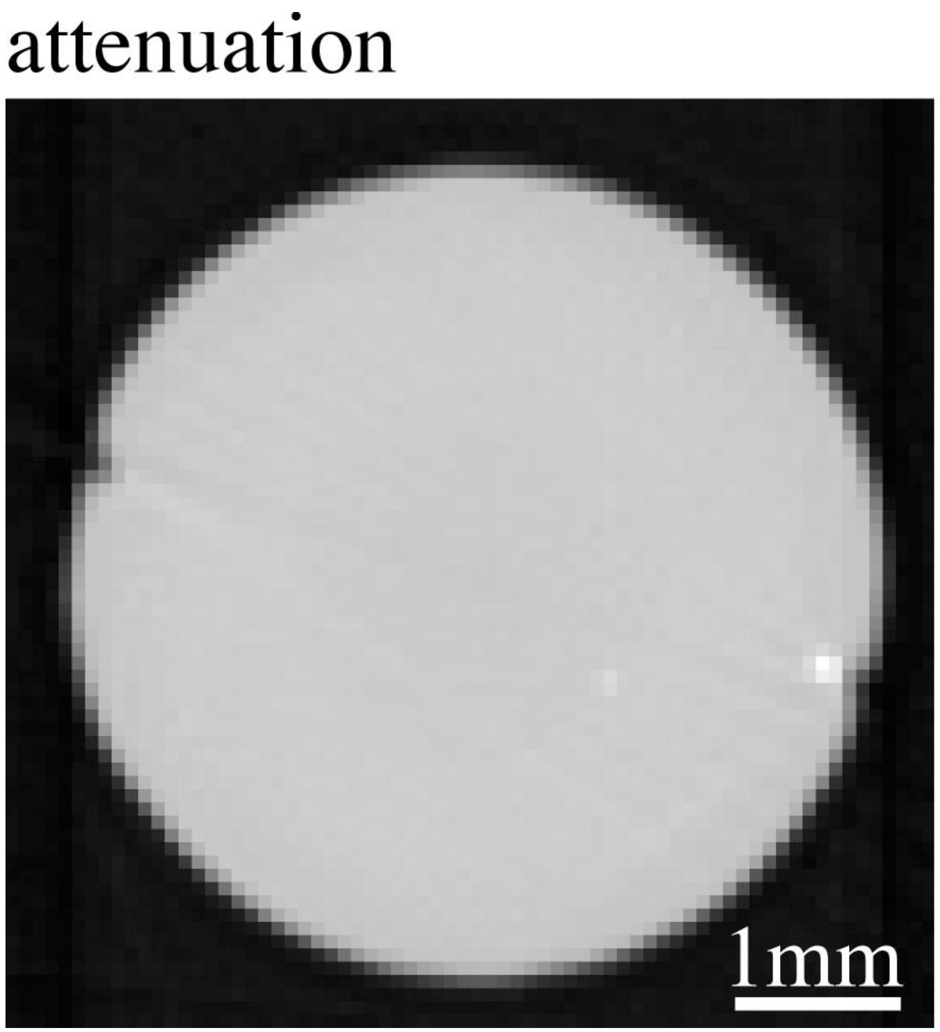

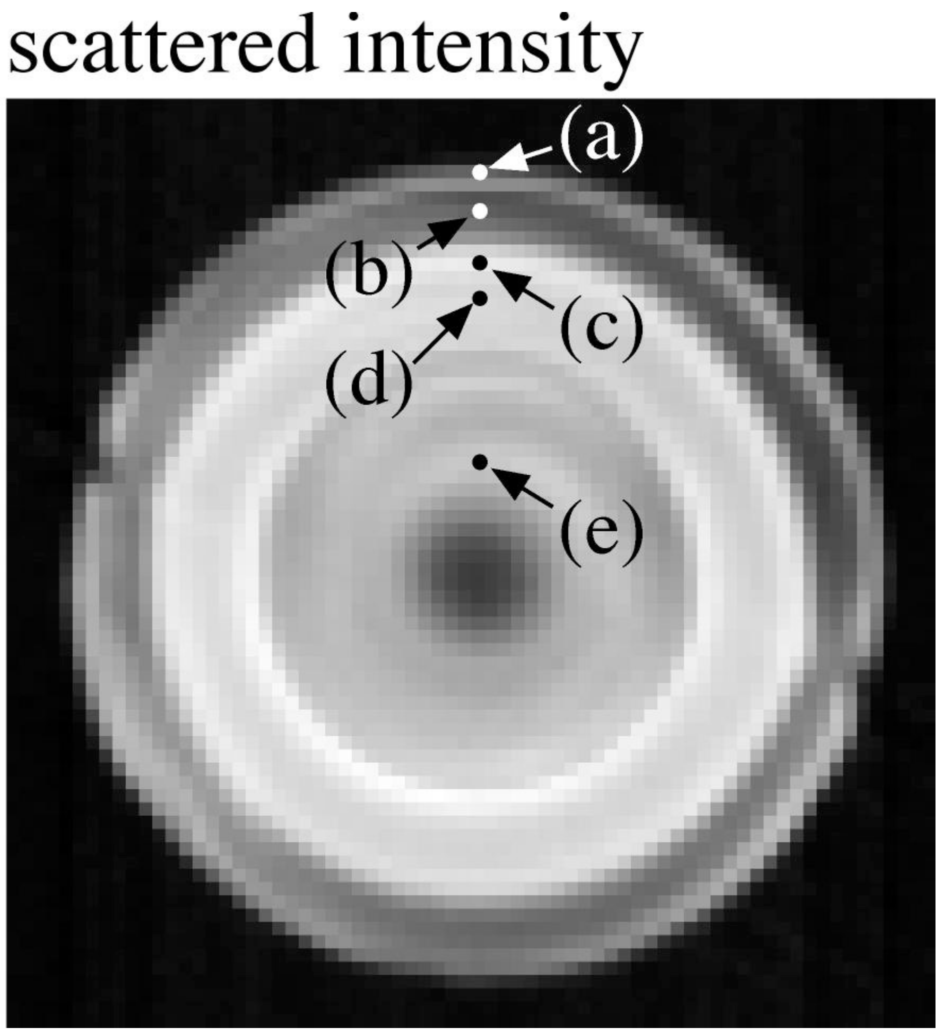

integral scattering cross section along rotation axis

SAXS Tomography

Sample with fibre texture:

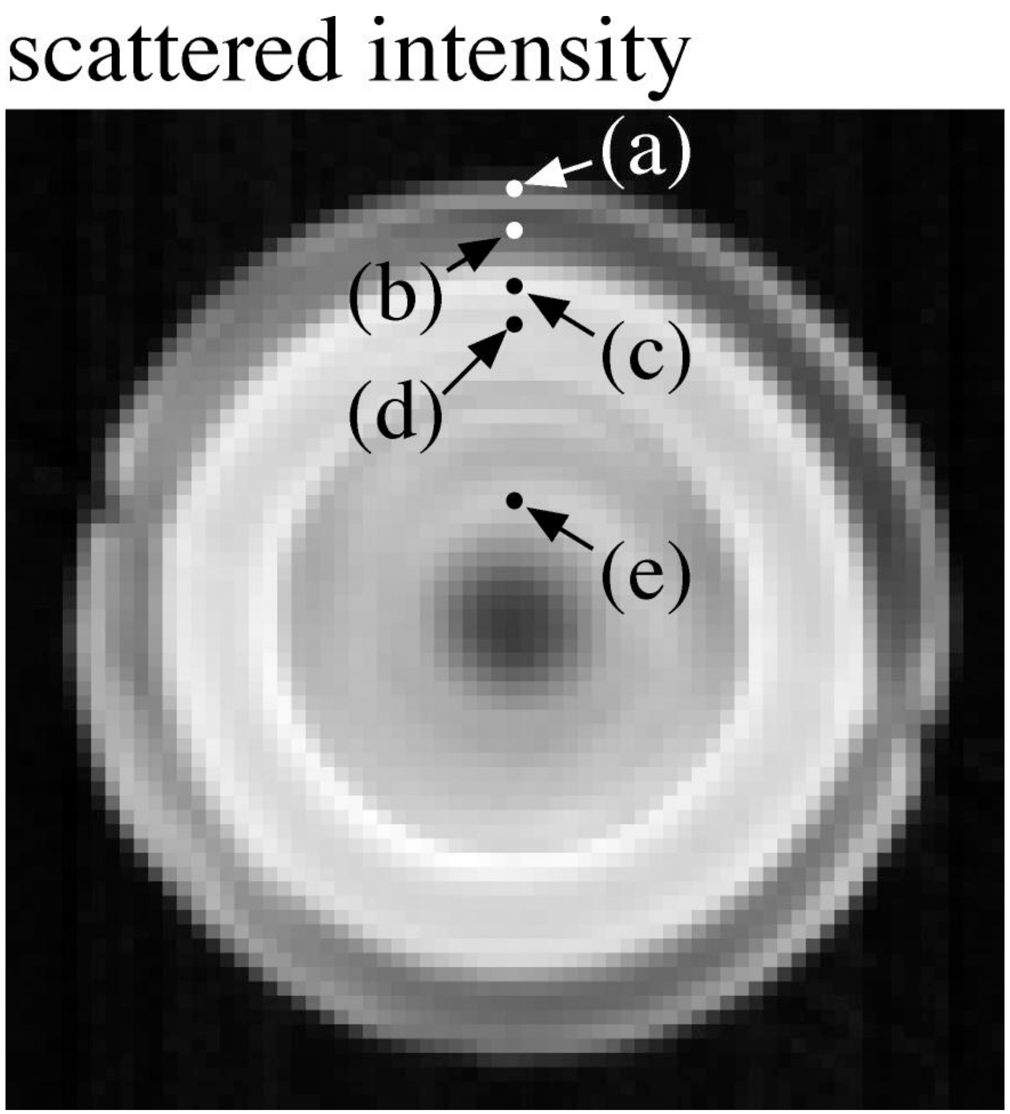

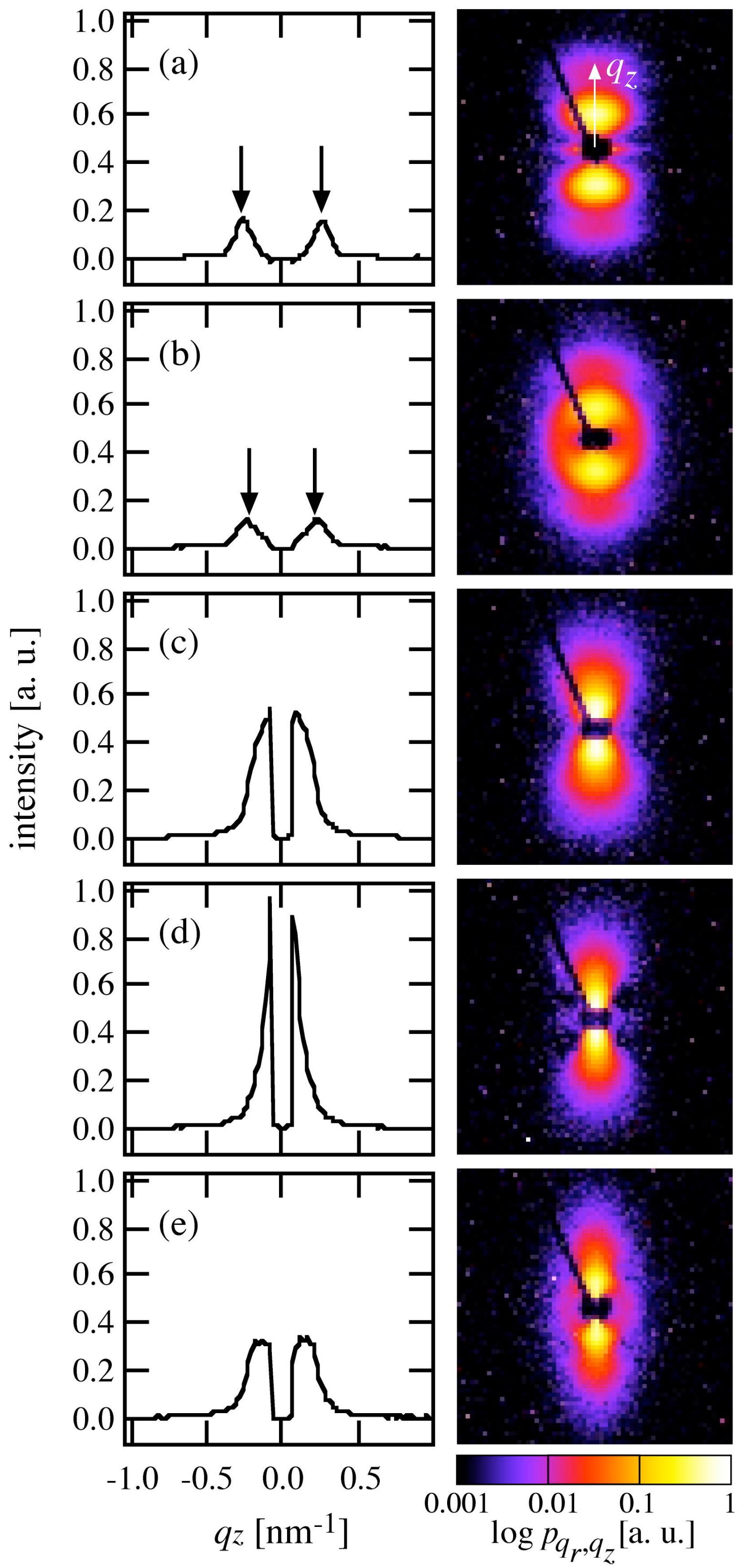

inhomogeneous nanostructure

scattering cross section in each pixel (rotation symmetry)!

C. Schroer, et al., Appl. Phys. Lett. **88**, 164102 (2006)

SAXS Tomography in 3D

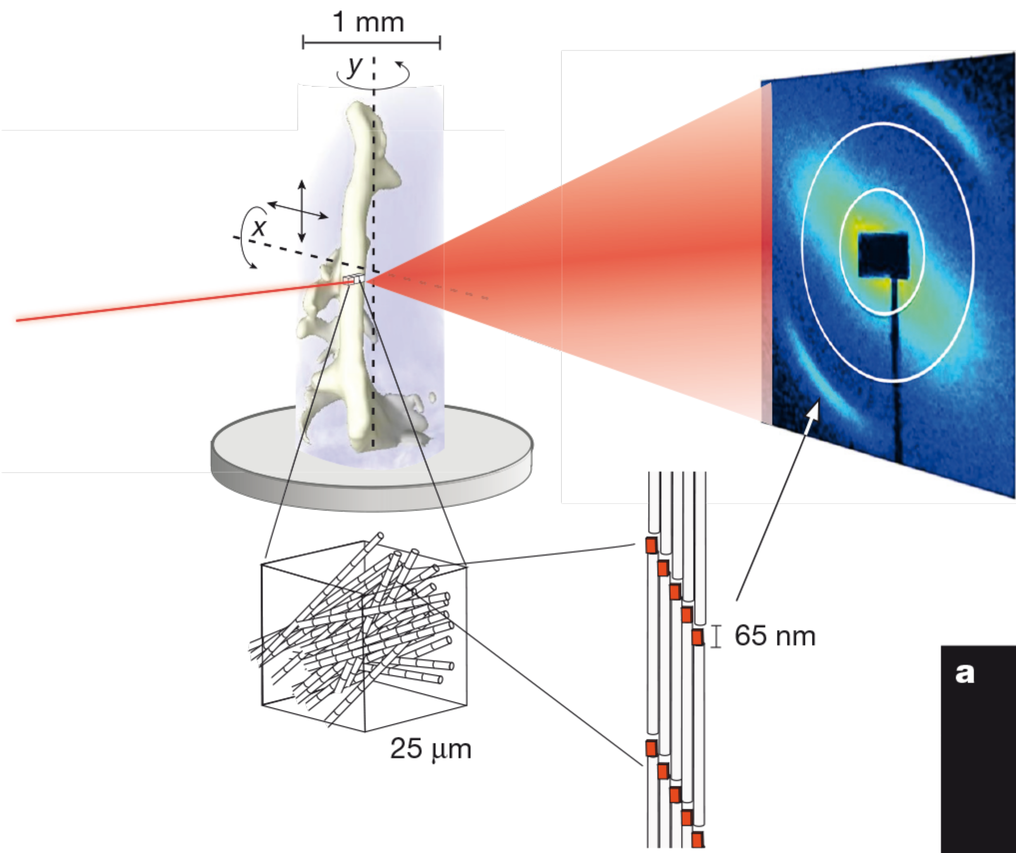

general SAXS-tomographic oroblem

in general: measure 6 dimensional information!

Scan in 4 dimensions and record 2D patterns (coarse mesh due to time limitations)

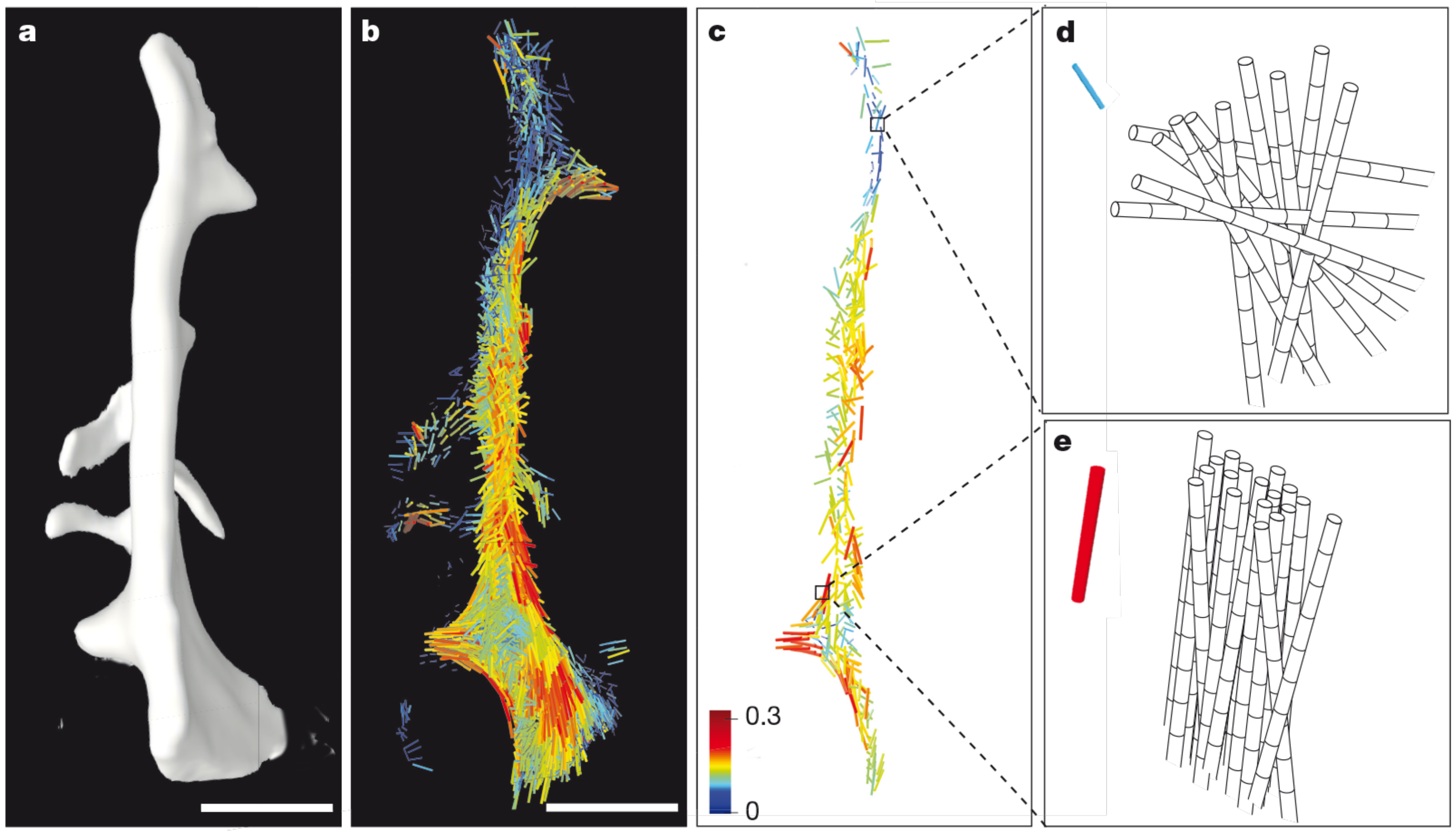

Liebi, M., et al., Nature, **527**(7578), 349–352. (2015).

Conventional X-Ray Microscopy

X-ray microscopy as a quantitative local measurement:

- Full-field microscopy: attenuation and phase contrast

  → measure complex refractive index of sample

- scanning microscopy:

  → all x-ray analytical techniques can be used as contrast:

  - x-ray fluorescence (XRF): chemical composition (quantitative analysis)
  - x-ray absorption spectroscopy (XAS): chemical state of given element (e. g. oxidation)
  - x-ray diffraction and scattering (SAXS & WAXS): local nanostructure
  - …

Full-field and scanning microscopy require x-ray optics

→ resolution limited by numerical aperture of optics

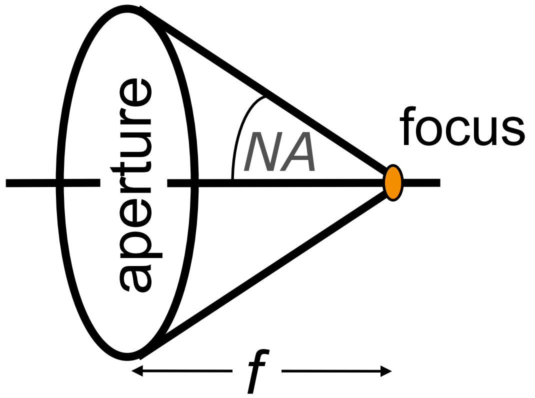

Wednesday: what are the limits and how can we overcome them?